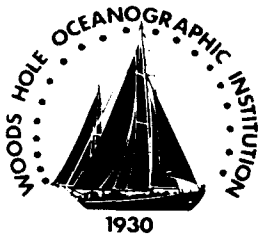DTIC
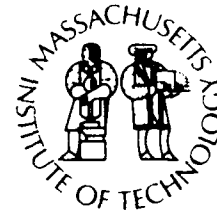
Woods Hole Oceanographic Institution

Massachusetts Institute of Technology

Joint Program
in Oceanography
and
Oceanographic Engineering

1930

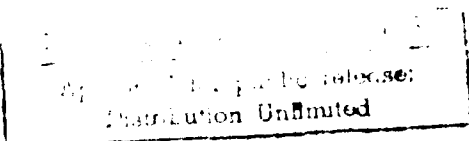DOCTORAL DISSERTATION·····

Nonlinear Diffraction of Ocean Gravity Waves

by

Yehuda Agnon

June 1986

WHOI-86-22

Nonlinear Diffraction of Ocean Gravity Waves

by

Yehuda Agnon

Woods Hole Oceanographic Institution
Woods Hole, Massachusetts 02543

and

The Massachusetts Institute of Technology
Cambridge, Massachusetts 02139
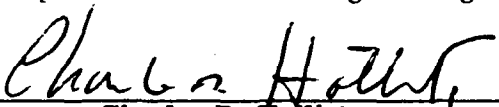
June 1986

Doctoral Dissertation

Approved for Distribution

Robert C. Spindel, Chairman
Department of Ocean Engineering

Charles D. Hollister
Dean of Graduate Studies

NONLINEAR DIFFRACTION OF OCEAN GRAVITY WAVES

by

YEHUDA AGNON

B.Sc., Hebrew University
(1979)

M.Sc., Hebrew University
(1980)

SUBMITTED IN PARTIAL FULFILLMENT
OF THE REQUIREMENTS FOR THE
DEGREE OF

DOCTOR OF SCIENCE

at the

MASSACHUSETTS INSTITUTE OF TECHNOLOGY

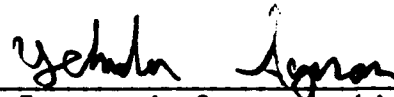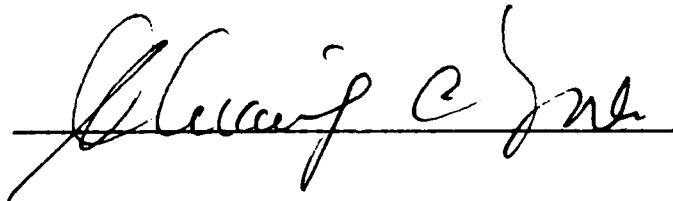and the

WOODS HOLE OCEANOGRAPHIC INSTITUTION

May, 1986

© Massachusetts Institute of Technology 1986

Signature of Author _____
Joint Program in Oceanographic Engineering
Massachusetts Institute of Technology
Woods Hole Oceanographic Institution
May, 1986

Certified by _____
Chiang C. Mei
Thesis Supervisor

Accepted by _____
William D. Grant
Chairman, Joint Committee on Oceanographic Engineering

NONLINEAR DIFFRACTION OF OCEAN GRAVITY WAVES

ABSTRACT

In an irregular sea, waves having different wave numbers interact nonlinearly, giving rise to long waves at the difference frequency and wavenumber. The long waves are associated with motions that have large characteristic time and space scales.

The method of multiple scales in time and in space, in conjunction with perturbation expansions, enables us to separate the flow into components for the general case when there are wave-trains propagating in different directions. In particular, it is of great interest to study the effect of modification of the short waves by diffraction, refraction, reflection and radiation. Using the method of matched asymptotics we determine the long-wave, that consists of forced waves travelling with the short-wave groups and of an additional wave that propagates away from the "zone of modification" at the long-wave velocity $(gh)^{1/2}$. The resulting theory has a wide range of applications. We have studied the following problems:

a) **Slow Sway of a Moored Floating Body in Water of Finite Depth** Both large and small amplitude cases were studied, as well as the effect of different geometries and mooring stiffness. New analytical results for a block with small clearance underneath are included and the existence of resonance is displayed. Periodic and different transient inputs were studied.

b) Wave Trapping on a Shelf

Normal and obliquely incident slowly varying waves were studied, retaining short wave reflection. For the obliquely incident waves trapping can occur. This trapped wave cannot be excited from off the shelf by any linear mechanism. The shelf response is computed and singular resonance is found. The transient response, however, is finite. It too is determined.

c) Excitation of Interfacial Waves in the Lee of a Breakwater

The method of multiple scales is used to determine the non-resonant interaction of surface waves with internal waves in a two layer fluid. We study the effect of diffraction by a long breakwater. While the short waves are decaying behind the breakwater, free long internal waves are propagating directly into that shadow zone.

The present method of analysis, and in particular the multiple scales expansion, proves to be a useful tool in studying modulation and nonlinearity in several aspects at wave propagation, and can be extended to the study of a heretofore unexplored aspect of harbour resonance. The ideas will be sketched in the Epilogue.

Thesis Supervisor: Chiang C. Mei

Title: Professor of Civil Engineering

3

ACKNOWLEDGEMENTS

It is a special pleasure to thank Professor Chiang C. Mei for his continuous friendship and guidance. I hope to be able to emulate his example.

I thank my teachers and members of my committee for their encouragement: professors Bill Grant, Ole Madsen, Ken Melville and Nick Newman, as well as Willem Malkus and Gene Terray who participated in my thesis defense.

I thank Antoinette DiRenzo and Jim Rodgers who took great pains to type the thesis.

I am grateful to Professor H.S. Choi from Korea who has contributed to the work presented here, and has supplied computer programs as did Professor J.N. Newman.

Numerous friends have cheered me through my studies. Among them Mickey Stiassnie, Pat Dixon and many more firends in the Parson's Lab family, MIT and WHOI.

Support from the Fluid Mechanics Program of the Office of Naval Research (contract N00014-80-C-531 NR 4332-228), the Late Gershon Meirbaum Foundation, WHOI/Education, the Fulbright Fellowship and the Arthur T. Ippen Fellowship is gratefully acknowledged.

Finally I thank my family who shared the way with me and Efrat who has been with me throughout this wonderful period of our life.

TABLE OF CONTENTS

5

1. INTRODUCTION

1.1 Survey of Literature

During the last fifteen years there has been an increasing interest in the low frequency effects of irregular waves interacting with floating bodies. The low frequency force and motion can be sufficiently large and are important to the design of moored and dynamically positioned offshore structures. They can also affect the behaviour of ships as well as that of icebergs.

Moored offshore platforms are subject to seas with narrow-banded spectra. The moored vessel may have natural frequencies of horizontal plane motions (sway, surge, yaw) at the order of 0.01 Hz, which are much lower than the dominant frequencies of the incident sea, typically 0.1 Hz. It has been observed that the horizontal response of a moored vessel is indeed the largest at the low frequency range around its natural period (Verhagen & Van Sluijs (1970), Hsu & Blenkarn (1970), Remery & Herman (1971); see Fig. 1.1). At these frequencies the prime source of forcing is associated with the modulation periods of short-wave groups. Nonlinear interaction of the high frequency waves forces waves at the difference (beat) frequencies and wavenumbers.

Several authors have approached the long period motion within the potential theory. A comprehensive review of this topic has been given by Ogilvie (1983), who also cites a few references that treat viscous effects. In a regular wave train the steady drift force, which is second order in wave slope, can be computed from the first order (linear) solution. In irregular waves, Newman (1974) has found that

7
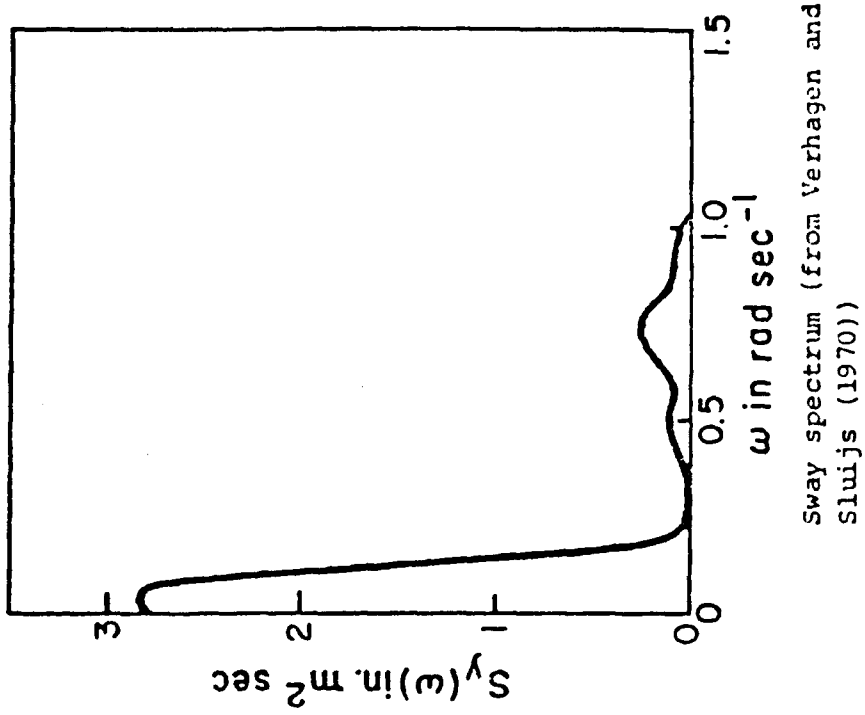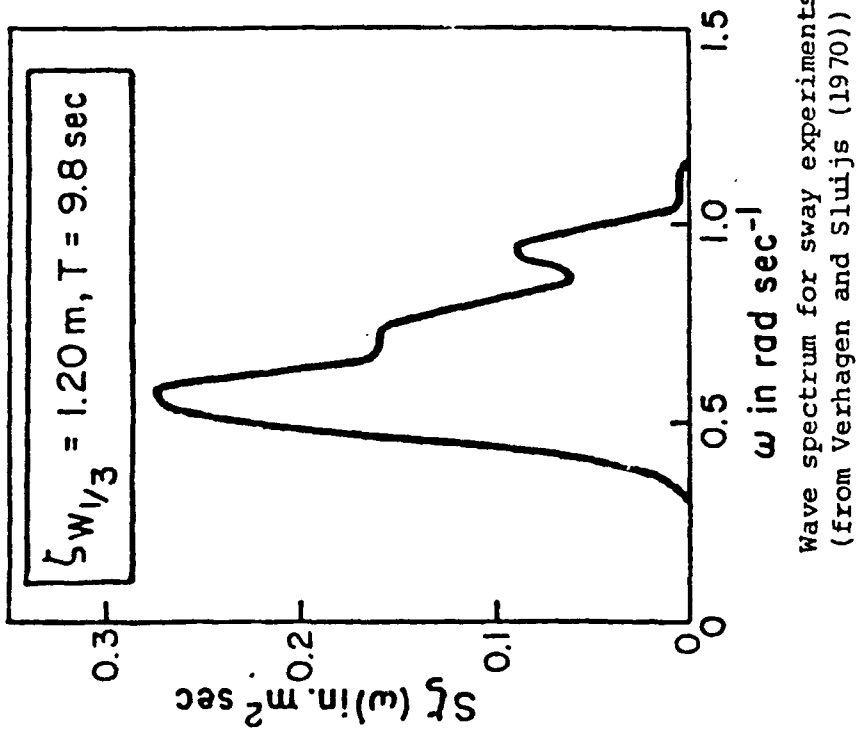
Figure 1.1   The Sway Response to a Narrow Banded Wave

8

the slow drift force can be written as a quadratic "transfer" function of the wave components. The coefficients of this function can be expanded as functions of the difference frequencies. He suggests that for small frequency differences the coefficients can be approximated by their values at zero difference – thus the slowly varying drift force is almost as simple as the steady drift force.

Newman's result has been supported by Martinsen (1983) following an idea suggested by Hsu & Blenkarn (1970). In the time domain, the slowly varying wave is viewed as a regular wave train for any given instant, with amplitude and frequency of the irregular wave at that instant and place. The slowly varying force is then assumed to be given by the steady drift force that would correspond to a regular wave train that has those instantanous and local characteristics. Martinsen points out in addition that for certain geometries, small frequency changes may result in large changes in the steady drift force; this was not included in the analysis of Roberts (1981) who used the same approach to study drift motion in random seas with nonlinear restoring forces.

In computing the slow drift force, the pressure is integrated over the wetted surface of the body and the low frequency terms are collected. Nearly all of these terms have corresponding terms in the expression for the steady drift force due to a regular wave train, with the exception of a term that includes a slowly varying potential. This potential has not been included by Newman, Martinsen or Roberts. Bowers (1976) computed the low frequency potential forced by two regular wave trains without diffraction effects. A similar approach was followed by Pinkster (1980). When the water depth is small compared with the wave-

length of the slow wave, this potential becomes large and needs to be considered.

Triantafyllou (1982) has observed that for finite depth the slow potential is of first order. He used a multiple time expansion to study large amplitude ($O(1)$) motion; this technique was also employed by Molin & Bureau (1980). Using more traditional arguments, Faltinsen & Løken (1979) have calculated the contribution of the slowly varying potential by introducing a related boundary value problem and using Green's Theorem for two dimensional bodies in water of infinite depth. They have concluded from computed results that the contribution of the term in question is small when the wave spectrum is narrow banded.

The related problem of diffraction by fixed coastal structures is also of engineering importance. The linear problem has been extensively studied in the literature (see Mei (1983)). In particular, the propagation of waves which are short compared with the structure's dimensions can be approximated by the theory of geometric optics and the parabolic approximation. Not much theory is available on the nonlinear aspects.

Interaction of the long waves that accompany groups of short waves can also occur when the wave motion is modified by topography (refraction) or by coastal structures such as islands or harbours (diffraction). Mei & Benmoussa (1984) have discussed the refraction of slowly varying waves due to slowly varying depth where the length scales of the variations are comparable. They have found a nonlinear mechanism for producing free long waves which do not propagate in the same direction as the wave group. In particular long waves can be trapped over a

ridge. Foda and Mei (1981) have studied such trapping using high order theory. Symonds and Bowen (1984) have studied trapping of long-waves by breaking short-waves.

Bowers (1977) has studied a problem that is essentially one dimensional, where a narrow rectangular wave flume resonates a very narrow rectangular basin. He has shown that the free long waves induced by incident short wave groups can resonate such a harbour. The resonant periods are much longer than those of the incident short waves, but may be close to their modulation period.

1.2 Scope of Thesis

In this thesis, both floating bodies and large fixed structures will be treated.

It is well known that wave motion with long periods is associated with long length scales. The modulation length scale and the long waves associated with it are expected to be much larger than the short wave-length. This suggests the introduction of multiple scales in space as well as in time. In Chapter 2 a general theory is presented for the interaction of short waves with long waves in water of finite depth. The motion of a floating body that performs slow drift motion in water of finite depth is our first application. Both large and small drift displacements are studied in Chapter 3. The effects of the determining factors, the mooring stiffness, and the body geometry are examined. Both two and three dimensional geometries are discussed in general terms. A special two-dimensional configuration which exhibits

11

damped resonance is that of a horizontal rectangular block with a narrow gap underneath it. This geometry is studied analytically, and compared to a block with no gap. Solutions for transient evolution that feature initial growth, approach to quasi-steady state and decay are also given.

Slowly varying wavetrains may interact with the sea bottom topography as well as with coastal structures such as islands and harbours. The characteristic length of these structures is much larger than that of the floating bodies. To illustrate the physics, we study a few simple geometrics. In Chapter 4 the interaction of slowly varying waves with a shelf/ridge is studied. For oblique incidence trapping of waves and resonance are found. The transient response of the shelf is also studied, displaying a 'wake' effect after the incident waves pass through.

In Chapter 5 we study the diffraction of slowly varying surface waves by a long breakwater in a two layer fluid. In particular, long interfacial waves are forced by the wave groups. We show that free long internal waves are emitted from the shadow boundary into the lee of the breakwater and compute their magnitude. In Chapter 6 the work is concluded. Limitations and possible extensions, including harbour resonance, are discussed.

THE INTERACTION OF SHORT PERIOD WAVES WITH LONG PERIOD WAVES

2.1 Introduction and Definitions

It is well known that progressive waves induce a depression in the mean water surface level, which includes the "set down", as well as a drift current, which includes "Stokes' drift". These quantities are averages over the short period of the surface wave. They are second order, proportional to the square of the wave steepness. Longuet-Higgins and Stewart (1962,1964) have obtained expressions that relate these mean quantities to the 'radiation stress' which stands for the momentum flux due to the wave propagation.

When the amplitude of the short waves varies slowly in time and space, the 'set down' and the drift vary correspondingly, at the same spatial and temporal rates. They are proportional to the square of the amplitude of the primary waves. This slow variation has the nature of a wave, and will be referred to as a long, or low frequency, wave. By carrying out a perturbation expansion of the wave potential and using the technique of multiple scales, we study the interaction between a rigid structure, groups of slowly varying waves that propagate in different directions, and the long period waves that are induced by them. Specific examples are: floating bodies, depth variations, and breakwaters.

Under the usual assumptions of potential theory (ideal incompressible fluid, irrotationality, no separation etc.) we may write Laplace Equation for the velocity potential $\phi(x, y, z, t)$:

$$\Delta\phi = 0 \qquad \text{in the fluid} \qquad (2.1.1)$$

where (x,y,z) are Cartesian coordinates, with the positive z axis pointing vertically upwards, and t denotes time. Writing g for gravity acceleration,

13

P for pressure and ρ for the fluid density, we may write Bernoulli's Equation:

$$- \frac{P}{\rho} = g \, z + \phi_t + \frac{1}{2} \left| \nabla \phi \right|^2 \qquad (2.1.2)$$

We let the pressure at the free surface be zero. Assuming small wave steepness, and Taylor expanding the free surface boundary condition for ϕ around the rest position of the free surface, we get:

$$\phi_{tt} + g\phi_z = [-\frac{1}{2}(\nabla\phi)^2 + \frac{1}{g}\phi_t\,\phi_{zt}]_t - \nabla_h \cdot (\nabla_h \phi\,\phi_t)$$

$$+ 0(\nabla_h\,\phi^3, \, (\phi^3)_t) \qquad (z = 0) \qquad (2.1.3)$$

(cf. Benney (1962)).

At the rigid bottom, the kinematic boundary condition is:

$$\phi_z = \nabla_h\,\phi \cdot \nabla_h\,h \qquad (z = -h) \qquad (2.1.4)$$

where $\nabla_h \equiv (\partial/\partial x, \, \partial/\partial y)$ is the horizontal gradient, and $h = h(x, \, y)$ is the bottom depth.

The water is assumed to be of intermediate depth, comparable to the wave length:

$$kh = 0(1) \qquad (2.1.5)$$

We shall study only bathymetries that are piecewise horizontal (∇h is zero) for which (2.1.4) reduces to:

$$\phi_z = 0 \qquad (z = -h) \qquad (2.1.6)$$

There are two small parameters that are associated with the peturbation expansion for slowly varying small amplitude waves. The first one is the wave steepness:

$$\varepsilon = 0(k \,\,\varepsilon A) \ll 1 \qquad (2.1.7)$$

where k is the central wavenumber and εA is the free surface amplitude of the short wave.

14

The second parameter is the modulation ratio:

$$\mu = O(\mu\Omega/\omega) \ll 1 \qquad (2.1.8)$$

where $\omega = O(g/h)^{1/2}$ is the central frequency of the short wave, and $\mu\Omega$ is the frequency of modulation of the short wave, or - equivalently, its frequency bandwidth. For simplicity, we shall choose ϵ equal to μ, so as to render the effects of dispersion and nonlinearity comparable.

The vastly different spatial and temporal scales of the short waves and their envelopes, suggest the introduction of multiple scales. This will enable us to distinguish between quantities of different magnitudes and obtain a consistent analysis of the different orders.

2.2 The Multiple-Scales Analysis

Since the wave envelopes have typical temporal scales of $O(\epsilon\omega)^{-1}$ and spatial scales of $O(\epsilon k)^{-1}$, we define the stretched coordinates:

$$(x_1, y_1, t_1) = \epsilon(x, y, t) \qquad (2.2.1)$$

Since the fluid depth, h, is assumed to be much smaller than the long scale, there is no need to stretch the vertical coordinate.

The potential, Φ, and the free surface displacement, ζ, are expanded in powers of the small parameter ϵ:

$$(\Phi, \zeta) = \epsilon(\Phi_1, \zeta_1) + \epsilon^2(\Phi_2, \zeta_2) + \ldots \qquad (2.2.2)$$

where Φ_n and ζ_n are functions of the fast and the slow coordinates:

$$\{\Phi_n = \Phi_n (x, y, z, t, x_1, y_1, t_1), \ \zeta_n = \zeta_n(x, y, t, x_1, y_1, t_1)\} = O(1) \qquad (2.2.3)$$

All quantities in this work are $O(1)$ with powers of ϵ signifying the order.

The partial derivatives become:

15

$$\partial/\partial t \; (\epsilon^n \; \phi_n) = \epsilon^n \; [\phi_{n_t} + \epsilon \; \phi_{n_{t_1}}] \qquad (2.2.4)$$

etc.

Expanding (2.1.1) in this fashion, we obtain, after separating the orders:

$$\Delta \phi_1 = 0 \qquad (2.2.5a)$$

$$\Delta \phi_2 = -2\phi_{1xx_1} - 2\phi_{1yy_1} \qquad (2.2.5b)$$

$$\vdots$$

In the same way, (2.1.3) gives at $(z = 0)$:

$$\phi_{1tt} + g\phi_{1z} = 0 \qquad (2.2.6a)$$

$$\phi_{2tt} + g\phi_{2z} = - 2\phi_{1tt_1} - [\frac{1}{2} (\nabla\phi_1)^2 - \frac{1}{g} (\phi_{1t} \; \phi_{1z})_t]_t - \nabla_h \cdot (\phi_{1t} \; \nabla_h \phi_1) \qquad (2.2.6b)$$

$$\vdots$$

and from (2.1.6), at $(z = -h)$:

$$\phi_{1z} = 0 \qquad (2.2.7a)$$

$$\phi_{2z} = 0 \qquad (2.2.7b)$$

$$\vdots$$

The dependence on fast time, t, is in the form $e^{-im\omega t}$ where m is an integer. We further expand ϕ_n, ζ_n in terms of these time harmonics, defined by:

$$(\phi_n, \; \zeta_n) = \sum_{m=-n}^{n} (\phi_{nm}, \; \zeta_{nm}) e^{-im\omega t} \qquad (2.2.8)$$

where ϕ_{nm} are complex, containing the phase information. We require $\phi_{nm}^* = \phi_{n,-m}$ (where $(\;)^*$ is the complex conjugate) so that ϕ_{nm} are real.

In the following sections, we shall solve the perturbation equations at the different orders and harmonics that are required to determine the leading

order slow motion and long waves. The first order first harmonic potential ϕ_{11}, represents the short waves. Because of the use of multiple scales, the long wave potential, too, is first order. It is the zeroth harmonic, ϕ_{10}. By focusing on the long spatial scales we shall obtain a governing equation for ϕ_{10}, in terms of the solution for ϕ_{11}. In this chapter, only the general form of the solution will be studied. The specifics of the near field solution and matching to the far field are left to the following chapters. We begin by studying the short waves potential, ϕ_{11}.

2.3 The Short Waves Away from the Body

Extracting the first order first harmonic equations, for the primary short wave potential, from (2.2.5a, 2.2.6a, 2.2.7a), we obtain:

$$\Delta\phi_{11} = 0 \qquad\qquad (-h < z < 0) \qquad\qquad (2.3.1)$$

$$\phi_{11z} - \sigma\phi_{11} = 0 \qquad\qquad (z = 0) \qquad\qquad (2.3.2)$$

where $\sigma = \dfrac{\omega^2}{g}$

$$\phi_{11z} = 0 \qquad\qquad (z = -h) \qquad\qquad (2.3.3)$$

These equations are formally the same as the linearized equations for purely periodic waves with frequency ω.

We focus our attention on a form of the solution that is general enough for the classes of problems studied in the present work. This form assumes periodicity of the short wave in the y direction:

$$\phi_{11} = f_0(z) \, [s_0^+(\alpha_1, y_1, t_1)e^{i\alpha x + i\gamma y} + s_0^-(x_1, y_1, t_1)e^{-i\alpha x + i\gamma y}]$$

$$+ \sum_{n=1}^{\infty} f_n(z) \, [s_n^+(x_1, y_1, t_1) \, e^{\alpha_n x + i\gamma y} + s_0^-(x_1, y_1, t_1)e^{-\alpha_n x + i\gamma y}]$$

$$(2.3.4)$$

w ; $n = 0, 1, 2...$ are the eigenfunctions:

$$f_0 = \frac{\sqrt{2} \cosh k(z+h)}{(h + \sigma^{-1} \sinh^2 kh)^{1/2}}$$

(2.3.5a)

$$f_n = \frac{\sqrt{2} \cos k_n(z+h)}{(h - \sigma^{-1} \sin^2 kh)^{1/2}} \qquad n = 1, 2,...$$

with k and k_n the positive real roots of

$$k \tanh kh = \sigma$$

(2.3.5b)

$$k_n \tan k_n h = -\sigma$$

The wave numbers (α_n, γ) satisfy:

$$\alpha^2 + \gamma^2 = k^2 \qquad n = 0$$

(2.3.6)

$$\alpha_n^2 + \gamma^2 = -k_n^2 \qquad n = 1, 2,...$$

We may also write: $\alpha = k \sin\theta$, $\gamma = k \cos\theta$, where θ is the direction of pro-pagation of the propagating modes. In any given region either $\{s_n^+\}$, or $\{s_n^-\}$ $n = 1,2...$ may be present, and their contribution is decaying exponentially. These modes are called the <u>evanescent</u> modes. When the water depth, h, takes on different but constant values, the wavenumbers and eigenfunctions must change according to the dispersion relation (2.3.5b).

The propagation of the wave envelopes for the propagating modes, s_0^+ and s_0^-, can be found from solvability conditions for the second order first har-monic potential ϕ_{21}. In view of (2.3.4), the governing equations for the propagating modes, e.g., the component associated with s_0^+, can be separated from (2.2.5b, 2.2.6b, 2.2.7b), to get:

$$\Delta\phi_{21} = f_0[2i\alpha \, s_{0x_1}^+ + 2i\gamma \, s_{0y_1}^+] \qquad (-h < z < 0) \qquad (2.3.7)$$

$$\phi_{21_z} - \sigma\phi_{21} = \frac{2i\omega}{g} s_{0t_1}^+ f_0 \qquad (z = 0) \qquad (2.3.8)$$

$$\phi_{21_z} = 0 \qquad (z = -h) \qquad (2.3.9)$$

For solvability of ϕ_{21}, we must have:

$$s_0^+ = s_0^+ (t_1 - \mu x_1 - \mu y_1) \qquad (2.3.10)$$

where

$$\mu = \frac{\partial \alpha}{\partial \omega} \; ; \quad \nu = \frac{\partial \gamma}{\partial \omega} \qquad (2.3.11)$$

(cf. Mei (1983, p. 52)).

The propagation of s_0^- is found in the same way. It is:

$$s_0^- = s_0^- (t_1 + \mu x_1 - \nu y_1) \qquad (2.3.16)$$

We stress that the details of $s_0^\pm$ are still unknown, only the dependence

on x_1, y_1, and t_1 is fixed. Further information must await the study of the

neighborhood of the body where evanscent modes are important.

2.4 The Long Waves Away from the Body

We now turn to the long waves. They are associated with the zeroth

harmonic of the potential, and of the surface elevation. Due to the intro-

duction of stretched coordinates, it is the first order slow potential that

gives rise to second order free surface displacement

$$-\frac{1}{g} \frac{\partial}{\partial t} \epsilon\phi_{10} = -\frac{1}{g} \epsilon^2 \phi_{10t_1} = 0(\epsilon^2) \qquad (2.4.1)$$

We shall proceed to find the governing equation for ϕ_{10}.

The interaction of short period waves and long period waves is different

in open water, over large horizontal scales, from that in regions of wave

generation, such as the neigborhood of a floating body, a depth

discontinuity, or other structures, where evanescent short waves exist. Each region will be studied separately and the resulting solutions will be matched asymptotically to determine their values. The region where the evanescent modes are important — that is — within a few short waves from the wave generation area — is referred to as the 'near field'. We denote the potential in the near field by

$$\psi = \phi \qquad kx = 0(1) \qquad kx_1 \ll 1 \qquad (2.4.2)$$

The region in which only propagating modes need to be considered, a few wave groups away from the wave generation area, is called 'the far field' and the potential there is denoted by ϕ

$$\phi = \phi \qquad kx \gg 1 \qquad kx_1 = 0(1) \qquad (2.4.3)$$

see Figure 2.1.

With this notation we shall study separately the specific characteristics of the potential in each region.

The short scale variation of ϕ_{10} is found by collecting the zeroth harmonic from (2.2.5a), (2.2.6a) and (2.2.7a):

$$\Delta\phi_{10} = 0 \qquad (-h < z < 0) \qquad (2.4.4)$$

$$\phi_{10z} = 0 \qquad (z = 0, -h) \qquad (2.4.5)$$

The eigenfunctions for these equations are:

$$g_n(x, y) \cos \frac{n\pi z}{h} \qquad n = 0, 1,\ldots \qquad (2.4.6a)$$

where

$$(\Delta_h - n^2\pi^2/h^2)\, g_n = 0 \qquad (2.4.6b)$$

For all $n \neq 0$, the solutions decays exponentialy away from the near field. We conclude that ϕ_{10}, the far field component of ϕ_{10} is independent

20
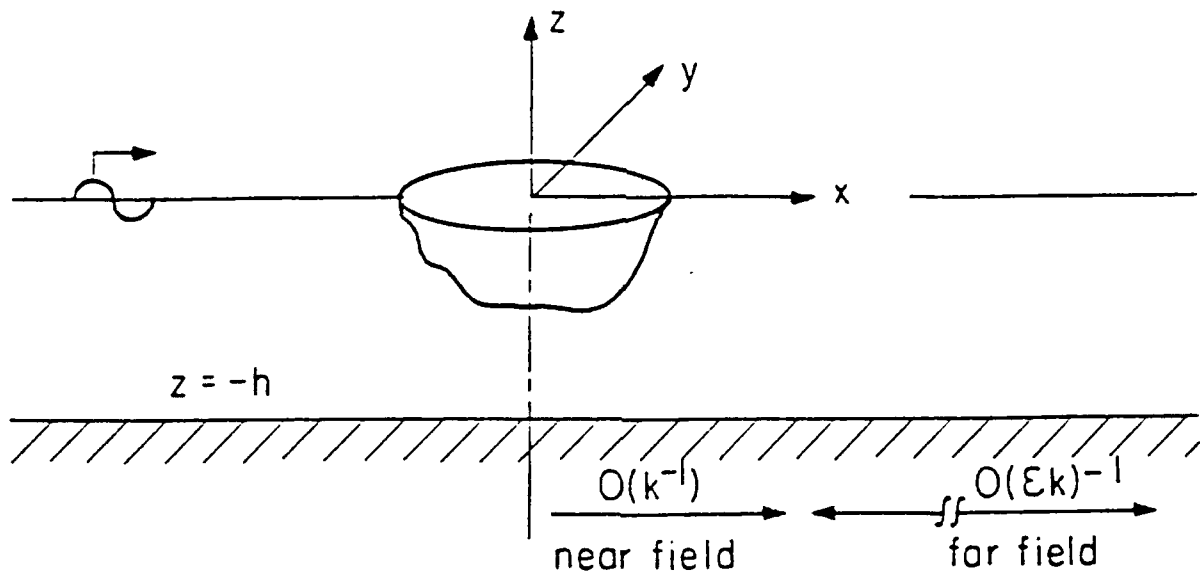
Figure 2.1 Definition Sketch

of the short scale (x, y, z):

$$\phi_{10} = \phi_{10}(x_1, y_1, t_1) \tag{2.4.7}$$

Let us now seek the governing equations for ϕ_{10}, mainly from (2.1.3). To second order in ϵ, ϕ_{10z} is zero at $(z=0)$. However, by integrating (2.1.1) from $-h$ to 0 with respect to z, and using (2.1.6), we find:

$$\phi_z \Big|_{z=0} = \int_{-h}^{0} \phi_{zz} \, dz = - \int_{-h}^{0} \nabla_h^2 \phi \, dz \tag{2.4.8}$$

also

$$[\nabla_h^2 \phi]_{30} = \nabla_1^2 \phi_{10} + (\nabla_h \cdot \nabla_1 + \nabla_1 \cdot \nabla_h)\phi_{20} + \nabla_h^2 \phi_{30} \tag{2.4.9}$$

where $\nabla_1 \equiv (\partial/\partial x_1, \partial/\partial y_1)$

The first term on the right hand side of (2.4.9) is only a function of the long space scales (x_1, y_1) while the other two terms are functions of short (x, y) as well. The third order zeroth harmonic of (2.1.3) is

$$(g \, \phi_z)_{30} + \phi_{10t_1 t_1} \qquad (z=0)$$

We substitute (2.4.9) into (2.4.8) and the resulting equation into (2.4.10). The long spatial scale component of (2.4.10) is thus given by:

$$\phi_{10t_1 t_1} - gh \, \nabla_1^2 \phi_{10} \tag{2.4.11}$$

On the right hand side of (2.1.3), the long scale component of $\{0[(\phi^3)_x]$, $0[(\phi^3)_y]\}$ is of order $0(\epsilon^4)$ while the zeroth harmonic of $\{0[(\phi^3)_t]\}$ is $0(\epsilon^4)$. The third order zeroth harmonic of the other terms on the right hand side of (2.1.3) is

22

$$[-\left|\nabla\phi_{11}\right|^2 + (\sigma \ \phi_{11} \ \phi_{11}^* + *)]_{t_1}$$

$$\text{(2.4.12)}$$

$$- \{[\nabla_1(\nabla_h \ \phi_{11} \ i\omega \ \phi_{11}^*) + \nabla_h(\nabla_1 \ \phi_{11} \ i\omega \ \phi_{11}^*)] + *\}$$

We note that in the far field, in the absence of evanescent modes in (2.3.4), the terms of (2.4.12) have components of the form:

$$(s_0^- \ s_0^{+*} e^{-2i\alpha x} + *) \ , \quad \left|s_0^+\right|^2 \ , \quad \left|s_0^-\right|^2$$

Clearly, only the last two terms contribute to the long spatial scale component. This means that ϕ_{10} is induced only by the self interaction of each propagating short wave with itself. Cross interactions between the propagating modes, or with the evanescent modes, give rise to higher order, short scale waves. In the second square brackets of (2.4.12) only the first term is purely long scale in space, and the last term is discarded since it depends on short space scale.

When only the self interaction terms are taken on the right hand side of (2.1.3) the result is:

$$\phi_{10t_1t_1} - gh \ \nabla_1^2 \ \phi_{10} = f_0^2(0) \ [(\sigma^2 - k^2) \frac{\partial}{\partial t_1} - 2\omega\alpha \frac{\partial}{\partial x_1} - 2\omega\gamma \frac{\partial}{\partial y_1}] \ \left|s_0^+\right|^2$$

$$\text{(2.4.13)}$$

$$+ f_0^2(0) \ [(\sigma^2 - k^2) \frac{\partial}{\partial t_1} + 2\omega\alpha \frac{\partial}{\partial x_1} - 2\omega\gamma \frac{\partial}{\partial y_1}] \ \left|s_0^-\right|^2$$

which is the differential equation governing the far field slow potential $\phi_{10}(x_1, y_1, t_1)$.

An alternative way to arrive at Equation (2.4.13) is by observing that the total second order, zeroth harmonic surface elevation (from Bernoulli's equation (2.1.2)) is:

$$\zeta_{20} = -\frac{1}{g}\left[\phi_{10t_1} + \nabla\phi_{11} \cdot \nabla\phi_{11}^* - (\sigma\,\phi_{11}\,\phi_{11z}^* + *)\right] \qquad (z = 0) \qquad (2.4.14)$$

Let $(h + \bar{\zeta})\,U$ denote the horizontal flux across the fluid column and expand it into orders and harmonics:

$$U = \frac{1}{(h+\bar{\zeta})} \int_{-h}^{\zeta} \nabla_h \Phi = \sum_{n=1}^{\infty} \sum_{m=-n}^{n} U_{nm}\, e^{-im\omega t} \qquad (2.4.15)$$

then since $\bar{\zeta} = O(\varepsilon^2)$,

$$hU_{20} = h\nabla_1\,\phi_{10} + (\zeta_{11}\,\nabla_h\,\phi_{11}^* + *)\big|_{z=0} + \int_{-h}^{0} \nabla_h\,\phi_{20}\,dz \qquad (2.4.16)$$

In the far field $\nabla_h\phi_{20}$ is zero (see Equation (3.3.23)).

When the long scale parts of (2.4.14, 2.4.16) are substituted into the equation of continuity:

$$\bar{\zeta}_{20t_1} + h\nabla_1 \cdot \bar{U}_{20} = 0 \qquad (2.4.17)$$

where the overbar stands for the long scale component, the ϕ_{10} terms make up (2.4.11) while the terms due to the short waves make up (2.4.12). Hence, the wave equation for ϕ_{10}, (2.4.13) can be retrieved. Finally, a third and more formal way to obtain (2.4.13) is by studying solvability conditions for ϕ_{30}; this is lengthy and will be omitted.

The form of (2.4.13) can be further simplified. By making use of the relations for the propagation of the wave envelopes (2.3.10) and (2.3.11), (2.4.13) becomes:

$$\phi_{10t_1t_1} - gh\nabla_1^2\,\phi_{10} = f_0^2(0)\,[\sigma^2 - k^2 - 2\omega(\alpha\mu + \gamma\nu)]\,[\,|s_0^+|^2 + |s_0^-|^2]_{t_1} \qquad (2.4.18)$$

which is hyperbolic. Finally we write:

$$\alpha\mu + \gamma k\nu = \frac{\alpha^2}{kC_g} + \frac{\gamma^2}{kC_g} = k/C_g \qquad (2.4.19)$$

(2.4.18) then becomes:

$$\phi_{10t_1t_1} - gh\nabla_1^2 \phi_{10} = f_0^2(0) [\sigma^2 - k^2 - 2\omega k/C_g][|s_0^+|^2 + |s_0^-|^2]_{t_1} \qquad (2.4.20)$$

This is a generalization of the theory of Longuet-Higgins and Stewart (1962, 1964) for a single wavetrain.

The wave Equation (2.4.13) or (2.4.20) governs the long wave in the far field. The specific solutions will depend on the particular problem at hand and will be determined by matching to the nea field. In the following chapters we shall study a few examples of the application of the present theory to problems that involve wave propagating in different direction at the same location.

3. SLOW SWAY OF A FLOATING BODY

3.1 Introduction and General Considerations

We first deal with the slow motion of moored floating bodies in slowly varying waves. The linearized theory does not account for low frequency responses due to narrow banded incident swells. It has been observed, however, that such responses exist, and can be very large. It is also known that the resonant frequency of a mooring system usually lies below the swell frequencies, while it can fall inside the range of the lower, modulational frequencies.

In general, a floating body has six degrees of freedom. Among them, three modes of motion induce buoyancy restoring forces and moments. These are: heave, pitch and roll. To leading order, the buoyancy forces and moments are proportional to the displacements. For example, a heave motion with amplitude H will induce a buoyancy force with amplitude $-\rho g H A_{wp}$, where A_{wp} denotes the water-plane area. H can be large only for a bottle shaped body, on which we shall comment later.

For a body that is not bottle shaped, the only interesting slow motions are horizontal: surge, sway and yaw. We shall examine a sway problem to illustrate our approach. The geometry chosen is that of a rectangular horizontal cylinder in beam seas. The cylinder axis lies on the y axis and the waves are incident from $(x \to -\infty)$ (Figure 3.1). The problem is then two dimensional, with

$$\partial/\partial y = 0 \qquad (3.1.1)$$
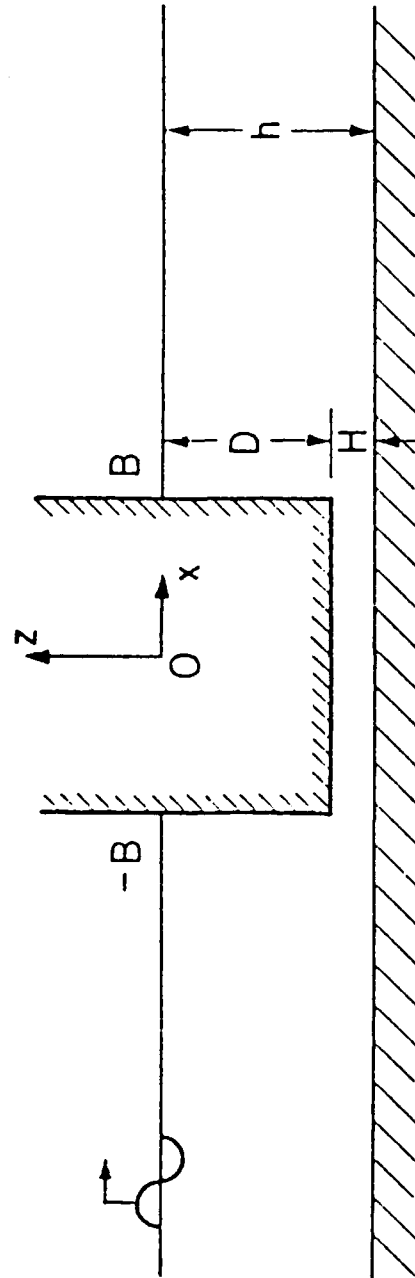
for all quantities.

26

Figure 3.1 A Rectangular Cylinder in Beam Seas

27

We assume that the body performs sway motion only, to the leading order, at both fast and slow time scales. This assumption simplifies the presentation and will be shown to be valid for some cases. Computed results for the general motion will be presented in the other cases. The mooring is modelled by a linear spring.

The wave field is coupled with the motion of the body through boundary conditions on the body surface. The incoming waves are diffracted and reflected by the presence of the body. Waves are further radiated by the body motion caused by waves. The effect of sway is expressed by the kinematic boundary condition. Denoting the sway displacement by X:

$$\phi_x = X_t \qquad \text{on } S^{\pm} = \left\{ x = X(t) \pm B; \; -D \leq z \leq \zeta \right\} \qquad (3.1.2)$$

$$\phi_z = 0 \qquad \text{on } b = \left\{ z = -D; \; -B \leq x - X \leq B \right\} \qquad (3.1.3)$$

$S^{\pm}$ are the sides of the body, which has breadth 2B and draught D (see Figure 3.1). B and D are assumed to be comparable to the depth h which is of the order of the wavelength $2\pi/k$. The boundaries of the body at rest are given by

$$S_0^{\pm} = \{ x = \pm B; \; -D \leq z \leq 0 \}, \quad \bar{b}_0 = \{ z = -D; \; -B \leq x \leq B \}$$

The effect of the waves on the body motion is given by the dynamic boundary condition:

$$MX_{tt} + K_0 X = \int_{S^-} P \, dz - \int_{S^+} P \, dz \qquad (3.1.4)$$

where M is the mass of the body and K_0 is the elastic constant of the mooring system. The right hand side is the hydrodynamic force where the pressure P is given by (2.1.2). We shall see that the driving force for the slow motion

(zeroth harmonic) is $O(\epsilon^2)$. The magnitude of X depends on the mooring stiff-ness: If K_0 is $O(\epsilon)$, X must be $O(\epsilon)$ (small displacement) in order to balance the hydrodynamic force. This case is studied in Section 3.3. The mass of the body is $O(1)$ so that the inertia of the body for the slow motion is $O(\epsilon^3)$ since,

$$MX_{tt} = \epsilon^2 MX_{t_1 t_1} \tag{3.1.5}$$

It is negligible if X is $O(\epsilon)$ (small displacement).

On the other hand, if K_0 is $O(\epsilon^2)$, X must be $O(1)$ in order to balance the slow drift force. The body inertia is then $O(\epsilon^2)$. This case will be studied in Section 3.4.

As a special but interesting case, we shall see that large blockage by the cylinder may give rise to large added mass and damping coefficients, rendering X at $O(\epsilon)$ regardless of the mooring.

The problem will be studied separately in the near field , within a few short waves from the body, and in the far field, a few wave groups away from the body on either side. We examine the form of ϕ in the far field where it is denoted $\bar{\phi}$. Because of radiation conditions, the only waves in addition to the incident waves must be propagating away from the body. Since the equations for ϕ_{11} are linear, (2.3.10) and (2.3.16) for s_0^+ and s_0^- may be written as:

$$s_0^+ = A_0(t_1 - x_1/C_g) \; ; \quad s_0^- = RA_0(t_1 + \frac{x_1}{C_g}) \quad (x_1 < 0)$$
$$s_0^+ = TA_0(t_1 - x_1/C_g) \; ; \quad s_0^- = 0 \quad\quad\quad (x_1 > 0) \tag{3.1.6}$$

where R and T are complex reflection and transmission coefficients,

respectively. We shall see later that they include both diffraction and radiation effects. The equation for ϕ_{10}, (2.4.20), becomes:

$$\frac{\phi_{10t_1t_1} - gh\,\phi_{10x_1x_1}}{f_0^2(0)\,[(\sigma^2 - k^2)\,C_g + 2\omega k]} = \left\{ \begin{array}{l} \dfrac{\partial}{\partial x_1}\left|A_0^2(x_1 - C_g t_1)\right| + \left|R\,A_0(x_1 + C_g t_1)\right|^2 \\[2mm] \dfrac{\partial}{\partial x_1}\left|T\,A_0(x_1 - C_g t_1)\right|^2 \end{array} \right. \qquad (3.1.7)$$

to the left and the right of the body, respectively.

The forcing terms produce waves which propagate at velocities C_g and $-C_g$. There are also free waves which propagate away from the origin at velocities $(gh)^{1/2}$ and $-(gh)^{1/2}$. These are solutions to the corresponding homogeneous equation. Formally, the solution can be written as:

$$\phi_{10} = \left\{ \begin{array}{l} \phi_{10}^{I}\,(x_1 - C_g t_1) + \phi_{10}^{R}\,(x_1 + C_g t_1) + \phi_{10}^{-}\,(x_1 + \sqrt{gh}\,t_1) \qquad (x_1 < 0) \\[3mm] \phi_{10}^{T}\,(x_1 - C_g t_1) + \phi_{10}^{+}\,(x_1 - \sqrt{gh}\,t_1) \qquad\qquad\qquad (x_1 > 0) \end{array} \right.$$

$$(3.1.8)$$

The values of $\phi^{(\alpha)}$ (α = I, R, or T) at $(x_1 = 0)$ can be obtained from (3.1.7) and (3.1.8)

$$\phi_{10t_1}^{(\alpha)} = \overset{(I)}{\chi^{(\alpha)}}\left|A_0^2\right|\frac{f_0^2(0)}{gh/C_g^2 - 1}\left[(k^2 - \sigma^2) + \frac{2\omega k}{C_g}\right)\right] \qquad \begin{array}{l}[\chi] = [1] \\ [\chi^{(R)}] = [|R|^2] \\ [\chi^{(T)}] = [|T|^2] \end{array} \qquad (3.1.9)$$

$\phi_{10}^{\pm}$ will be determined through matching to the near field ψ_{10}. In order to perform the matching, we shall need the inner expansion of (3.1.8) as $(x_1 \to 0)$ for $(x_1 > 0)$ and $(x_1 < 0)$, which is

$$\phi_{10} \sim \left[\phi_{10}^{I} + \phi_{10}^{R} + \phi_{10}^{-}\right]_{x_1 = 0} + x_1\left[\frac{\phi_{10}^{I}}{-C_g} + \frac{\phi_{10}^{R}}{C_g} + \frac{\phi_{10}^{-}}{\sqrt{gh}}\right]_{t_1} \qquad (x_1 < 0)$$

$$(3.1.10a)$$

30

$$\phi_{10} - [\phi_{10}^{T} + \phi_{10}^{+}]_{x_1} = 0 + x_1 \left[\frac{\phi_{10}^{T}}{-C_g} + \frac{\phi_{10}^{+}}{-\sqrt{gh}}\right]_{t_1} \qquad (x_1 > 0)$$

$$(3.1.10b)$$

where we have replaced derivatives with respect to x_1 by derivatives with respect to t_1, expanding (3.1.8) in the form:

$$G \sim G(0) + x_1 \frac{\partial G}{\partial x_1} = G(0) + x_1 \frac{\partial G}{\partial t_1} C_g \qquad (3.1.11)$$

We now turn to specific problems. The first case examined will be that of slow sway of small amplitude ($O(\varepsilon)$).

3.2 The Solution for the Fast Motion

When the mooring is somewhat stiff,

$$K_0 = \varepsilon K = O(\varepsilon) \qquad (3.2.1)$$

the slow sway displacement (and the fast one) is

$$X = O(\varepsilon) \qquad (3.2.2)$$

which can be expanded into harmonics:

$$X = \sum_{n=1}^{\infty} \varepsilon^n \sum_{m=-n}^{n} X_{nm} \exp(-im\omega t) \qquad (3.2.3)$$

The boundary conditions on the body (3.1.2 - 3.1.4) can be Taylor-expanded about the rest position, $S_0^{\pm}$.

At the first order, first harmonic, we get for the short wave potential, ϕ_{11}:

$$\phi_{11_x} = -i\omega X_{11} \qquad \text{on} \qquad S_0^{\pm} \qquad (3.2.4)$$

31

$$\Phi_{11_z} = 0 \qquad\qquad \text{on } \overline{b}_0 \qquad\qquad (3.2.5)$$

$$-\omega^2 M X_{11} = -i\omega\left[\int_{S_0^-} \Phi_{11} dz - \int_{S_0^+} \Phi_{11} dz\right] \qquad (3.2.6)$$

Together with (2.3.1 - 2.3.3) and the radiation condition, these equations define the problem for ψ_{11}, which is the near field of Φ_{11}. Formally these equations are identical to the equations for the linear, time harmonic problem of a rectangular cylinder swaying freely in regular waves. This problem was solved by Mei and Black (1969), using a variational method. We shall employ the equivalent Galerkin method in order to solve for the dynamics of the sway motion as well as its kinematics. To start with, we break the problem down into a diffraction problem and a radiation problem.

The diffraction problem deals with a fixed body. We break it down further into a symmetric and an antisymmetric problem. The analysis is confined to $(x < 0)$. Starting with the symmetric (S) problem, (2.3.4) becomes:

$$\psi_{11}^S = f_0 a_0 (e^{ik(x+B)} + R_S \, e^{-ik(x+B)}, + \sum_{n=1}^{\infty} a_n f_n \, e^{k_n(x+B)}, \quad (x < -B) \quad (3.2.7)$$

under the body, the potential has the form

$$\psi_{11}^S = \overline{A}_0 F_0 + \sum_{n=1}^{\infty} A_n F_n \cosh K_n x \qquad (x > -B) \quad (3.2.8)$$

For the antisymmetric (A) problem:

$$\psi_{11}^A = f_0 b_0 (e^{ik(x+B)} + R_A \, e^{-ik(x+B)}) + \sum_{n=1}^{\infty} b_n \, e^{k_n(x+B)} \quad (x < -B) \quad (3.2.9)$$

$$\psi_{11}^A = B_0 F_0 x + \sum_{n=1}^{\infty} B_n F_n \sinh K_n x \qquad (x > -B) \quad (3.2.10)$$

32

The eigenfunctions under the body satisfy (2.3.3, 3.2.5) and are given by:

$$F_0 = (h-D)^{1/2}; \quad F_n = \sqrt{2/(h-D)} \, \cos K_n (z+h), \quad n = 1, 2, \ldots \quad (3.2.11)$$

R_S and R_A are the reflection coefficients.

There are two continuity conditions that apply at the boundary between the fluid region under the body and the region to its left: both the potential ψ_{11} and ψ_{11} must be continuous. Let us define:

$$U_A = \psi_{11x}^A \; ; \quad U_S = \psi_{11x}^S \quad (x = -B) \; (-h \le z \le -D) \quad (3.2.12a)$$

$$= 0 \qquad\qquad = 0 \qquad\qquad (-D \le z \le 0) \quad (3.2.12b)$$

U_A and U_S are the complex amplitudes of the horizontal velocity. Using the orthonormality of $\{f_n\}$ and that of $\{F_n\}$ we can express $\{a_n\}$, $\{A_n\}$ in terms of U_S, and $\{b_n\}$, $\{B_n\}$ in terms of U_A:

$$a_0 = \frac{1}{ik(1-R_S)} \int_{-H}^{-D} U_S \, f_0 \qquad B_0 = \frac{1}{ik(1-R_A)} \int_{-H}^{-D} U_A \, f_0 \, dz$$

$$(3.2.13a)$$

$$a_n = \frac{1}{k_n} \int_{-H}^{-D} U_S \, f_n \, dz; \qquad b_n = \frac{1}{k_n} \int_{-H}^{-D} U_A \, F_0 \, dz \quad (n \ge 1)$$

$$B_0 = \int_{-H}^{D} U_A \, F_0 \, dz$$

$$(3.2.13b)$$

$$A_n = -\frac{1}{K_n \sinh K_n B} \int_{-H}^{-D} U_s \, F_n \, dz \; ; \quad B_n = \frac{1}{K_n \cosh K_n B} \int_{-H}^{-D} U_A \, F_n \, dz \; (n \ge 1)$$

$\bar{A}_0$ does not affect, hence, cannot be determined from U_S.

We may now use (3.2.13) to write down the continuity condition on ψ_{11}^S, ψ_{11}^A at $(x = -B)$. Eliminating R_S (or R_A) and keeping a_0 and b_0, we get:

$$-2b_0 f_0 = \int_{-h}^{-D} dz' \, G^A(z,z') \, U_A(z') \qquad (-h < z < -D) \qquad (3.2.14)$$

$$\bar{A}_0 F_0 - 2a_0 f_0 = \int_{-h}^{-D} dz' \, G^S(G,z') \, U_S(z') \qquad (-h < z < -D) \qquad (3.2.15)$$

where

$$G^{\begin{bmatrix}S\\A\end{bmatrix}}(z,z') = \frac{f_0(z) \, f_0(z')}{ik} + \sum_{n=1}^{\infty} \frac{f_n(z) \, f_n(z')}{k_n} + \begin{bmatrix}0\\B\end{bmatrix} F_0(z) \, f_0(z')$$

$$(3.2.16)$$

$$+ \sum_{n=1}^{\infty} \begin{bmatrix}\coth K_n B\\ \tanh K_n B\end{bmatrix} \frac{F_n(z) \, F_n(z')}{K_n}$$

Using the Galerkin method to solve this integral equation, we approximate U_S and U_A by:

$$U_S \simeq - \sum_{n=1}^{N} K_n \, A_n \, F_n \, \sinh K_n \, B \qquad (3.2.17a)$$

$$U_A \simeq B_0 \, F_0 + \sum_{n=1}^{N} K_n \, B_n \, F_n \, \cosh K_n \, B \qquad (3.2.17b)$$

Multiplying (3.2.14) by $\{F_0, \ldots F_N\}$ and integrating from $-h$ to $-D$ with respect to z, we get $N+1$ equations for $\{B_0, B_1 K_1 \cosh K_1, \ldots, B_N K_N \cosh K_N B\}$. Multiplying (3.2.15) by $\{F_1, \ldots, F_N\}$ we get N linear algebric equations for $\{-A_1 K_1 \sinh K_n B, \ldots, -A_N K_N \sinh K_N B\}$. Details are given in Appendix A. Having obtained an approximation for the velocity $(x = -B)$ we can determine R_S, R_A and the force on $\bar{S}_0$ from (3.2.13).

The diffraction problem for a wave incident from the left is solved by superposition of the symmetric and the antisymmetric solutions. We have:

$$R_d = \frac{1}{2} (R_S + R_A) \; ; \quad T_d = \frac{1}{2} (R_S - R_A) \; ; \quad F = F_A \qquad (3.2.18)$$

here R_d, T_d, and F are respectively the reflected wave, the transmitted

wave and the force due to diffraction, per unit incident wave amplitude, and

$$F_A = \rho i \omega \int_{S_0^-} \psi_{11}^A \, dz \qquad (3.2.19)$$

The solution of the radiation problem for sway is done in the same way,

with (3.2.12b) replaced by:

$$U_A = V \qquad (x = -B) \qquad (-D \le z \le 0) \qquad (3.2.20)$$

where V is the complex amplitude of the sway velocity (the sway potential is

antisymmetric), see Appendix A for details.

Having found the added mass, μ, and the damping coefficient, λ, for the

swaying cylinder, (3.2.6) becomes:

$$[-\omega^2 (M+\mu) - i\omega\lambda] \, X_{11} = A \, F_A \qquad (3.2.21)$$

for an incident wave amplitude A. If the left-going radiated wave has complex

amplitude R_r for a unit amplitude sway we find that

$$R = R_d + R_r \, X_{11}/A = \{R_d + R_r \cdot F_A / [-\omega^2(M+\mu) - i\omega\lambda]\} \qquad (3.2.22)$$

$$T = T_d - R_r \, X_{11}/A = T_d - R_r \cdot F_A / [-\omega^2(M+\mu) - i\omega\lambda]\}$$

As a special case, we shall be interested in a body which extends the

entire sea depth and slides on the bottom, that is:

$$D = h \qquad (3.2.24)$$

For this case, we obtained an analytical solution for the combined diffrac-

tion radiation problem of ψ_{11} (Agnon & Mei 1985a). This solution is given in

Appendix B.

As another interesting special case, we consider a narrow gap between
the bottom and the body:

$$h - D = O(\epsilon h) \tag{3.2.25}$$

In view of the narrowness, ψ_{11} in the gap represents a uniform flow which
depends on the pressure gradient between its two ends:

$$-\partial P/\partial x \simeq -i\omega\rho \; [\epsilon\psi_{11} \; (B, \; -h) - \epsilon\psi_{11} \; (-B, \; -h)]/2B = O(\epsilon) \tag{3.2.26}$$

The effect of this flow, when multiplied by the gap width, amounts to an
$O(\epsilon^2)$ flux. It is negligible outside the gap since it is equivalent to an
$O(\epsilon^2)$ sink-source pair. The potential outside the gap, ψ_{11}, is then given to
order $O(\epsilon)$ by the solution in Appendix B for a sliding body, as if the gap
did not exist.

We now turn to the slow sway.

3.3 Slow Sway of Small Amplitude

The slow potential Φ_{10}, which in the near field is denoted by ψ_{10}, is
governed by (2.4.4) and (2.4.5). For the boundary condition on the body, we
derive the second order zeroth harmonic from (3.1.2) – (3.1.4). Expanding
(3.1.2) about $S_0^{\pm}$ we get:

$$\psi_x \; (S^{\pm}) = \psi_x \; (S_0^{\pm}) + \psi_{xx} \; X + O(\epsilon^2) = X_t \tag{3.3.1}$$

where ψ_x, ψ_{xx} on the right hand side are evaluated at $S_0^{\pm}$ which are the
mean positions of the side walls.

The second order zeroth harmonic component is:

$$\psi_{10x_1} + \psi_{20x} + (\psi_{11xx} \; X_{11}^* + *) = X_{10t_1} \qquad \text{(on } S_0^{\pm}) \tag{3.3.2}$$

36

where X_{20t} is zero, since

$$X_{20} = X_{20}(t_1) \tag{3.3.3}$$

To find the dynamic boundary condition, we note that:

$$\frac{d^2}{dt^2} \epsilon \, X_{10} = \epsilon^3 \, X_{10t_1t_1} = O(\epsilon^3) \tag{3.3.4}$$

$$\psi_t(S^{\pm}) = \psi_t(S_0^{\pm}) + \psi_{tx} \, X + O(\epsilon^3) \tag{3.3.5}$$

$$\int_0^{\zeta} \psi_t \, dz = \psi_t \, (z=0) \, \zeta + O(\epsilon^3) \tag{3.3.6}$$

and

$$\int_0^{\zeta} z \, dz = \frac{1}{2} \zeta^2 \tag{3.3.7}$$

The integral of the pressure on $S^{\pm}$ will have contributions from integration between $-h$ and zero and from integration between zero and ζ_{11}. The contribution to the latter due to the quadratic terms in the expression for the pressure (2.1.2) is $O(\epsilon^3)$. The only contribution at $O(\epsilon^2)$ is that evaluated in (3.3.6), (3.3.7).

Hence, the second-order, zeroth harmonic of (3.1.4) is:

$$KX_{10} = -\rho \, [\int_{S_0^-} P'_{20} dz - \int_{S_0^+} P'_{20} dz + \delta(i\omega\psi_{11} \, \zeta_{11}^* + *) + \delta(g\zeta_{11} \, \zeta_{11}^*)] \tag{3.3.8}$$

where

$$P'_{20} = \psi_{10t_1} + |\nabla\psi_{11}|^2 + (i\omega\psi_{11}^* \, X_{11_x} + *) + gz \tag{3.3.9}$$

(from the Bernoulli equation (2.1.2) and from (3.3.5)),
and

$$\delta G \equiv G(-B, \, 0) - G(B, \, 0) \tag{3.3.10}$$

Equation (3.1.3) simply gives:

$$\psi_{20_z} = 0 \quad \text{on} \quad \bar{b}_0 \quad \text{and} \quad (z = -h) \qquad (3.3.11)$$

We note that the kinematic boundary condition (3.3.2) couples ψ_{10}, which is a function of long spatial scale, with ψ_{20}, which is a function of short spatial scale. The right hand side of (3.3.8) (see also (3.3.9)) can be split into contributions due to ψ_{10} and ψ_{11}. Since ψ_{11} is formally the same as ψ_{11} for a regular wave train, the terms involving ψ_{11} have the same form as the terms in the expression for the steady drift force in a regular wave-train. In Appendix D we evaluate these terms and obtain an expression which agrees with that obtained by Maruo (1960), by Newman (1967) and by Longuet-Higgins (1977), using conservation of momentum and maintaining that there is no energy absorbed by the body. The contribution of the short waves is:

$$\rho g \left| A \right|^2 \left| R \right|^2 \frac{C_g}{C} \qquad (3.3.12)$$

where A, the amplitude of the incident short wave ζ_{11}^I is given by:

$$A = \frac{2i\omega \, f_0(0)}{g} A_0 \qquad (3.3.13)$$

A_0 is the amplitude of the incident short wave potential ϕ_{11}^I and $(C \equiv \omega/k)$ is its phase speed. Equation (3.3.8) can now be written as:

$$KX_{10} = -\rho \left[\int_{S_0^-} \psi_{10} dz - \int_{S_0^+} \psi_{10} dz \right]_{t_1} + \rho g \left| A \right|^2 \left| R \right|^2 \frac{C_g}{C} \qquad (3.3.14)$$

The form of ψ_{10} in the near field will depend on the specific geometry of the body. Denoting the gap width by H, we distinguish among three cases, according to the width of the gap between the body and the bottom:

a) large gap: $H / h = O(1)$,

b) small gap: $H / h = O(\varepsilon)$,

c) no gap: $H = 0$.

These three cases are studied in the following subsections. Each case represents a different asymptotic limit. Together they give a picture of the dependence of the body's response on the size of the gap.

3.3.1 The Large Gap Case

A geometry common in practice is one in which the gap between the body and the bottom is comparable to the water depth.

The variation of ψ_{10} with respect to (x, z) is governed by Laplace Equation (2.4.4) and by homogenous Newmann conditions on the mean free surface and the bottom (2.4.5). The flux through S_0^+, S_0^- is $O(\varepsilon^2)$, because of (3.3.2), and the flux at the matching boundaries to the far field

$$S_\infty^\pm = \{x, z \mid 1 \ll kx \ll \varepsilon^{-1}, \quad -h < z < 0\} \qquad (3.3.15)$$

(see Figure 3.2), is $O(\varepsilon^2)$ because of (3.1.10).

Since the cross section of the gap is $O(1)$, the flux through it, which is the horizontal gradient of the slow potential is $\nabla_h \varepsilon \psi_{10}$. It must be matched to the far field according to

$$\nabla_h \varepsilon \psi_{10} = O(\varepsilon^2 \phi_{10x_1} / H) = O(\varepsilon^2) \qquad (3.3.16a)$$

Hence, the spatial variation of the slow potential in the near field with respect to the short scale is second order in ε, except in the vicinity of sharp corners. This is in agreement with the $O(\varepsilon)$ kinematic boundary condition:
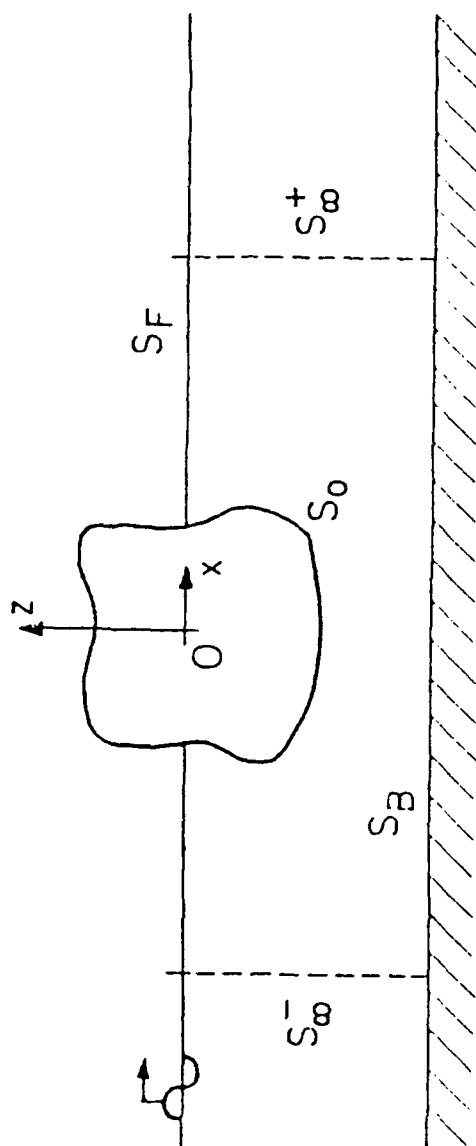
Figure 3.2   The Near Field of a 2-Dimensional Problem

$$\psi_{10x} = 0 \quad \text{on} \quad S_0^{\pm} \qquad (3.3.16b)$$

Thus, ψ_{10} is only a function of time almost everywhere in the near field:

$$\psi_{10} = \psi_{10}(t_1) \, (1 + O(\varepsilon)) \qquad (3.3.17)$$

Integrating across the hull, we get

$$\int_{S_0^-} \psi_{10t_1} \, dz - \int_{S_0^+} \psi_{10t_1} \, dz = 0 \qquad (3.3.18)$$

The dynamic boundary condition (3.3.14) becomes:

$$K \, X_{10} = \rho g \, \left|A\right|^2 \left|R\right|^2 \frac{C_g}{C} \qquad (3.3.19)$$

Formally this result is the same as that for the steady drift motion in a regular (unmodulated) wave train, and agrees with Newman's (1974) theory, in which the slow drift force is approximated by the steady drift-force formula.¶

The present theory allows us, however, to find the long wave field, and the vertical force as well. To determine the wave potential we match the slow potential and its gradient – on both sides of the near field – with the corresponding quantities in the far field. Matching of the potential gives:

$$\phi_{10}(0^-, t_1) = \psi_{10}(t_1) = \phi_{10}(0^+, t_1) \qquad (3.3.20)$$

To the far field observer, the near field shrinks to a line at $(x_1 = 0)$ across which the potential ϕ_{10} is connected via ψ_{10}. Combining (3.3.10) and (3.3.20), we have:

$$\phi_{10}^+(t_1) - \phi_{10}^-(t_1) = \phi_{10}^I(t_1) + \phi_{10}^R(t_1) - \phi_{10}^T(t_1) \quad (x_1 = 0) \qquad (3.3.21)$$

¶   In the large gap case, large slow sway is possible (for weaker mooring). This will be studied in Section 3.4. The results presented there include (3.3.19).

41

In order to determine the unknown ϕ_{10}^+, ϕ_{10}^- we need a further condition on the jump in $\partial\phi_{10}/\partial x_1$. This condition is related to the horizontal flux. At the second order zeroth harmonic, the flux across S_∞^+, where $kx \gg 1$ and $x_1 \ll 1$ is

$$\overline{\int_{-h}^{\zeta} \frac{\partial\psi}{\partial x}\Big|_{S_\infty^+} dz} = \overline{\zeta_1 \frac{\partial\psi_1}{\partial x}\Big|_{\substack{z=0\\S_\infty^+}}} + \int_{-h}^{0} \overline{\frac{\partial\psi_{20}}{\partial x}\Big|_{S_\infty^+}} dz \qquad (3.3.22)$$

This flux should be matched to the far-field flux:

$$\overline{\int_{-h}^{\zeta} \frac{\partial\phi}{\partial x}\Big|_{x_1=0^+}} = h \frac{\partial\phi_{10}}{\partial x_1}\Big|_{x_1=0^+} + \overline{\zeta_1 \frac{\partial\phi_1}{\partial x}\Big|_{\substack{x_1=0^+\\z=0}}} \qquad (3.3.23)$$

The overbar stands for averaging over a short period $2\pi/\omega$ and short spatial scale $2\pi/k$. We now insist that $(\phi_{20_x} \to 0)$ as $(|x| \to \infty)$ so that

$$\int_0^{O(x_1)} \phi_{20_x} dx = \phi_{20} = O(1) \text{ and not } O(\varepsilon^{-1}) \text{ as } x = O(1/\varepsilon)$$

In the near field, however, ψ_{20x} may contain a constant term. To evaluate this term we write the governing equations for ψ_{20}. From (2.2.5b), (2.2.6b), (2.2.7b) and (3.1.3), we get:

$$\left(\frac{\partial^2}{\partial x^2} + \frac{\partial^2}{\partial z^2}\right) \psi_{20} = 0 \qquad\qquad (-h < z < 0) \qquad (3.3.24)$$

$$\frac{\partial\psi_{20}}{\partial z} = 0 \qquad\qquad (z = -h) \qquad (3.3.25)$$

$$g \frac{\partial\psi_{20}}{\partial z} = -\left[i\omega\psi_{11}^*\psi_{11x} + *\right]_x \equiv gh \, \nabla_h \cdot \tilde{U} \qquad (z = 0) \qquad (3.3.26)$$

42

where $\tilde{U} = (U,V)$ is defined by:

$$gh\tilde{U} \equiv - [i\omega\psi_{11}^* \nabla_h\psi_{11} + *]_{z=0} \qquad (3.3.27)$$

The kinematic condition on the body is obtained from (3.3.2), and is:

$$\psi_{20_x} = -(X_{11} \psi_{11_{xx}}^* + *) + X_{10t_1} \qquad \text{on } S_0^{\pm} \qquad (3.3.28)$$

Thus ψ_{20} accounts for the short scale variation of the slow potential. We must now find the last term in (3.3.22). It turns out that it is not necessary to solve explicitly for ψ_{20}. Because of Laplace Equation (3.3.24), we may apply Gauss' theorem to ψ_{20} in a control volume that is bound by the surfaces $(z = -h)$ and $(z=0)$ on bottom and top, the surfaces S_∞^+ and S_∞^- on the right and left, and the rest position of body the surface S_0 (see Figure 3.2). We shall write the flux of ψ_{20} through these surfaces in terms of U and add them up to find the value of the last term in (3.3.22).

By Gauss' theorem,

$$[\int_{S_\infty^+} - \int_{S_\infty^-} + \int_{S_0^+} - \int_{S_0^-}] \, dz \, \psi_{20x} + [\int_{-\infty}^{-B} + \int_{B}^{\infty}] \, \psi_{20z}\Big|_{z=0} \, dx$$

$$(3.3.29)$$

$$+ \int_{-B}^{B} \psi_{20z}\Big|_{z=-D} \, dx - \int_{-\infty}^{\infty} \psi_{20z}\Big|_{z=-h} \, dx = 0$$

Now, the integrals along the free surface are

$$[\int_{-\infty}^{-B} + \int_{B}^{\infty}] \, \psi_{20z} \, dz = h(\int_{-\infty}^{-B} + \int_{B}^{\infty}) \, U_x \, dx = h \, U\Big|_{-\infty}^{-B} + hU\Big|_{B}^{\infty} \qquad (z=0) \qquad (3.3.30)$$

after using (3.3.26).

43

The integrals along the vertical walls of the body are

$$\left(\int_{S_0^+} - \int_{S_0^-}\right)dz\ \psi_{20x} = -\left\{\int_{S_0^+} - \int_{S_0^-}\right\}[X_{11}\ \psi_{11xx}^* + *]dz + \left(\int_{S_0^+} - \int_{S_0^-}\right)X_{10t_1}\ dz$$

(3.3.31)

Since $\psi_{11_{xx}} = -\psi_{11_{zz}}$ we have:

$$\int_{-D}^{0}(X_{11}\ \psi_{11_{xx}}^* + *)dz = [-X_{11}\ \int_{-D}^{0}\psi_{11_{zz}}^*\ dz + *]$$

$$= (-X_{11}\ \psi_{11_z}^*(\pm B,\ 0) + *) = (-\frac{i\omega}{g}\psi_{11}^*\ \psi_{11_x}(\pm B,\ 0) + *)$$

$$= -hU(\pm B)$$

(3.3.32)

(making use of $\psi_{11_z} = \frac{\omega^2}{g}\psi_{11}$ at $(z=0)$ and $\psi_{11_x} = -i\omega X_{11}$ at $(x = \pm B)$).

When we combine (3.3.23) and (3.3.32), we get an expression for the net

flux across the body through the gap (the body is rigid and impermeable):

$$\int_{S_0^+}\psi_{20_x}\ dz - \int_{S_0^-}\psi_{20_x}\ dz = hU\ \Big|_{-B}^{-B} + D\ X_{10t_1} - D\ X_{10t_1} = hU\ \Big|_{-B}^{+B}$$

Because of Equations (3.3.24) and (3.3.30) we get:

$$\int_{S_\infty^+}\psi_{20_x}\ dz - \int_{S_\infty^-}\psi_{20_x}\ dz = hU\ \Big|_{+\infty}^{+B} - hU\ \Big|_{-\infty}^{-B} - hU\ \Big|_{-B}^{+B} = -hU\ \Big|_{-\infty}^{+\infty}$$

(3.3.34)

$U(\pm\infty)$ are given by (3.3.27):

$$gh\ U(-\infty) = -\{i\omega A_0^* f_0^*(0)\ [ikA_0 f_0(0)] + i\omega R^* A_0^* f_0^*(0)\ [-ikR\ A_0 f_0(0)]\} + *$$

$$= 2\omega k|A_0|^2(1-|R|^2)f_0^2(0)$$

(3.3.35a)

44

$$gh \ U(\infty) = - \{i\omega A_0^* \ T^* f_0(0)[ikA_0 \ T \ f_0(0)] + *\}$$

$$= 2\omega k \left|A_0\right|^2 \ \left|T\right|^2 \ f_0^2(0) \tag{3.3.35b}$$

Because the body is freely floating as far as the high frequencies are concerned, there is no energy transfer to the body; hence,

$$\left|R\right|^2 + \left|T\right|^2 = 1 \tag{3.3.36}$$

That is the energy carried away by the short waves is equal to that brought in by the incident waves. Combining (3.3.35) and (3.3.36) we get;

$$U(+\infty) = U(-\infty) \tag{3.3.37}$$

We are now ready to match (3.3.22) to (3.3.23). The quadratic terms in the two equations are equal, since ϕ_{11} is continuous in the passage between the near field and the far field. Matching the gradients of ϕ_{10} and ψ_{20}, and substituting (3.3.34) and (3.3.36) we get:

$$\phi_{10x_1} \left.\begin{array}{c} 0^+ \\ \Big| \\ 0_- \end{array}\right. dz = \int_{S_\infty^+} \psi_{20_x} \ dz - \int_{S_\infty^+} \psi_{20_x} \ dz = hU(\infty) - hU(-\infty) = 0 \tag{3.3.38}$$

From (3.1.9) and (3.3.36) we immediately obtain:

$$\phi_{10}^R + \phi_{10}^T = \phi_{10}^I \quad \text{at} \quad (x_1 = 0) \tag{3.3.39}$$

Matching the gradients of ϕ_{10} as they appear in (3.1.10), and using (3.3.38), we see that the locked wave contribution is eliminated by virtue of (3.3.39). We are left with:

$$-\phi_{10}^-(t) = \phi_{10}^+(t) \quad \text{at} \quad (x_1 = 0) \tag{3.3.40}$$

45

Using (3.3.39) we write the right hand side of (3.3.21) in terms of ϕ_{10}^{R}. The left hand size is written in terms of ϕ_{10}^{+}, making use of (3.3.40). The result is simply:

$$\phi_{10}^{+}(t_1) = \phi_{10}^{R}(t_1) \quad \text{at} \quad (x_1 = 0) \tag{3.3.41}$$

Thus, the free long wave propagating to the right is equal to the long wave locked to the reflected wave group. Substituting (3.3.40) and (3.3.41) into (3.1.8) and (3.3.20) we get:

$$\psi_{10}(t_1) = \phi_{10}(t_1) = \phi_{10}^{I}(t_1) \quad (x_1 = 0^{\pm}) \tag{3.3.42}$$

ϕ_{10} at $(x_1 = 0)$ is the same as if the body were absent! This is similar to the Froude-Krylov approximation in the linearized theory of long waves past a small body.

As an aside, when calculating the vertical slow drift force, there will again be terms due to ψ_{11}, which are formally the same as those terms for a regular wave and terms due to the slow potential, as in (3.3.8), (3.3.9). The vertical drift force due to ψ_{10} for a general hull shape, is:

$$-\rho\, \epsilon^2 \int_{\text{body surface}} \psi_{10t_1} \, dx \, dy = -\epsilon^2 \, \rho\psi_{10t_1} A_{wp} \tag{3.3.43}$$

where A_{wp} is the water plane area. As pointed out in the introduction to this chapter, when the water plane area is $O(1)$, the heave displacement is $O(\epsilon^2)$. The contribution to the heave-inducing force due to ψ_{11} and the correction due to ψ_{10} are comparable, yet the slow heave is too small to be interesting in practice. When the body is shaped as a bottle

$$A_{wp} = O(\epsilon) \tag{3.3.44}$$

46

the heave amplitude becomes $O(\varepsilon)$, yet, from (3.3.43) we see that the effect

of $\psi_{,n}$ on the vertical force is $O(\varepsilon^2)$, resulting in a negligible, $O(\varepsilon^2)$,

effect on the heaving displacement. In contrast to the vertical motion,

there are cases where ψ_{10} may play an important role in the sway motion.

This happens when ψ_{10} varies appreciably across the body surface, as discus-

sed in the following subsections.

Numerical results will be presented later.

3.3.2 The Small Gap Case

When the gap between the body and the seabed is narrow, the analysis of

Section 3.3.1 does not apply, and the slow potential affects the slow sway.

This can happen when a ship is moored in very shallow water, which is only

slightly deeper than its draught and is encountering beam seas. We let:

$$H \equiv h - D = O(\varepsilon h) \tag{3.3.45}$$

First, let us show that the heave and roll amplitudes, both fast and slow,

are $O(\varepsilon^2)$ and can be neglected. The body is forced by the incident and

diffracted waves, and is restrained by buoyancy and the radiated wave force.

For the fast motion, the forcing is $O(\varepsilon)$:

$$P = -\rho \, \varepsilon \Phi_{11_t} = O(\varepsilon) \tag{3.3.46}$$

and it is $O(\varepsilon^2)$ for the slow motion:

$$-\rho \frac{d}{dt} \, \varepsilon \Phi_{10} = -\rho \, \varepsilon^2 \, \Phi_{10t_1} = O(\varepsilon^2) \tag{3.3.47}$$

The radiated potential for the fast flow acts as an added mass; this added

mass is usually $O(1)$. In the present case, however, the narrowness of the

gap makes the heave added mass and roll added moment of inertia much larger
- $O(\varepsilon^{-1})$. Their dominant parts are due to the flow inside the gap. This
flow is primarily horizontal, since the gap is narrow.

Denote the fast heave and roll displacement by Z and θ, the associated
potentials in the gap by $\phi^{(Z)}$ and $\phi^{(\theta)}$, and the related added mass and moment
of inertia by μ_Z and I_θ, respectively.

The equations of continuity for $\phi^{(2)}$, $\phi^{(\theta)}$ are:

$$-H \phi_{xx}^{(Z)} + (-i\omega) Z = 0 \qquad (3.3.48)$$

$$-H\phi_{xx}^{(\theta)} + (-i\omega) \theta x = 0 \qquad (3.3.49)$$

Since Z is constant in x and θx is linear in x.

$\phi^{(Z)}$ is symmetric and $\phi^{(\theta)}$ is antisymmetric, so that;

$$\phi^{(Z)} = - i\omega \frac{Z}{H} \frac{x}{2}^2 \qquad (3.3.50)$$

$$\phi^{(\theta)} = - i \omega \frac{\theta}{H} \frac{x^3}{6} \qquad (3.3.51)$$

from which we find μ_Z and I_θ to be:

$$\mu_Z = - \frac{\rho}{\omega^2 Z} \int_{-B}^{B} \phi_t^{(Z)} dx = \rho \frac{B^3}{3H} = O(\varepsilon^{-1}) \qquad (3.3.52)$$

$$I_\theta = - \frac{\rho}{\omega^2 \theta} \int_{-B}^{B} \phi_x^{(\theta)} dx = \rho \frac{B^5}{15H} = O(\varepsilon^{-1}) \qquad (3.3.53)$$

Since $\omega = O(1)$, and the forcing is $O(\varepsilon)$, the fast heave and roll displacement
are $O(\varepsilon/\varepsilon^{-1}) = O(\varepsilon^2)$, and may be neglected.

For the slow heave and roll, the dominant terms of the restoring force
and moment are due to buoyancy. The inertia term being $O(\varepsilon^3)$. For heave the
buoyancy force is

$$-2B\rho g Z = O(Z) \qquad\qquad (3.3.54)$$

while the restoring moment for roll is

$$-g \, M \, m_c \, \theta = O(\theta) \qquad\qquad (3.3.55)$$

where m_c the metacentric height is assumed to be $O(B)$. Since the forcing for slow motion is $O(\epsilon^2)$, we find that the slow heave and roll, too, are $O(\epsilon^2)$. Therefore, the only first order slow motion present is sway.

Because of the narrow gap under the body, strong blockage occurs. The slow current under the body becomes large ($O(\epsilon)$) and there is a large pressure gradient due to the potential difference in ψ_{10} between the two ends of the gap. Apart from the difference in ψ_{10} between the two sides of the gap, the flow in the gap has only an $O(\epsilon^2)$ effect on mass flux which does not cause any additional effect on ψ_{10}.

In order to determine ψ_{10}, we define ψ_0 to be the sum of $\epsilon\psi_{10}$ and $\epsilon\overline{\psi_{20}}$:

$$\psi_0 \equiv \epsilon\psi_{10} + \epsilon^2 \overline{\psi_{20}} \qquad\qquad (3.3.56)$$

ψ_0 is the long scale slow potential in the near field. The slow potential has a component with short length scale: $2\pi/2k$, and a component with a long scale: $O(\epsilon^{-1} \, 2\pi/2k)$. The kinematic boundary condition on the body, (3.3.2), combines both long scale and short scale zeroth harmonic potential. The long spatial scale component can be separated by integrating (3.3.2) along $S_0^{\pm}$, keeping only the propagating modes contribution, and not that of the evanescent modes that give rise to short scale ψ_{20}. The integral of the last term on the left hand side of (3.3.2) was evaluated in (3.3.32). The long scale

part associated with the propagating modes is given by $U(\pm\infty)$ at the far field, which was given in (3.3.35) and (3.3.37). We note that $U(\pm\infty)$ is just Stokes' drift.

We are now ready to write the resulting kinematic boundary condition on the body. Separating the long scale component of (3.3.32) we get

$$\int_{-D}^{0} \overline{(\tilde{X}_{11} \psi_{11xx}^{*} + *)}dz = -h\overline{U(\pm B)} = -hU(\pm\infty) \qquad \text{on} \qquad S_0^{\pm}$$

When substituting this result in place of the last term of (3.3.1) averaged over S_0 and recalling that the difference between h and D is $O(\epsilon)$, we get the boundary condition for ψ_0 defined in (3.3.56), in the form:

$$\psi_{0_x} = X_{10t_1} - U(\pm\infty) \qquad \text{on} \qquad S_0^{\pm} \qquad (3.3.57)$$

ψ_0 also satisfies the rigid lid boundary conditions:

$$\psi_{0_z} = 0 \qquad (z = 0, -h) \quad \text{and on} \quad \overline{b}_0 \qquad (3.3.58)$$

Recall that both ψ_{10} and ψ_{20} satisfy (3.3.24). ψ_{20z} is equal to zero on the free surface while the short scale part accounts for the inhomogeneous term in (3.3.26). With (3.3.57) and (3.3.58) ψ_0 is the potential for a steady flow ϵv past a body moving at a steady velocity $X_{10t_1} - U(\pm\infty)$, with a parametric dependence on t_1.

It is known for a stationary body in long waves that the outer approximation of the near field in terms of $(x" \equiv x - X_0)$ is

$$\psi_0 \sim Q(t_1) + \epsilon(v - X_{10t_1} + U)x" \pm \epsilon(v - X_{10t_1} + U)c$$

where c is the blockage coefficient. By a Gallilean transformation, we go to the stationary frame of reference in which the body is moving at the velocity $X_{10t_1} - U$. The outer approximation of the near field potential must then be

$$\psi_0 \sim Q(t_1) + [v - X_{10t_1} + U](\pm \varepsilon c) + v\varepsilon x \qquad (x \to \pm\infty) \qquad (3.3.59)$$

where Q is an unknown integration constant and εv is the unknown current, ψ_{0x}, at $x \to \pm\infty$. c is the blockage coefficient which is known to be a large quantity

$$c = \frac{Bh}{H} + 0(\log\varepsilon) = 0(\varepsilon^{-1}) \qquad (3.3.60)$$

(cf. Flagg and Newman (1971)).

The outer expansion of the near field, (3.3.59), has to be matched to the inner expansion of the far field, (3.1.10). This matching gives:

$$Q(t_1) + [v - X_{10t_1} + U] \, \varepsilon c = [\phi_{10}^T + \phi_{10}^+]_{x_1 = 0}$$

$$Q(t_1) + [v - X_{10t_1} + U] \, \varepsilon c = [\phi_{10}^I + \phi_{10}^R + \phi_{10}^-]_{x_1 = 0}$$

$$(3.3.61)$$

$$v = [-\frac{\phi_{10}^I}{C_g} + \frac{\phi_{10}^R}{C_g} + \frac{\phi_{10}^-}{\sqrt{gh}}]_{t_1}$$

$$v = [-\frac{\phi_{10}^T}{C_g} - \frac{\phi_{10}^+}{\sqrt{gh}}]_{t_1}$$

Using (3.3.37) and integrating the last two equations in (3.3.61) with respect to t_1, we eliminate Q and v with the results:

$$\phi_{10}^{+} = -\phi_{10}^{-} \qquad (x_1 = 0) \qquad\qquad (3.3.62)$$

and

$$\phi_{10}^{T} + \phi_{10}^{+} - (\phi_{10}^{I} + \phi_{10}^{R} + \phi_{10}^{-}) = 2c_1\{[-\frac{\phi_{10}^{T}}{C_g} - \frac{\phi_{10}^{+}}{\sqrt{gh}}]_{t_1} - X_{10t_1} + U\} \qquad (3.3.63)$$

where $c_1 \equiv \epsilon c$.

The large blocking by the narrow gap, causes a jump in $\phi_{10} = \psi_{10}$ between the two sides of the block given by (3.3.63), although the gradients of the slow potential, on either side of the body, are $O(\epsilon^2)$. This jump is important to the dynamic boundary condition on the body, (3.3.14), which can be written in terms of the far field potentials. Since ψ_{10} does not change appreciably on either side of the body. This gives:

$$K X_{10} = \rho h[\phi_{10}^{+} + \phi_{10}^{T} - (\phi_{10}^{I} + \phi_{10}^{R} + \phi_{10}^{-})]_{t_1} + \rho g |A|^2 |R|^2 \frac{C_g}{C} \qquad (x_1 = 0)$$
$$(3.3.64)$$

We now wish to eliminate $\phi_{10}^{\pm}$ between (3.3.62) and (3.3.63). From (3.3.62) and (3.3.64) we get after using (3.3.37):

$$\pm 2\phi_{10t_1}^{\pm} = \frac{KX_{10}}{\rho h} + 2\phi_{10t_1}^{R} - \frac{g}{h} |A|^2 |R|^2 \frac{C_g}{C} \qquad (3.3.65)$$

Differentiating (3.3.63) with respect to t_1 we can substitute its right hand side in the left hand side of (3.3.64) and finally substitute for $\phi_{10t_1}^{+}$ using (3.3.65). This yields:

$$X_{10t_1t_1} + \frac{K}{2\rho h\sqrt{gh}} X_{10t_1} + \frac{K}{2\rho h c_1} X_{10}$$

$$(3.3.66)$$

$$= [-(\frac{C_g}{\sqrt{gh}} |R|^2 + 1 - |R|^2) \frac{C_g}{gh - C_g^2} \frac{g}{2h} S \frac{\partial}{\partial t_1} + \frac{C_g}{C} |R|^2 \frac{g}{2h c_1}] |A|^2$$

where

$$S \equiv \frac{2C_g}{C} - \frac{1}{2} \tag{3.3.67}$$

is a factor appearing in the radiation stress. Equations (3.1.6), (3.1.7), and (3.1.9) have been used (details are given in Appendix C). From (3.3.65) we get the free surface elevation associated with $\phi_{10}^{\pm}$, through the Bernoulli equation

$$\zeta_{20}^{\pm} = -g \; \phi_{10t_1}^{\pm} \tag{3.3.68}$$

In the limit as $H \to 0$, $c_1 \to \infty$, the last term on both sides of (3.3.66) vanish and the resulting equation may be integrated with respect to t_1, to give:

$$X_{10t_1} + \frac{K}{2\rho h\sqrt{gh}} X_{10} = - \left(\frac{C_g}{\sqrt{gh}} \left|R^2\right| + 1 - \left|R\right|^2\right) \frac{C_g}{gh - C_g^2} \frac{g}{2h} S \left|A\right|^2 \tag{3.3.69}$$

Equation (3.3.69) is identical to the equation for a sliding block (Agnon and Mei 1985) to be discussed in Section 3.3.3. At the other limit, as the gap becomes large, $H = O(1)$, $c_1 = O(\epsilon)$ and the last term on each side of (3.3.66) becomes the dominant term, we get:

$$K \; X_{10} = \rho g \; \frac{C_g}{C} \left|R\right|^2 \left|A\right|^2 \tag{3.3.70}$$

Equation (3.3.70) is the same as the result (3.3.19) for a wide gap. Therefore, (3.3.66) may be regarded as practically valid for all gap widths.

We shall now solve (3.3.66) explicitly to study different wave envelope forms and their effect on the slow sway, as listed below:

a) A Steady Sinusoidal Envelope

b) A Sudden Start of a Sinusoidal Envelope

c) A Gradual Start of a Regular Wave

d) A Sinusoidal Wave Packet

a) A Steady Sinusoidal Envelope

Let the incident wave amplitude be:

$$A = a \sin \Omega t_1 \qquad \text{at} \qquad (x_1 = 0) \tag{3.3.71}$$

The solution to (3.3.66) is then:

$$X_{10} = \text{Re}[X'_{10} e^{-2i\Omega t_1} + X''_{10}] \tag{3.3.72}$$

where

$$X'_{10} \equiv D / (-4\Omega^2 - \frac{2i\Omega K}{2\rho h\sqrt{gh}} + \frac{K}{2\rho h c_1})/2 \tag{3.3.73}$$

$$X''_{10} \equiv \frac{1}{2} \frac{g\rho}{K} \frac{C_g}{C} a^2 \left| R \right|^2 \tag{3.3.74}$$

and

$$D \equiv -2i\Omega \left(\frac{C_g}{\sqrt{gh}} \left| R \right|^2 + 1 - \left| R \right|^2 \right) \frac{C_g}{gh - C_g^2} \frac{g}{2h} S a^2 + \frac{C_g}{C} \frac{g}{2h c_1} \left| R \right|^2 a^2 \tag{3.3.75}$$

In Figure 3.3, $\underline{X}'_{10} = h \left| X'_{10} \right| / a^2$, the normalized slow sway amplitude is plotted versus $\underline{\Omega} \equiv \Omega/\omega$, the wave modulation ratio, for three values of K. The resonance peak occurs near $2\Omega/\omega = \sqrt{K/2\rho h c_1}$. $2\rho h c_1$ may be regarded as the apparent mass. X''_{10} will be discussed in Section 3.3.3 and plotted in Figure 3.5.

In all the computations presented in this section $kh = 1$, $\underline{M} \equiv M/\rho h^2 = 1$ and $\underline{c}_1 \equiv c_1/h = 1$. The nomalized elastic constant is $\underline{K} \equiv K_0/(\epsilon \rho g h)$. A corresponding choice of physical parameters would be, depth $h = 10$ m deep, the vessel width $B = 10$ m, the wavelength $\lambda = 2\pi \cdot 10 \simeq 63$ m which corresponds to a wave period of 7.2 sec.
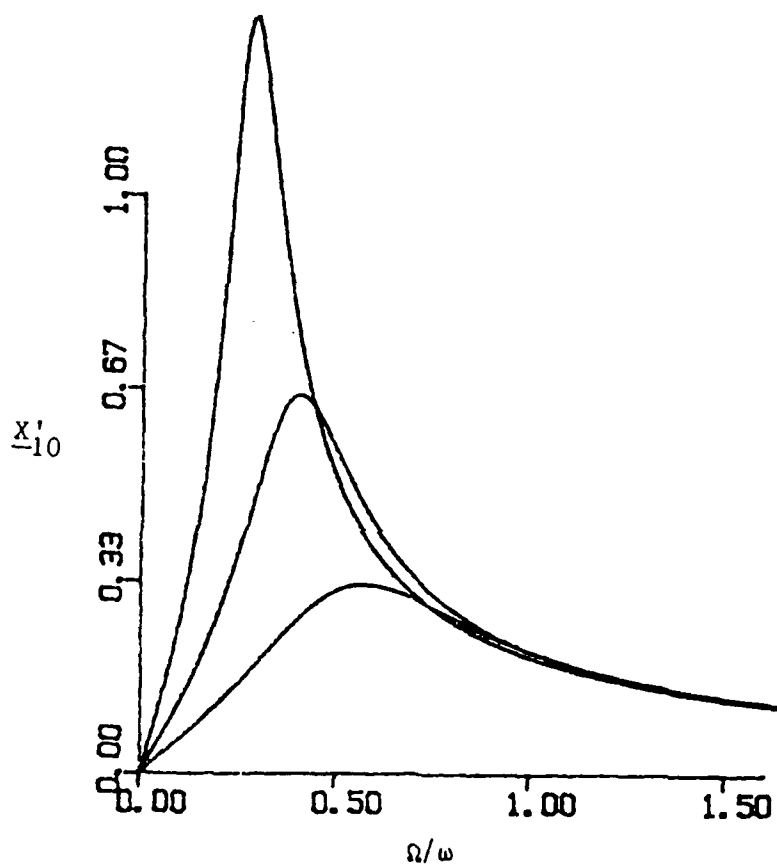
Figure 3.3 Normalized Amplitudes of the Slow Sway Displacement

$\underline{X}'_{10} = h\left|X'_{10}\right|/a^2$ for a Sinosoidal Envelope;

$\dfrac{K}{\rho gh} = 0.5, 1., 2., kh = 1, c_1/h = 1$ (Narrow Gap).

The gap width is $5\varepsilon/1 = 0.5$ m if ε is 0.1, and the spring constants are $0.1(0.5, 1, 2) \cdot 10 \cdot 10 \cdot 1 = (5, 10, 20) \, 10^3$ Newton/m per meter length of the cylinder. Each unit of the abscissa (Ω/ω) translates to 72 sec. period of the modulation envelope and each unit of the ordinate $\underline{X}'_{10}$ translates to slow sway amplitude of ~ 1 m for incident wave of 3 m amplitudes (or 6 m waveheight) and is proportional to the square of the waveheight.

In nondimensional form, Equations (3.3.73) through (3.3.75) become:

$$\underline{X}'_{10} = \underline{D}/(-4\underline{\Omega}^2 \, \underline{\omega}^2 - 2i\underline{\Omega} \, \underline{\omega} \, \underline{K} + \frac{\underline{K}}{2\underline{c}_1})/2 \qquad (3.3.73')$$

$$\underline{X}''_{10} = \frac{1}{2\underline{K}} \frac{\underline{C}_g}{\underline{C}} \left|R\right|^2 \qquad (3.3.74')$$

$$\underline{D} = -i\underline{\Omega} \, \underline{\omega} \, (\underline{C}_g \left|R\right|^2 + 1 - \left|R\right|^2) \frac{\underline{C}_g}{1-\underline{C}_g^2} \frac{\left|R\right|^2}{\underline{c}_1} \qquad (3.3.75')$$

where

$$\underline{C}_g \equiv C_g/\sqrt{gh} \, , \qquad \underline{C} \equiv C/\sqrt{gh}$$

and

$$\underline{\omega} \equiv \omega\sqrt{h/g}$$

b) A Sudden Start of a Sinusoidal Envelope

Let

$$A = H(t_1) \, a \, \sin \Omega t_1 \qquad (3.3.76)$$

where H is the Heaviside step function. The solutions of the homogeneous equation corresponding to (3.3.66) are:

$$X_{10} \propto e^{\alpha_1 t_1}, \; e^{\alpha_2 t_1}$$

with

$$\alpha_{1,2} = \frac{-K}{4\rho h\sqrt{gh}} \pm [\frac{K^2}{16\rho^2 h^2 gh} - \frac{K}{2\rho h c_1}]^{1/2} \qquad (3.3.77)$$

and we assume that the square root does not vanish so that $\alpha_1 \neq \alpha_2$ (when = $\alpha_1 = \alpha_2$ the solutions are $e^{\alpha_1 t_1}$ and $t_1 e^{\alpha_1 t_1}$, the results are not qualitatively different in any significant manner). In nondimensional form, Equation (3.3.77) becomes:

$$\underline{\alpha}_{1,2} = [-\underline{K} \pm (\underline{K}^2 - \frac{8\underline{K}}{\underline{c}_1})^{1/2}]/4$$

With $X_{10}(0) = X_{10t_1}(0) = 0$ we get:

$$X_{10} = Re\{X_{10}''[1 - \frac{\alpha_2 e^{\alpha_1 t_1} - \alpha_1 e^{\alpha_2 t_1}}{(\alpha_2 - \alpha_1)}]$$

$$\qquad (3.3.78)$$

$$+ X_{10}'' [e^{-2i\Omega t_1} - \frac{(\alpha_2 + 2i\Omega) e^{\alpha_1 t_1} - (\alpha_1 + 2i\Omega) e^{\alpha_2 t_1}}{\alpha_2 - \alpha_1}]\}$$

where X_{10}' and X_{10}'' have been defined in (3.3.73) and (3.3.74)

c) A Gradual Start of a Regular Wave Train

Let

$$A = a [H(t_1) H(\frac{\pi}{2\Omega} - t_1) \sin \Omega t_1 + H(t_1 - \frac{\pi}{2\Omega})] \qquad (3.3.79)$$

Then X_{10} is given by (3.3.78) for $0 \leq t_1 \leq \pi/2\Omega$ and

$$X_{10} = Re \{2X_{10}'' [1 - \frac{\alpha_2 e^{\alpha_1(t_1 - \pi/2\Omega)} - \alpha_1 e^{\alpha_2(t_1 - \pi/2\Omega)}}{\alpha_2 - \alpha_1}]$$

$$+ [\alpha_2 \, X_{10} \, (\pi/2\Omega) - X_{10t_1} \, (\pi/2\Omega)] \, \frac{e^{\alpha_1(t_1-\pi/2\Omega)}}{\alpha_2 - \alpha_1} \qquad (3.3.80)$$

$$- [\alpha_1 \, X_{10} \, (\pi/2\Omega) - X_{10t_1} \, (\pi/2\Omega)] \, \frac{e^{\alpha_2(t_1-\pi/2\Omega)}}{\alpha_2 - \alpha_1}\} \; (\tfrac{\pi}{\Omega} < t_1)$$

as $(t_1 \uparrow \infty)$ X_{10} tends to $2X_{10}''$ which is the steady drift force and is also the

value given by (3.3.19) and (3.3.70).

d)   A Sinusoidal Wave Packet

Let

$$A = H(t_1) \, H(\tfrac{\pi}{\Omega} - t_1) \, a \sin \Omega \, t_1 \qquad (3.3.81)$$

then X_{10} is given by (2.92) for $0 \leq t_1 \leq \pi/\Omega$ and

$$X_{10} = \mathrm{Re}\{[\alpha_2 \, X_{10} \, (\pi/\Omega) - X_{10t_1} \, (\pi/\Omega)] \, \frac{e^{\alpha_1(t_1-\pi/\Omega)}}{\alpha_2 - \alpha_1}$$

$$\qquad (3.3.82)$$

$$- [\alpha_1 \, X_{10} \, (\pi/\Omega) - X_{10t_1}(\pi/\Omega)] \, \frac{e^{\alpha_2(t_1-\pi/\Omega)}}{\alpha_2 - \alpha_1}\} \qquad (\tfrac{\pi}{\Omega} \leq t_1)$$

In nondimensional form, Equations (3.3.78), (3.3.80), and (3.3.82) are modi-

fied by changing $(\alpha_{1,2})$ to $(\underline{\alpha}_{1,2})$; Ω to $\underline{\omega} \, \underline{\Omega}$, and X_{10}' and X_{10}'' to $\underline{X}_{10}'$ and $\underline{X}_{10}''$.

In Figure 3.4, a typical example of the displacement X_{10} from (3.3.78,

3.3.80, and 3.3.82) is plotted versus nondimensional slow time, Ωt_1. There

is a considerable overshooting before a steady or a quasi-steady state is

reached. For the gradual start of a regular wavetrain (Case C), the over-

shoot can be an order of magnitude larger than the steady state value, where

Φ_{10} has no effect. This transient drift force also alternates direction, and
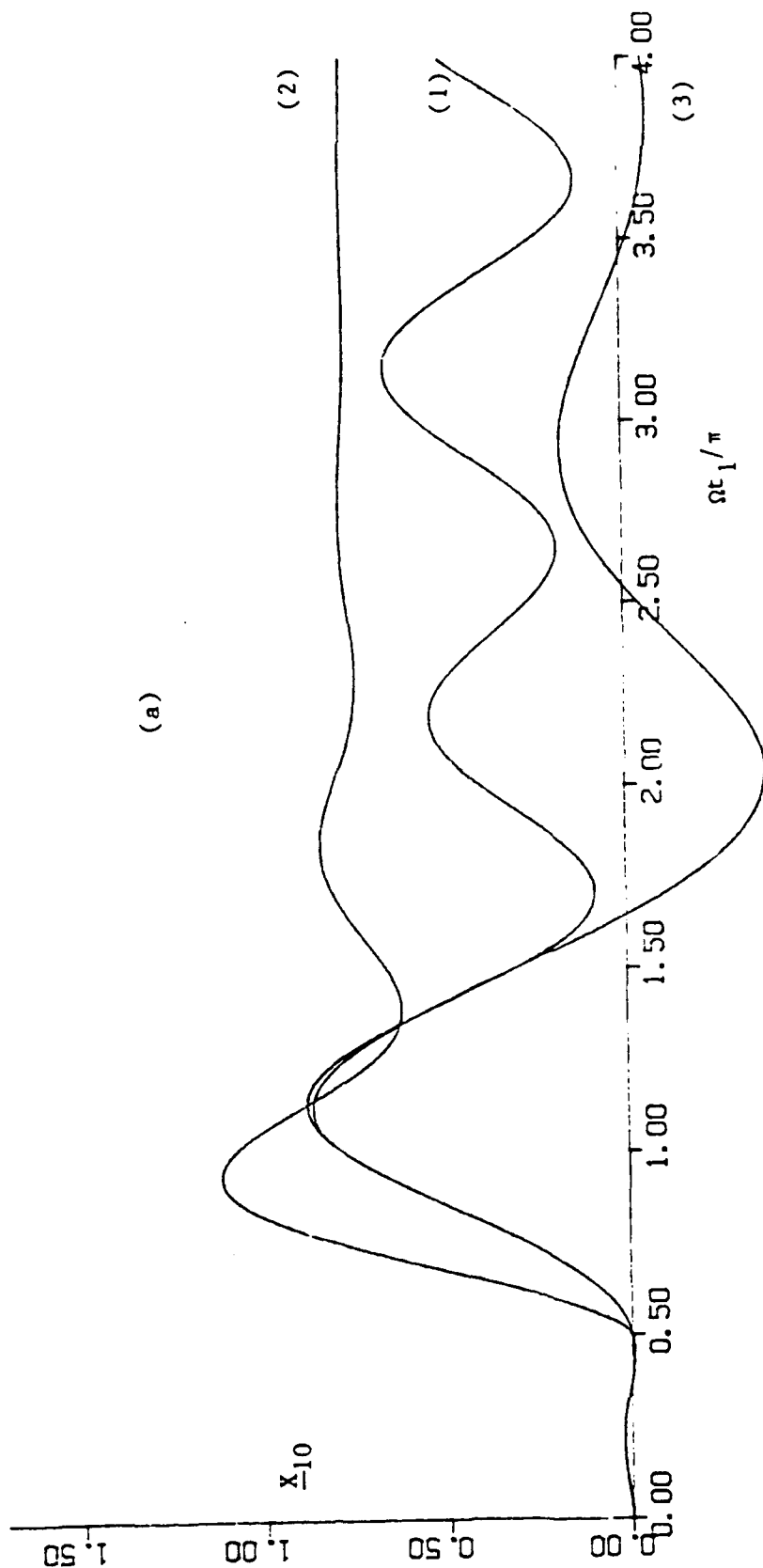
58

(a)

Figure 3.4   Transient Slow Displacement for a Block With a Narrow Gap.
(1) A Sinosoidal Envelope Starting From Rest; (2) A Uniform
Envelope Starting From Rest; (3) A Pulse Envelope.

$C_1 = 1$, $kh = 1$, $\Omega/\omega = 1$.

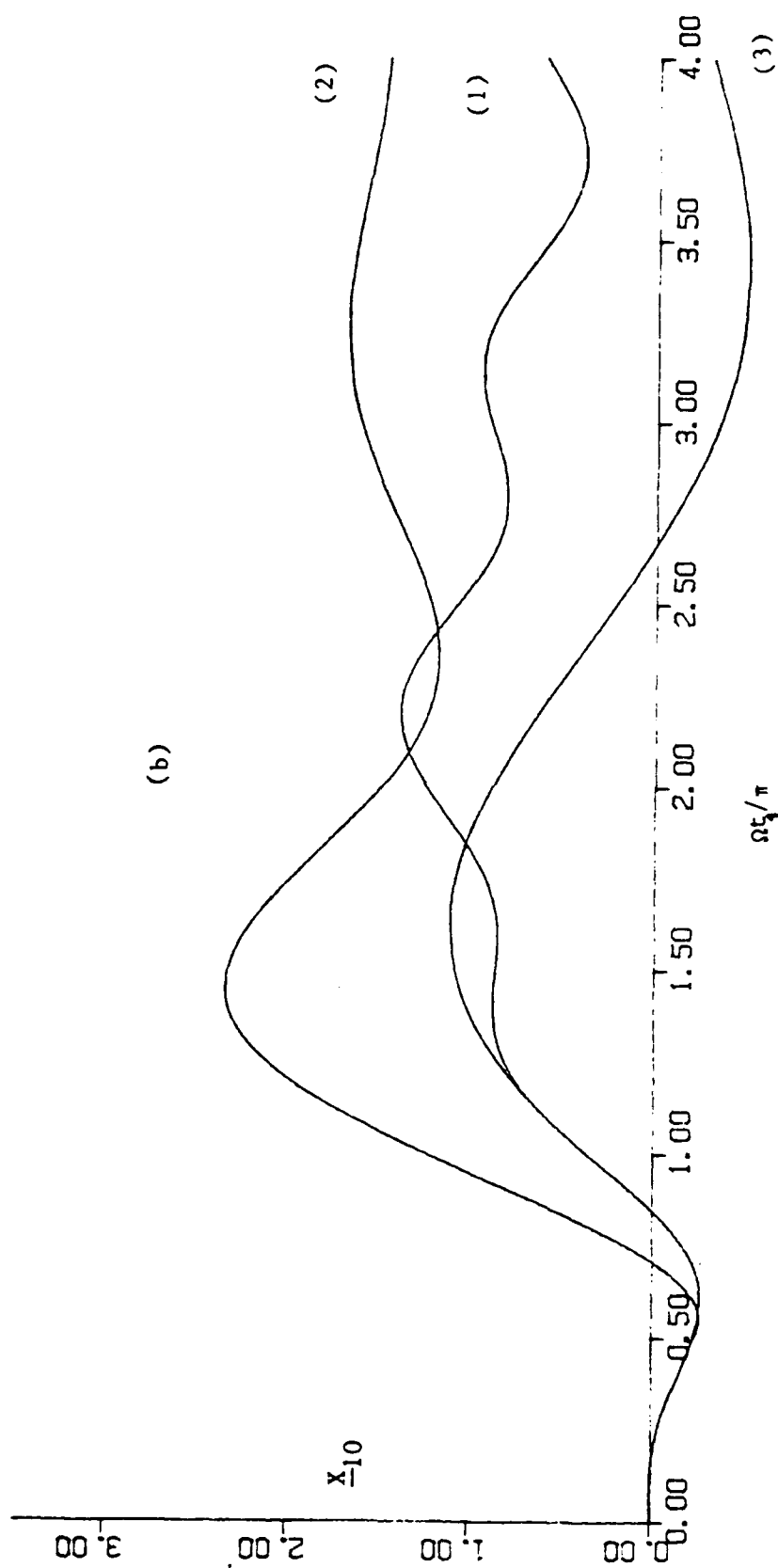In Plot a) $K/\rho gh = 1$ and in Plot b) $K/\rho gh = 0.5$.

X_{10}

$\Omega t_g / \pi$

(b)

(1)

(2)

(3)

Figure 3.4

60

becomes large when directed both to the lee of the body and in the opposite direction. The modulation ratio is 1 ($\Omega = \epsilon\omega$) so that the envelope period is 72 sec for the parameters given in Case a. The normalized elasticity constant is 1.

3.3.3 The Case of No Gap

Finally we examine the case of complete blocking. There is no connection between the two sides of the body, which slides on the seabed. This case was studied by Agnon & Mei (1985a). The dynamic boundary condition, (3.3.57), can now be directly matched to (3.1.10), the far field inner expansion, since there is no flow underneath the body, and the gradient of ψ_{10} is uniform throughout the near field. The kinematic boundary condition is now:

$$X_{10t_1} = \phi_{10x_1} \qquad (x_1 = 0^\pm) \qquad (3.3.83)$$

Combining (3.1.10), (3.3.64), and (3.3.83) we can eliminate ϕ_{10} in the same way that (3.3.66) is obtained in Appendix B to get:

$$X_{10t_1} + \frac{K}{2\rho h \sqrt{gh}} X_{10} + [\frac{C_g}{\sqrt{gh}} |R|^2 + 1 - |R|^2] \frac{gC_g}{2h} \frac{S|A|^2}{gh - C_g^2} = 0 \qquad (3.3.84)$$

which is (4.31) of Agnon & Mei (1985a) where the notation for S is different. This is the differential equation for the slow sway of the body. The first term signifies the effect of radiation damping, the second term the effect of mooring, and the third term, the wave momentum flux. Because of the slow motion, inertia is ineffective.

The general solution to (3.3.84) is easily found:

$$X_{10}(t_1) = - [\frac{C_g}{\sqrt{gh}} R^2 + (1-R^2)] \frac{gC_g S}{2h(gh-C_g^2)} e^{-\beta t_1} \int_0^{t_1} |A|^2 (-C_g \tau) e^{\beta \tau} \, d\tau \qquad (3.3.85)$$

where

$$\beta \equiv \frac{K}{2\rho h\sqrt{gh}} \qquad (3.3.86)$$

We can see immediately that if the mooring stiffness K increases, it takes less time for the slow motion to reach equilibrium under persistent forcing, or to decay when forcing is removed. Let us specify the incident envelope to be such that

$$A = \begin{cases} a \sin \Omega t_1 & (0 < t_1 < T_1) \\ 0 \text{ otherwise} \end{cases} \qquad (3.3.87)$$

where a is the maximum amplitude of the incident wave potential; then the slow displacement is

$$(3.3.88)$$

$$X_{10}(t_1) = \begin{cases} -\hat{X}_{10}\{1 - e^{-\beta t_1} - \text{Re}[(1 - \frac{2i\Omega}{\beta})^{-1}(e^{-2i\Omega t_1} - e^{-\beta t_1})]\} & (0 < t_1 \leq T_1) \\ X_{10}(T_1) e^{-\beta(t_1 - T_1)} & (t_1 > T_1) \end{cases} \qquad (3.3.89)$$

where

$$\hat{X}_{10} = (\frac{C_g}{\sqrt{gh}} R^2 + 1 - R^2) \frac{\sqrt{gh}}{2K} \frac{C_g}{gh - C_g^2} S \frac{\rho g a^2}{gh - C_g^2} > 0 \qquad (3.3.90)$$

Note that $\hat{X}_{10}$ is independent of Ω, is inversely proportional to the spring constant K, and is positive.

Let us consider three sub-cases:

a)   A Sinusoidal Envelope:

If we let $T_1 \uparrow \infty$ in Equation (3.3.87), then the incident wave envelope is sinusoidal for all $t_1 < \infty$. The limit for quasi-steady state $\Omega t_1 \gg 1$ is

$$X_{10}(t_1) = -\hat{X}_{10} + \hat{X}_{10}[1 + (\frac{2\Omega}{\beta})^2]^{-1/2} \cos 2\Omega(t_1 - \tau) \qquad \Omega t_1 \to \infty \qquad (3.3.91)$$

where τ is the phase angle:

$$\tan \tau \equiv \frac{2\Omega}{\beta} \qquad (3.3.92)$$

The ratio β/Ω measures the importance of mooring relative to radiation damping. Thus X_{10} oscillates about the mean $-\hat{X}_{10}$. In Figure 3.5, the dimensionless $\underline{\hat{X}}_{10} = \hat{X}_{10} h/a^2$ is plotted for three values of $\underline{M}$. For comparison the first-order high-frequency displacement X_{11} is also shown. Relative to the mean, the amplitude of the oscillatory part is

$$\hat{X}_{10} [1 + (\frac{2\Omega}{\beta})^2]^{-1/2} \qquad (3.3.93)$$

which decreases as β/Ω increases. Thus for tighter mooring, the body wanders less. A typical history of $X_{10}(t)$, normalized by a^2/h, is shown by curve a in Figure 3.6. Throughout Figure 3.6 we have chosen the modulation frequency to be ε times the short-wave frequency, namely $\Omega = \omega$. We have also set $\underline{M} = 1$ and $K_0 = \varepsilon \rho g h$.

The reflected $\bar{\zeta}_{20}^R$ and transmitted $\bar{\zeta}_{20}^T$ travel outwards at the group velocity. Their amplitudes depend only on R and are plotted in Figure 3.7a for three different values of M. The radiated long waves which travel at the speed $\sqrt{gh}$ depend further on K through X_{10t_1}; their amplitudes are equal by virtue of Equation (3.3.65) and are plotted in Figure 3.7b only for $K = \rho g h$.

b)   A Constant Envelope:

If we let the incoming wave have the form

$$A = \begin{cases} a \sin \Omega t_1 & (0 < t_1 < \pi/2\Omega) \\ a & (\pi/2\Omega < t_1) \end{cases} \qquad (3.3.94)$$

63

Figure 3.5 Normalized Displacement Amplitudes of the Low- and High-Frequency Body Motion for $\underline{M} = 0.5$, 1, and 2.

$$\underline{X}_{11} \equiv \left| \max X_{11}/a \right|, \quad \hat{\underline{X}}_{10} = \hat{X}_{10}h/a^2$$

For Contrast, $\underline{X}''_{10} = X''_{10}h/a^2$ is Also Shown

The Elastic Mooring Constant is $K/\epsilon\rho\sqrt{gh} = 1$.

64
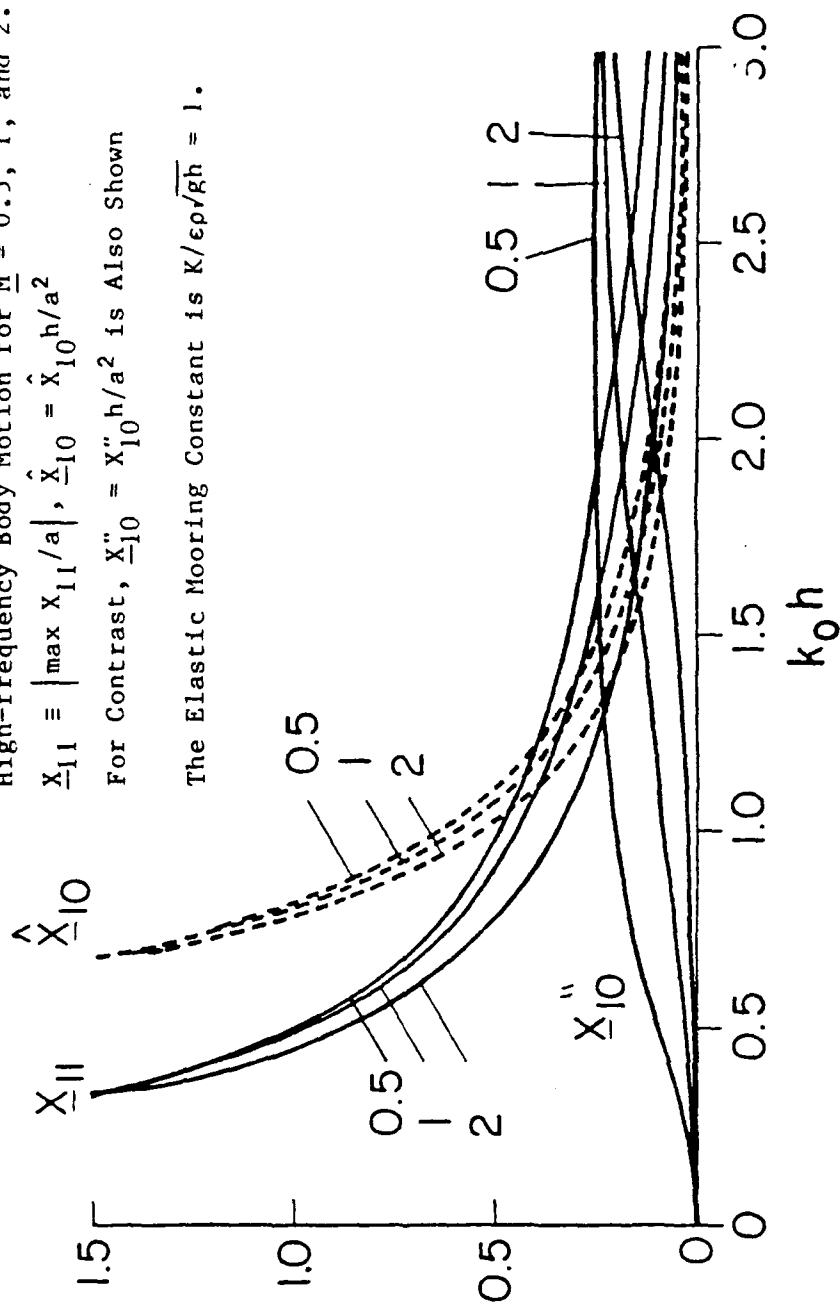
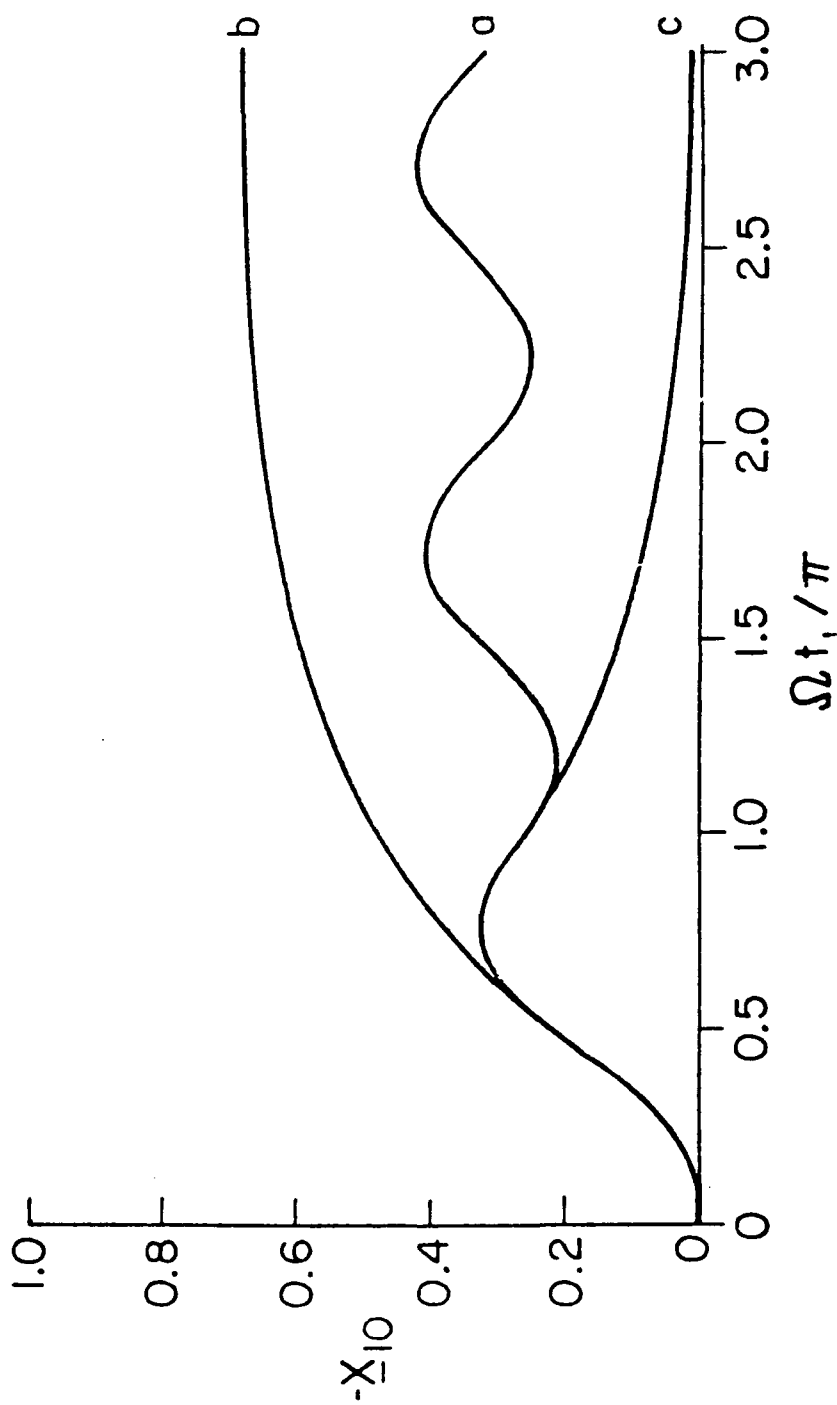Figure 3.6   Sliding Block: Slow Displacements Due to Various Transient
Incident Envelopes: a) Sinusoidal Envelope Started From Zero,
b) Uniform Envelope Started From Zero, c) Pulse Envelope.
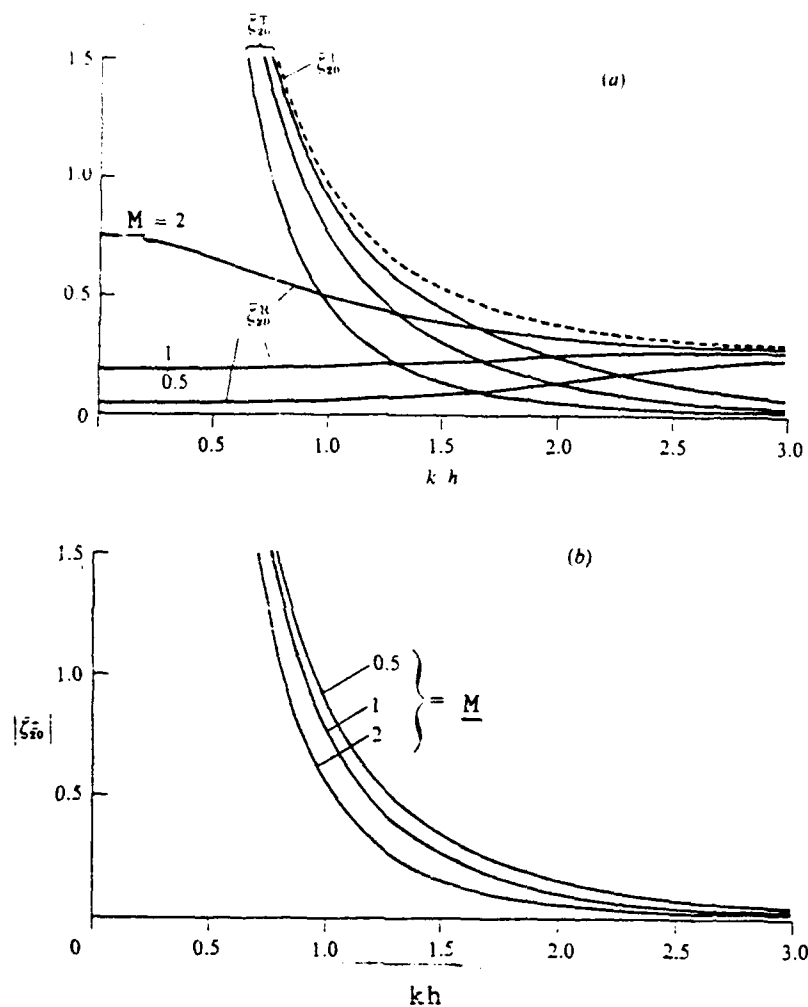
Figure 3.7 Sliding Block: (a) Normalized Amplitudes of the Long Waves Accompanying the Incident Group ζ_{20}^{T}, the Reflected Group ζ_{20}^{R} and the Transmitted Group ζ_{20}^{T}. (b) Normalized Amplitude of the Radiated Long Waves Travelling at the Speed $\sqrt{gh}$ to the Right ζ_{20}^{+} and to the Left ζ_{20}^{-}. Normalization Length is a^2/h, $\underline{K} = 1$.

we get in Equation (3.3.84) a constant forcing term when $t_1 > \pi/2\Omega$ and the solution tends asymptotically to $X_{10} = -2\hat{X}_{10}$ as follows:

$$X_{10} = -2\hat{X}_{10} + [2\hat{X}_{10} + X_{10}(\pi/2\Omega)]e^{-\beta(t_1 - \pi/2\Omega)} \tag{3.3.95}$$

For $0 < t_1 < \pi/2\Omega$ the solution $X_{10}(t_1)$ is still given by Equation (3.3.89). Note that X_{10} is negative, implying that the drift displacement is <u>opposite</u> to the direction of the incident waves.

When a cylinder is floating or immersed so that fluid is allowed to pass from one side to the other, the drift force due to normally and steadily incident waves is known to be

$$\rho g a^2 |R|^2 C_g/C \tag{3.3.96}$$

and is in the <u>same</u> direction as the incident waves (see, e.g., Longuet-Higgins, 1977). The corresponding displacement is just

$$2X_{10}'' = \rho g\ a^2 |R^2|\ C_g/CK \tag{3.3.97}$$

It is different both in sign and in magnitude (see Figure 3.5) from $-2\hat{X}_{10}$, the steady-state limit of X_{10} (see (3.3.95)). Does this contradict our result?

Observe first that Equation (3.3.97) can be gotten from Equation (3.3.64) if one sets

$$\Delta\phi_{10t_1} = 0 \tag{3.3.98}$$

In the long-time limit of a uniform wavetrain, the long wave described by ϕ_{10} becomes a steady current. For a two-dimensional body that does not

prohibit steady flow of water from one side to the other, Equation (3.3.98)

holds when viscous effects are ignored. Now, in the present example,

$\Delta\phi_{10t_1}$ does not vanish; indeed, it also contributes a new part in the jump

of mean sea level across the body, since

$$g\Delta\bar{\zeta}_{20} = -\Delta\phi_{10t_1} - \Delta[\overline{|\phi_{11x}|^2} + \overline{|\phi_{11z}|^2} - \overline{\sigma(\phi_{11}\overset{*}{\phi}_{11x} + *)}] \qquad (3.3.99)$$

The second part $\Delta[\ ]$ above can be calculated

$$\frac{1}{2}\frac{g}{h}a^2\ |R^2|\ (\frac{C_g}{C} - \frac{1}{2}) \qquad (3.3.100)$$

which is precisely the mean sea level change across a two-dimensional body

if fluid passage is allowed (Longuet-Higgins, 1977).

To confirm our result, let us give a more physical derivation of the

steady drift force on a fixed plate which seals off all communications

between two fluid regions $(x > 0)$ and $(x < 0)$. We assume that the envelope

of the incident wave train grows steadily from zero to a constant value.

The fluid on the right is never disturbed. In the fluid on the left the

steady-state spatial average of the normal radiation stress in the standing

wave is known to be

$$\bar{S}_{xx} = 2\hat{E}(\frac{2C_g}{C} - \frac{1}{2}\ ) = 2S\hat{E} \qquad \text{where } \hat{E} = \frac{1}{2}\ \rho g\ a^2 \qquad (3.3.101)$$

The steady-state mean set-down is also twice that of the incident progres-

sive wave, so that the corresponding hydrostatic pressure is

$$h\rho g\bar{\zeta}_{20} = -\ \frac{2S\hat{E}}{1 - C_g^2/gh} \qquad (3.3.102)$$

The sum of the two gives the drift force on the plate as $t_1 \to \infty$,

$$h\rho g\bar{\zeta}_{20} + \bar{S}_{xx} = -2S\hat{E}\left(\frac{1}{1 - c_g^2/gh} - 1\right) = -2S\hat{E}\left(\frac{c_g^2}{gh - c_g^2}\right) \qquad (3.3.103)$$

On the other hand, if we take $t_1 \to \infty$ in Equation (3.3.95) and $R = 1$ in Equation (3.3.90), we get the steady-state displacement whose product with K is precisely equal to the steady drift force given by Equation (3.3.103). Thus the mean set-down on the up-wave side is responsible for the negative drift force.

In Figure 3.6 the typical transient motion $X_{10}(t_1)$ is plotted as curve b for the case where the incident envelope becomes uniform after the first peak at $\Omega t_1 = \pi/2$.

c)   A Pulse Envelope:

Let the pulse envelope have the total duration $T_1 = \pi/\Omega$. After the pulse expires ($\Omega t_1 > \pi$), slow sway of the body gradually attenuates as shown by curve c in Figure 3.6. The rate of attenuation increases with K through β; see (3.3.89). The maximum of $X_{10}(t_1)$ lags behind the peak of the incident wave envelope at $\Omega t_1 = \pi/2$. This is due to the time constant $1/\beta \propto 1/K$.

To see the effect of the mooring force we plot in Figure 3.8 the effect of β/Ω for the same wave packet. For smaller β/Ω (or K), the maximum displacement is greater but is realized later.

The long waves are particularly interesting for this case. As shown in Figure 3.9, $\bar{\zeta}_{20}^{I}$, which accompanies the incident wave packet, is a solitary depression (set-down) travelling at the group velocity. The reflected and transmitted wave packets are also accompanied by set-downs $\bar{\zeta}_{20}^{R}$ and $\bar{\zeta}_{20}^{T}$ whose amplitudes are simply related to the reflection coefficient R. Ahead of
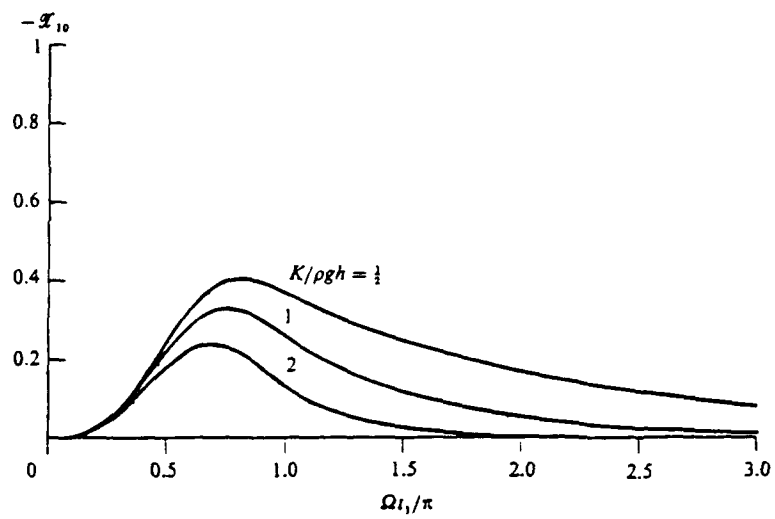
Figure 3.8 Effects of Elastic Mooring Constant on the Transient Slow
Displacement X_{10} of a Sliding Block Due to a Wave Packet for
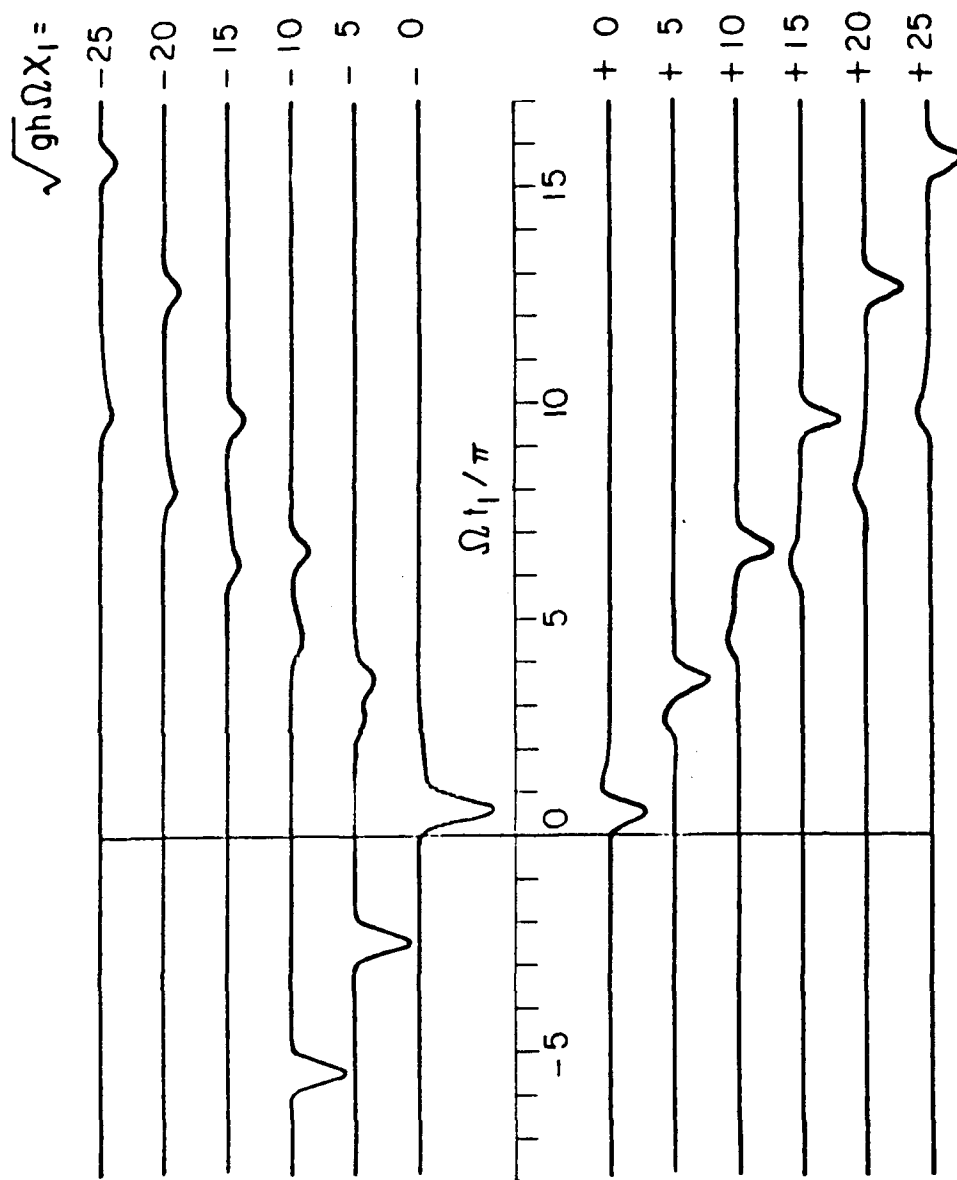$M = \rho h^2$ and $kh = 1.25$.

Figure 3.9   Scattering and Radiation of Long Waves Due to an Incident Wave Packet; kh = 1.25 $\underline{M}$ = 1, K = ρgh.

71

them are the two long waves $\overline{\zeta}_{20}^{\pm}$ travelling at speed $\sqrt{gh}$. Because $X_{10}(t)$ is pulse-like, X_{10t_1} and $\overline{\zeta}_{20}^{\pm}$ must have points of inflection (cf. (3.3.65)).

3.3.4 Comments on the Steady State "Set Down" and Drift Current

We wish to interpret the slow potential ϕ_{10} in the case of a uniform wave train. It is known that for a uniform wave train there can be an arbitrary second order mean free surface displacement and mean current (Mei (1983)). This can be written as:

$$\phi_{10} = ax_1 + bt_1$$

where a and b are undetermined. If we let the waves propagate onto otherwise calm water, with the envelope of the waves given, say, by (3.3.79):

$$A = a[H(t_1)\, H(\tfrac{\pi}{2\Omega} - t_1)\, \sin \Omega t_1 + H(t_1 - \tfrac{\pi}{2\Omega})] \tag{3.3.104}$$

or any other transient start of a uniform wave train, we find from (3.1.9) and (3.3.13) that ϕ_{10} will evolve to the form:

$$\phi_{10} = \frac{4\omega^2 a^2/g^2}{gh/C_g^2 - 1}\, [(k^2 - \sigma^2) + \frac{2\omega k}{C_g}]\, (t_1 - \frac{x_1}{C_g}) \tag{3.3.105}$$

once the waves have reached their full amplitude.

The usual practice in treating uniform wave train problems is to redefine the origin so that the mean set down is zero. We have seen that the initial value approach resulted in different mean water levels on the two sides of the sliding block contributing to a negative drift force.

72

On the rotating earth, Coriolis effect will affect the steady state drift current as shown by Ursell (1950). The Lagrangian drift U_{20} of (2.4.16) will approach zero.

However, reaching this steady state lasts on a time scale comparable to the Coriolis period, which is many hours long, and is much longer than the time scale considered by us, hence we may neglect rotation in the present study.

3.4 Large Amplitude Sway

In many practical situations, the mooring is very weak and the hydrodynamic blocking is small. This results in a slow sway displacement much larger than the wave amplitude. It is no longer feasible to carry out the Taylor expansion about the rest position of the body; a different approach is required.

Triantafyllou (1982) has used multiple time scales and a moving coordinate system to treat this problem, arriving at decoupled equations for the fast and slow motions. He did not account for the long spatial scales associated with the long period motion. As a result the diffraction of the locked long waves and the damping by radiation of long waves were not considered.

We carry out the multiple scale expansion in both time and space for the present problem, with a view to examining forces due to long wave diffraction and radiation damping.

We assume,

$$H = O(h) \qquad\qquad (3.4.1)$$

then there is no large blocking, and

$$K_0 = \epsilon^2 K = O(\epsilon^2)$$

73

so that

$$X = O(1) \qquad (3.4.2)$$

Let us write:

$$X = \sum_{n=0}^{\infty} \varepsilon^n \sum_{m=-n}^{n} X_{nm} \, e^{-im\omega t} \qquad (3.4.3)$$

$X_0 \equiv X_{00}$ is the slow sway motion of order unity; the corresponding velocity is small,

$$\partial X_0/\partial t = \varepsilon \, X_{0t_1} = O(\varepsilon) \qquad (3.4.4)$$

We define a moving coordinate system which follows the slow motion X_0, in order to study the fast potential, ψ_{11}. Let

$$(x', z', t') \equiv (x - X_0, z, t) \qquad (3.4.5)$$

be the moving coordinates in terms of which the velocity potential is

$$\Phi'(x', z', t') \equiv \Phi(x, z, t) \qquad (3.4.6)$$

The spatial gradient does not change:

$$\nabla'\Phi' = \nabla\Phi \qquad (3.4.7)$$

but the time derivative changes in accordance with the chain rule:

$$\Phi'_{t'} = \Phi_t - \varepsilon X_{0t} \, \Phi_x \qquad (3.4.8)$$

We define the near field as the region within a few short waves from the body. Let us denote the near field potential by ψ':

$$\psi' = \Phi' \qquad (3.4.9)$$

and expand it into orders and harmonics as in (2.2.2) and (2.2.8):

$$\psi' = \sum_{n=1}^{\infty} \varepsilon^n \sum_{m=-n}^{n} \psi'_{nm} \qquad (3.4.10)$$

for the first order fast potential ψ_{11} we obtain:

74

$$\Delta\psi'_{11} = 0 \qquad (-h < z < 0) \qquad (3.4.11)$$

$$\psi'_{11z} - \sigma\psi'_{11} = 0 \qquad (z = 0) \text{ where } \sigma = \frac{\omega^2}{g} \qquad (3.4.12)$$

$$\psi'_{11z} = 0 \qquad (z = -h) \text{ and on } \overline{b'_0} \qquad (3.4.13)$$

$$-\omega^2 M X_{11} = i\omega\rho [\int_{S'^-_0} \psi_{11} \, dz - \int_{S'^+_0} \psi_{11} \, dz] \qquad (3.4.14)$$

where $S'^{\pm}_0$ are the mean body surface moving in t_1 only. These equations are formally identical to those for ψ_{11} in Section 3.2 and are also formally the same as the equations for ψ_{11} in a regular wave train with no slow motion. Therefore, the solution is the same as that obtained in Section 3.2 for a body in regular waves. This means that the drift force, to the leading order $(O(\epsilon^2))$ is given by the "steady drift force" formula, Equation (3.3.12). We point out, however, that at the next order $(O(\epsilon^3))$ there is a contribution associated with the body velocity ϵX_{0t_1}. This contribution can be computed using the theory of a moving ship. Only a part of the effect of the current can be attributed to the $O(\epsilon)$ Doppler shift of Equation (3.4.8). The computation becomes more involved. We refer to Huijsmans and Hermans (1985) who solved a similar asymptotic problem for a slowly moving ship in very deep water. They found that the leading order correction, for a small forward speed, is proportional to that speed. We do not calculate that effect and merely write it symbolically in the form:

$$\rho g \, \lambda' \, \epsilon^2 |A|^2 \, \epsilon X_{0t_1} = O(\epsilon^3) \, \lambda'$$

for the leading order change in the drift force. This change is expected to be proportional to the forward speed (or equivalently the current). Since the changes occur in the second order potential, $\varepsilon^2 \phi_{21}$, the numerical value of λ' is expected to be $O(1)$. It might be larger at specific frequencies, for some bodies. We shall see that this damping-type term can be of the same order as the damping due to long-wave radiation and should thus be considered. The physical origin of the present term, however, is due to interaction of the body motion with the short waves.

Because the forward speed is small, $O(\varepsilon)$, the Doppler shift effect on ψ_{11} is negligible. The slow motion is related to ψ_0, which is a function of the long spatial scale x_1. Relative to that scale, X_0 is a small quantity and the change of mean position does not affect the slow motion hydrodynamics at the leading order.

We may therefore study the slow potential in the rest coordinate system (x, z, t). This is different from the approach taken by Triantafyllou (1982). The equations for the near field potential ψ_0 are:

$$\Delta\psi_0 = 0 \qquad (-h < z < 0) \qquad (3.4.15)$$

$$\psi_{0_z} = 0 \qquad (z = 0, -h) \text{ and on } \bar{b}_0 \qquad (3.4.16)$$

The velocity of the body is larger than in the small amplitude slow motion case, and is

$$\varepsilon\, X_{0t_1} = O(\varepsilon) \qquad (3.4.17)$$

We discard from (3.3.2) the second order terms

$$\varepsilon^2 u \equiv \varepsilon^2 [\psi_{20x} + (\psi_{11}\, X_{11}^* + *)] = O(\varepsilon^2) \qquad (3.4.18)$$

76

To the first order $O(\varepsilon)$ the slow kinematic boundary condition is

$$\psi_{10_x} = X_{0t_1} \qquad \text{o.. } S^\pm \quad (x = \pm B + X_0) \qquad (3.4.19)$$

The dynamic boundary condition is obtained in the same way as (3.3.14) was derived for the small amplitude slow sway. Including the body inertia, we write:

$$MX_{0t_1t_1} + K\, X_0 = -\rho \, [\int_{S^-} \psi_0 \; dz - \int_{S^+} \psi_0 \; dz]_{t_1} + \rho g \, |A|^2 \, |R|^2 \, \frac{C_g}{C} \qquad (3.4.20)$$

The slow potential ψ_0 can be separated into two parts: The first part $\psi_{10}^{(1)}$ is a function of t_1 only and is the near field of the slow potential of Section 3.3.1 given by (3.3.38) through (3.3.42). Its corresponding far field $\phi_{10}^{(1)}$ consists of the locked long waves which travel with the short wave groups (I, R, and T) and of the free diffracted wave $\phi_{10}^\pm$. In particular, $\psi_{10}^{(1)}$ satisfies

$$\psi_{10x}^{(1)} = 0 \qquad \text{on} \qquad S_0^\pm \; (x = \pm B) \qquad (3.4.21)$$

just as in (3.3.16b).

The remaining part of the slow potential, $\psi_0^{(2)}$, is related to the radiated wave, satisfying (3.4.19) and radiation conditions that state that the waves are outgoing from the body. $\psi_0^{(2)}$ is simply the solution to the linear problem for wave radiation by the slow sway motion. The order of $\psi_0^{(2)}$ and the corresponding $\phi_0^{(2)}$ will be determined later.

The present case is different from the case studied in Section 3.3.1 in that the radiation problem is important, due to the larger slow sway velocity. In addition to $\psi_{10}^{(1)}$, we have $\psi_0^{(2)}$ that is the potential of radiation due to the slow sway. This potential will have the effect of an added mass μ

77

and a damping coefficient $\epsilon\lambda$. These are derived in Appendix E by using matched asymptotics.

In the far field $\phi_0^{(2)}$ is given from (E.14) by:

$$\phi_0^{(2)} = \pm \epsilon \, \text{Re} \, \{X_{0t_1} \frac{c}{\epsilon i k_1 c - 1} e^{-2i\Omega(t_1 \mp \frac{x_1}{\sqrt{gh}})} \} \qquad \begin{array}{l} (x_1 > 0) \\ (x_1 < 0) \end{array} \qquad (3.4.22)$$

The force due to $\psi_{10}^{(1)}$ is $O(\epsilon^3)$ as shown for the identical ψ_{10} in Section 3.3.1. The force due to $\psi_0^{(2)}$ is given in terms of the added mass and damping coefficient at the low frequency 2Ω:

$$\epsilon^2 (\mu \, X_{0t_1 t_1} + \lambda \, X_{0t_1}) \qquad (3.4.23)$$

The introduction of the damping coefficient, $\epsilon\lambda$, is made possible by accounting for a free wave in the far field. This wave is radiated by the slow sway, carrying away energy, which results in damping. When $c = O(1)$, it is seen from (E.17) that $\epsilon\lambda$ is in fact $O(\epsilon^2)$. Multiplied by X_{0t_1} it will yield an $O(\epsilon^3)$ contribution, while the rest of the terms in the equation of motion are $O(\epsilon^2)$. However, near resonance, where the inertia and elastic force are nearly balanced, damping is important and serves to make the resonance finite. This effect was not accounted for in previous theories, where a rigid lid approximation results in using a zero frequency limit for the slow sway which excludes radiation damping (Triantafyllou (1982)). The equation of motion for the slow sway is

$$(M + \mu) \, X_{0t_1 t_1} + \lambda \, X_{0t_1} + K \, X_0 = \rho g |A|^2 \, (|R|^2 \frac{C_g}{C} + \epsilon\lambda' X_{0t_1}) \qquad (3.4.24)$$

where the last term on the right hand side indicates the third order effects for which the details have not been worked out. Note that terms in (3.4.24)

can be of different orders of magnitude. In particular μ and λ depend on the gap width H which influences the blockage coefficient c. If H/h is $O(1)$, then $c \simeq 2BD/h = O(1)$. It follows from (E.17) that λ is $O(\epsilon)$ and μ is $O(1)$. Damping is small. If the mooring constant is assumed to be $O(\epsilon^2)$ then Equation (3.4.24) predicts unbounded resonance at leading order. To obtain finite response at resonance it is necessary to calculate all the $O(\epsilon^3)$ terms which are tedious to work out. It is seen from (3.4.22) that when c is $O(1)$ the radiated potential is $O(\epsilon)$ and is comparable to $\epsilon\psi_{10}^{(1)}$.

There is a situation where (3.4.24) can be used without adding higher order corrections. This is when c is $O(1/\sqrt{\epsilon})$ which corresponds to an intermediate gap. We also choose intermediate mooring $K_0 = O(\epsilon^{3/2})$. From (E.17) we see that μ is $O(1/\sqrt{\epsilon})$ and $\epsilon\lambda$ is $O(\epsilon)$. Equation (3.4.24) is still at order ϵ^2 and X_0 decreases to $O(\sqrt{\epsilon})$. The damping term $\epsilon\lambda X_{0t_1}$, increases to $O(\epsilon^{5/2})$. The damping due to the modification of the short waves, $\epsilon\lambda'X_{0t_1}$, becomes $O(\epsilon^{7/2})$ (since X_0 decreased to $O(\sqrt{\epsilon})$).

In the results presented we shall use $c = O(1/\sqrt{\epsilon})$ and neglect the higher order effect of λ'. $\phi_0^{(2)}$ and $\psi_0^{(2)}$ are now $O(\sqrt{\epsilon})$ as seen from Equation (3.4.22) and are larger than $\epsilon\psi_{10}^{(1)}$.

In Figure 3.10 the value of the normalized $\underline{X}_0 \equiv hX_0/a^2$, the slow sway amplitude for a periodic envelope is plotted versus the modulation ratio Ω/ω for various choices of the parameters. It is clear from (3.4.24) and (E.17) that increasing c as well as increasing K will reduce $\underline{X}_0$. In Figure 3.11 transient responses corresponding to the inputs of Cases b, c, and d of Section 3.3 are plotted. Equations (3.3.71) through (3.3.82) can be carried over directly to the present case, with X_{10} replaced by X_0. The only modifications are:
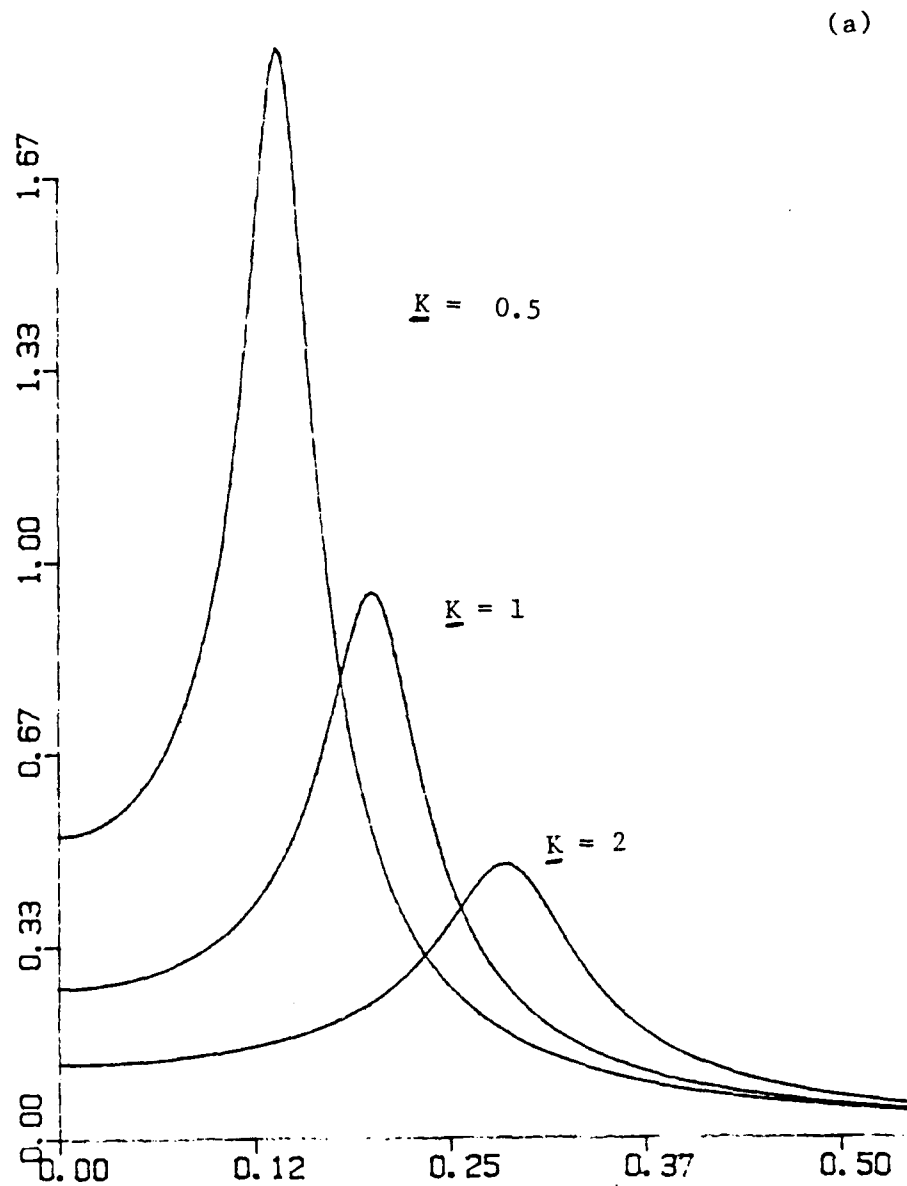
Figure 3.10 Amplitudes of the Normalized Slow Sway $h|X_0|/a^2$, versus the Modulation Ratio Ω/ω; $K/\rho gh = 0.5, 1.2$. (A) $kh = 1.2$, $\frac{c}{h} = 2.887$ (B) $kh = 1.6$, $\frac{c}{h} = 1.2$.
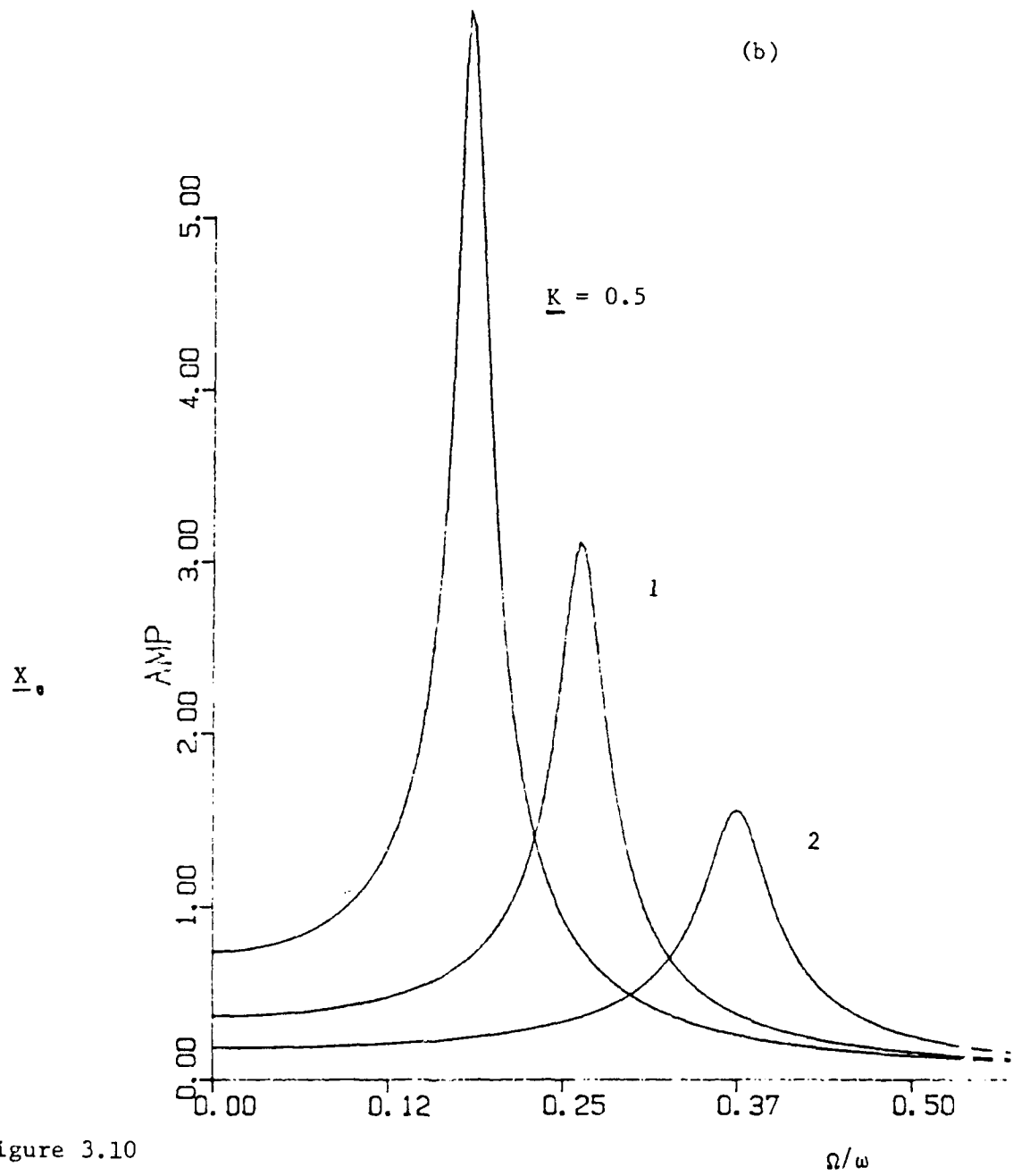
Figure 3.10

81

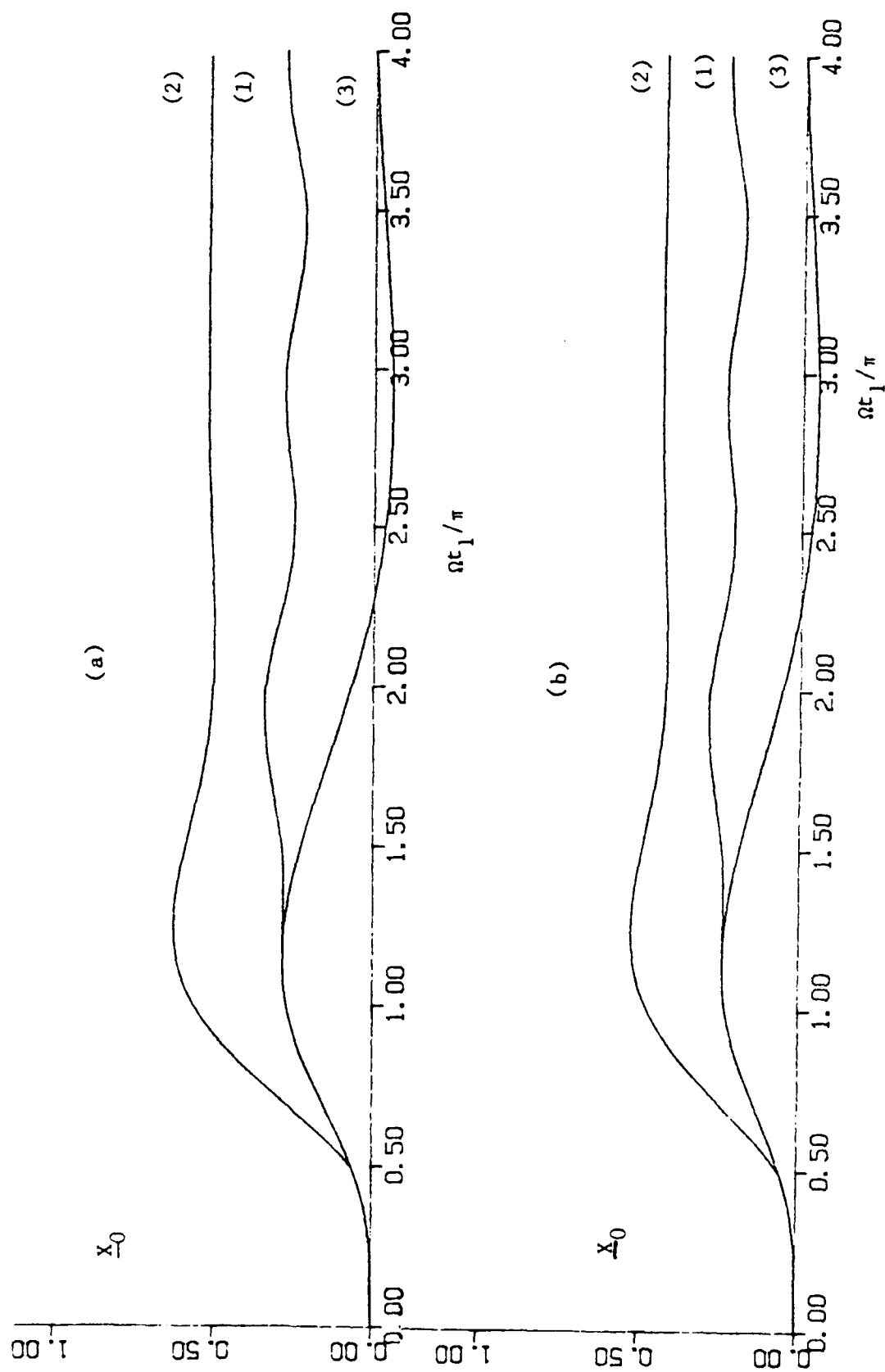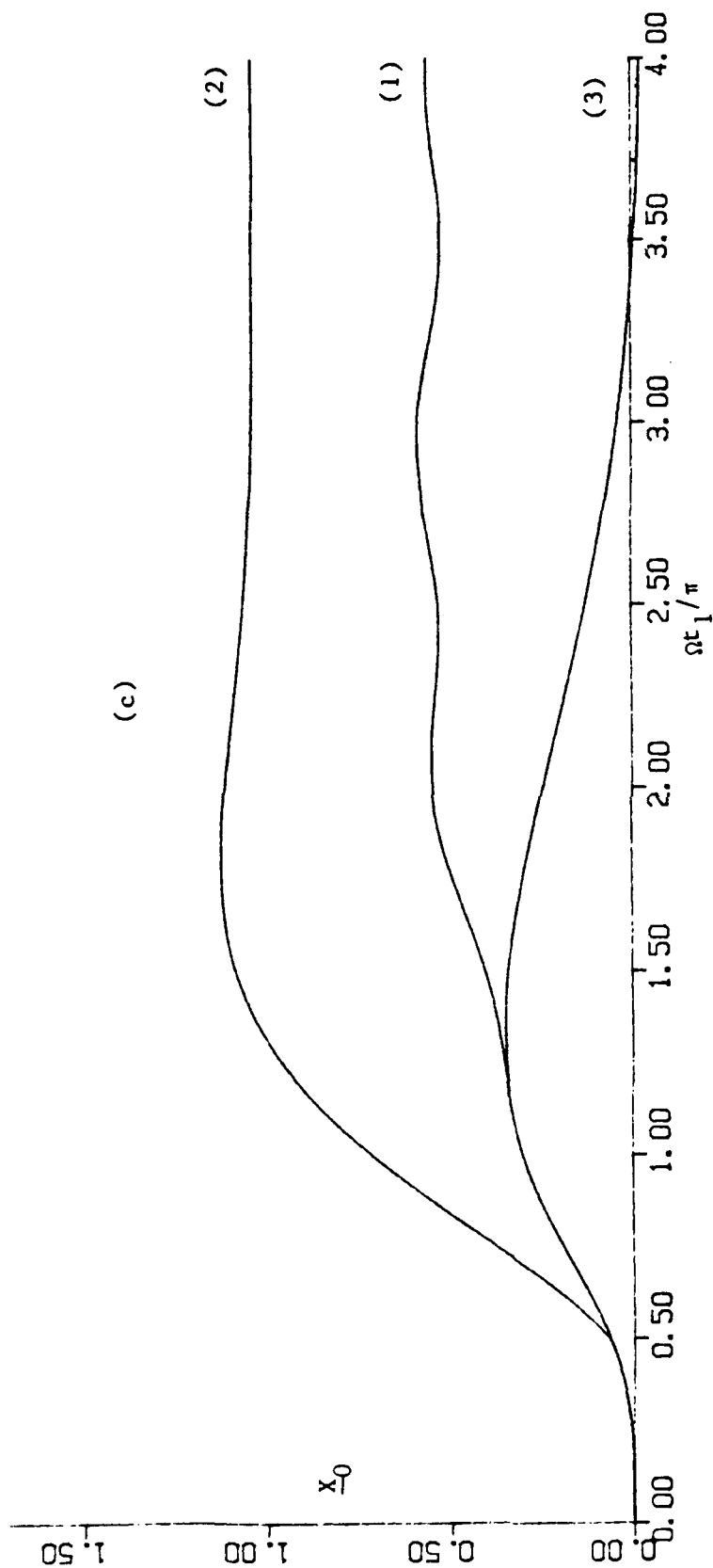Figure 3.11

82

Figure 3.11 Transient Slow Displacment for Large Amplitude Slow Sway. (1)
A sinosoidal Envelope Starting From Rest; (2) A Uniform
Envelope Starting From Rest; (3) A Pulse Envelope:

(a) kh = 1.2 $\frac{K}{} = 1$ c/h = 2.887,
(b) kh = 2 $\frac{K}{} = 1$ c/h = 2.887.
(c) kh = 1.2 $\frac{K}{} = .5$ c/h = 2.887

1) X_{10}' defined by (3.3.73) and (3.3.75) is replaced by

$$X_0' = -\frac{1}{2}\frac{C_g}{C}\frac{\rho g}{K}/[-(M + \mu)4\Omega^2 - 2i\Omega\lambda + K)$$ (3.4.25)

2) $\alpha_{1,2}$ of (3.3.77) is now given by:

$$\alpha_{1,2} = \frac{-\lambda \pm \sqrt{\lambda^2 - 4K(M + \mu)}}{2(M + \mu)}$$ (3.4.26)

The blockage coefficient corresponds to a cylinder that is 10 m wide and has a 7.5 m draft in water of 10 m depth. The spring constant is ϵ (0.1) times that of Section 3.3 and a unit sway motion is $1/\epsilon$ (10) fold larger: 10 m per unit for 3 m incident wave amplitude. We turn to the conclusions of the present chapter.

3.5 Conclusion

The response of a floating offshore structure in slowly varying waves depends on body geometry, mooring stiffness and wave characteristics. We have directed most of our attention to the slow sway motion, which is expected to be the largest, since it is not affected by the buoyancy force and moments. By a multiple scale analysis we have been able to separate the low frequency part of the second-order fluid motion from the high frequency part. By the notion of near and far fields, we have shown (i) that the slow drift problem can be solved without solving explicitly for any second order potential and (ii) that the slow motion in the near field is accompanied by the propagation of long waves in the far field.

The sway response of the two dimensional body depends on the so called blockage coefficient, which measures the obstruction by the body to the long period current around it, and on the mooring stiffness.

When the mooring is not too weak, the slow sway is comparable to fast sway, this was discussed in Section 3.3. In particular, when the blockage was not large, the body's response was passive, in agreement with Newman's (1974) generalization of the steady drift formula. We found that the long wave field is independent of the slow motion. These results are expected to be valid for three dimensional bodies that have O(1) dimensions, since the blockage of a uniform flow by such a body is small, regardless of the gap under it; this is because the fluid can flow around the three dimensional body.

When the blockage coefficient is large it has the effect of large added mass and damping coefficients. The differential equation of slow motion becomes second order and resonance occurs. The response for a transient may exhibit considerable overshooting. This case was solved analytically. For a long vessel with a narrow clearance underneath, we expect a similar blockage effect to make the slow potential dynamically important. Finally, we presented results for a sliding block where the blockage is infinite. No resonance occurs in this case.

When the mooring is very weak and the blockage is not large, the slow sway becomes O(1). We found two types of damping: one is due to the radiation of long waves and the other is due to the "forward speed" effect of the slow sway on the short waves. Both these effects are small. The long wave radiation was computed and the slow sway was found for intermediate gap

85

width. When the gap is $O(\varepsilon)$ or smaller the slow sway becomes $O(\varepsilon)$ even if the mooring is weak, since the added mass and damping coefficient become very large.

The heave motion too, was discussed. We have distinguished between a bottle shaped body and a regular shaped body. The slow potential's contribution to the vertical drift force is at leading order for a regular shaped body, but the resulting motion is $O(\varepsilon^2)$. For a bottle shaped body where the heave is large, the leading order slow vertical force is given by the steady drift formula and the slow potential effect is negligible.

We now turn to other applications of the theory.

4. TRAPPING AND RESONANCE OF LONG WAVES ON A SHELF

4.1 Introduction and Definition

It is well known that shallow water waves can be trapped on a shelf or on a ridge (or outside a canyon). These waves must be propagating on the ridge in a direction oblique to its axis. It is impossible by any linear mechanism for such waves to enter the ridge from the deeper sea; they must be generated by local forcing on the ridge. The wave length and period of the trapped modes are much longer than those of swell with typical periods of $O(20 \text{ sec})$, but can be close to the modulational frequency of swell groups, typically a few mintues.

We shall show that swell groups incident from the sea can excite trapped long waves on a shelf. If the excitation is resonant, these waves can be greater than second order, and cause large slow oscillations. Hence the long waves may present a hazard to off-shore platforms.

The subject of interaction of slowly varying waves with topography, and trapping on a shelf was studied by Foda and Mei (1981) and by Mei and Benmoussa (1984) who gave references to other work. The latter authors studied a slowly varying topography in which reflection by the sloping bottom is negligible. In the present work we study the case when reflection of the short waves is significant.

For demonstration of the physics, we choose a relatively simple bathymetry in the form of a rectangular step. The width of the shelf is comparable

to the wave group length, which is much greater than the short wave wave-length. The water depths are comparable to the short wave length. To solve for the flow potential, we perform a perturbation expansion in terms of the short wave steepness, and utilize multiple time and (horizontal) space scales.

At the leading order, the short waves are found by the solutions of a linear diffraction problem studied by Mei and Black (1969) using a variational method, or, equivalently, by Galerkin method. For convenience, the problem is solved as a superposition of a symmetric and an antisymmetric problem. In contrast to the procedure employed for a floating body (Agnon and Mei 1985a), the reflection by the shelf is very sensitive to the short wave wavelength. This is because the shelf is long; even small variations within a narrow banded spectrum give rise to large phase differences that affect reflection. An alternative and equivalent approach is to break down the shelf into two steps, matching their far fields (cf. Newman (1965)) while retaining the dependence of the wave amplitude on the slow (stretched) time.

After finding the short wave field, we examine separately the near field within a few short waves of the depth steps, and the far field, a few wave groups away. We find the forms of the potentials for the slow waves in each field, and match their asymptotic values to get the solution. It is found that two types of long waves exist. The first one is locked to the shortwave groups and propagates at the group velocity. The other is a shallow water wave generated at the shelf edges and radiated away from them in directions different from those of the short waves and the locked long waves. When the

88

depths and angle of incidence are such that the second long wave is trapped on the shelf, resonance can occur. The resonance obtained from the present approximation is unbounded, since there is no radiation damping due to complete trapping of the long waves. The onset of resonance, however, takes a very long time.

We present results for the amplitude of the free long waves due to periodic and transient inputs. The short waves are incident normally or obliquely.

The Cartesian coordinates (x, y, z) are the same as those of Section 2.1. The bathymetry is given by:

$$\text{depth} = h \qquad (|x| > L, \quad -\infty < y < \infty)$$
$$\text{depth} = h' \qquad (|x| < L, \quad -\infty < y < \infty) \tag{4.1.1}$$

where

$$h > h' \tag{4.1.2}$$

that is, we are studying a ridge that runs parallel to the y axis. The water is of intermediate depth:

$$\sigma h = O(1) ; \quad \sigma h' = O(1) \tag{4.1.3}$$

and the waves are incident from both left and right for the symmetric and antisymmetric problem. The width of the ridge, 2L, is assumed to be comparable to the length of the wave groups:

$$kL = O(\epsilon^{-1}) \tag{4.1.4}$$

The case of a shelf ending with a vertical coast is equivalent to a special case of the present problem where the incident waves from the left and the right are symmetric.

The regions within a few short waves from the ridge edges are called the near fields, and the potential there is denoted by ψ

$$\psi = \phi \qquad k(x \pm L) = O(1) \qquad\qquad (4.1.5)$$

The regions a few wave groups away from the ridge edges are called the far fields, and the potential there is denoted by ϕ:

$$\phi = \phi \qquad k(x_1 - L_1) = O(1) \; ; \quad k(x_1 + L_1) = O(1) \qquad (4.1.6)$$

where

$$(x_1, y_1, t_1; L_1) \equiv \epsilon(x, y, t; L) \qquad\qquad (4.1.7)$$

are stretched quantities used to study the wave groups and the long waves.

In each region the potential is expanded into orders and harmonics, as in Section 2.2. Let us first examine the short wave potentials, ψ_{11}, ϕ_{11}.

4.2 The Short-wave Potential

In the near fields, the equations for ψ_{11} are formally the same as the equations for the diffraction of regular waves by a step. Two approaches can be taken. One is to spectrally decompose the incident wave into its short wave components and to superpose the respective solutions to get the total diffraction wave field. It is well known that the diffraction by a long shelf is very sensitive to small changes in the wavenumber. Along the shelf, small phase differences due to dispersion have a large accumulating effect on the interference of waves reflected from the two edges, as seen in the results of Mei & Black (1969). An alternative way is to use the multiple scale analysis, and to follow the local wave amplitude of the wave group, which carries the

90

required phase information. Since the shelf is large, a wide spacing approximation can be employed, taking into account only the propagating modes for the interaction between the two edges (cf. Newman (1965)), as explained below.

Since the shelf is much longer than the wave length of the short waves, we may assume that only the propagating modes from each edge reach the opposite edge and that the evanescent modes may be neglected.

Consider an infinitely wide depth step at $(x = -L)$. Let the potential of a wave incident from the left of the step (from deep to shallow water) have a unit amplitude:

$$\phi_{11}^{I} = f_0 \exp(i\alpha x + i\gamma y) \qquad (x < -L) \qquad (4.2.1a)$$

with
$$\alpha = k \cos \theta; \quad \gamma = k \sin \theta$$

where θ is the angle of incidence, then the propagating modes of the reflected and transmitted waves are given by

$$\phi_{11}^{R} = R \, f_0 \exp(-i\alpha x + i\gamma y) \qquad (x < -L) \qquad (4.2.1b)$$

$$\phi_{11}^{T} = T \, f_0' \exp(i\alpha x + i\gamma y) \qquad (x > -L) \qquad (4.2.1c)$$

respectively, with $k'^2 = \alpha'^2 + \gamma^2$; R' and T' are used to denote the reflection and transmission coefficients for a wave incident from the shallow side of the depth step. The values of R, R', T, and T' are determined using the Galerkin method used in Section 3.2 for the floating rectangular cylinder. $\{F_n\}$ is replaced by $\{f_n'\}$ which are the eigenfunctions for the

onshelf potential. $\{f'_n\}$, k' are given by (2.3.5a, b) with h replaced by h'. Simple adjustments are made for oblique incidence as in Black (1970). Values of R, R', T, and T' are plotted in Figure 4.3. Energy conservation was verified by checking the numerical results against the identity:

$$(1 - |R|^2) \, C_g \cos \theta = |T| \, C_g'^2 \cos \theta$$

where $\tan \theta' = \gamma/\alpha'$

Now consider the shelf of finite width 2L. We denote the short wave potential in the far field off the shelf by:

$$\phi_{11} = (A \, e^{i\alpha x + i\gamma y} + B \, e^{-i\alpha x + i\gamma y}) \, f_0 \qquad (x < -L)$$

$$(4.2.2)$$

$$\phi_{11} = (C \, e^{i\alpha x + i\gamma y}) \, f_0 \qquad\qquad (x > L)$$

We study the case of waves incident from the left only. The case of waves incident from both sides and in particular symmetric incidence, which corresponds to a shelf of width L terminated by a vertical coast, can be treated in the same way.

The propagating modes on the shelf are given by:

$$\phi_{11} = (D \, e^{i\alpha' x + i\gamma y} + E \, e^{-i\alpha' x + i\gamma y}) \, f_0' \qquad (|x| < L) \qquad (4.2.3)$$

(see Figure 4.2). Matching the propagating modes in (4.2.2) and (4.2.3) and making use of the reflection and transmission coefficients for each step, we immediately get:

$$RA \, e^{i\alpha(-L)} + T'E \, e^{-i\alpha'(-L)} = B \, e^{-i\alpha(-L)}$$

$$(4.2.4)$$

$$TA \, e^{i\alpha(-L)} + R'E \, e^{-i\alpha'(-L)} = D \, e^{i\alpha'(-L)}$$

at $(x = -L)$, and

(a)

(b)
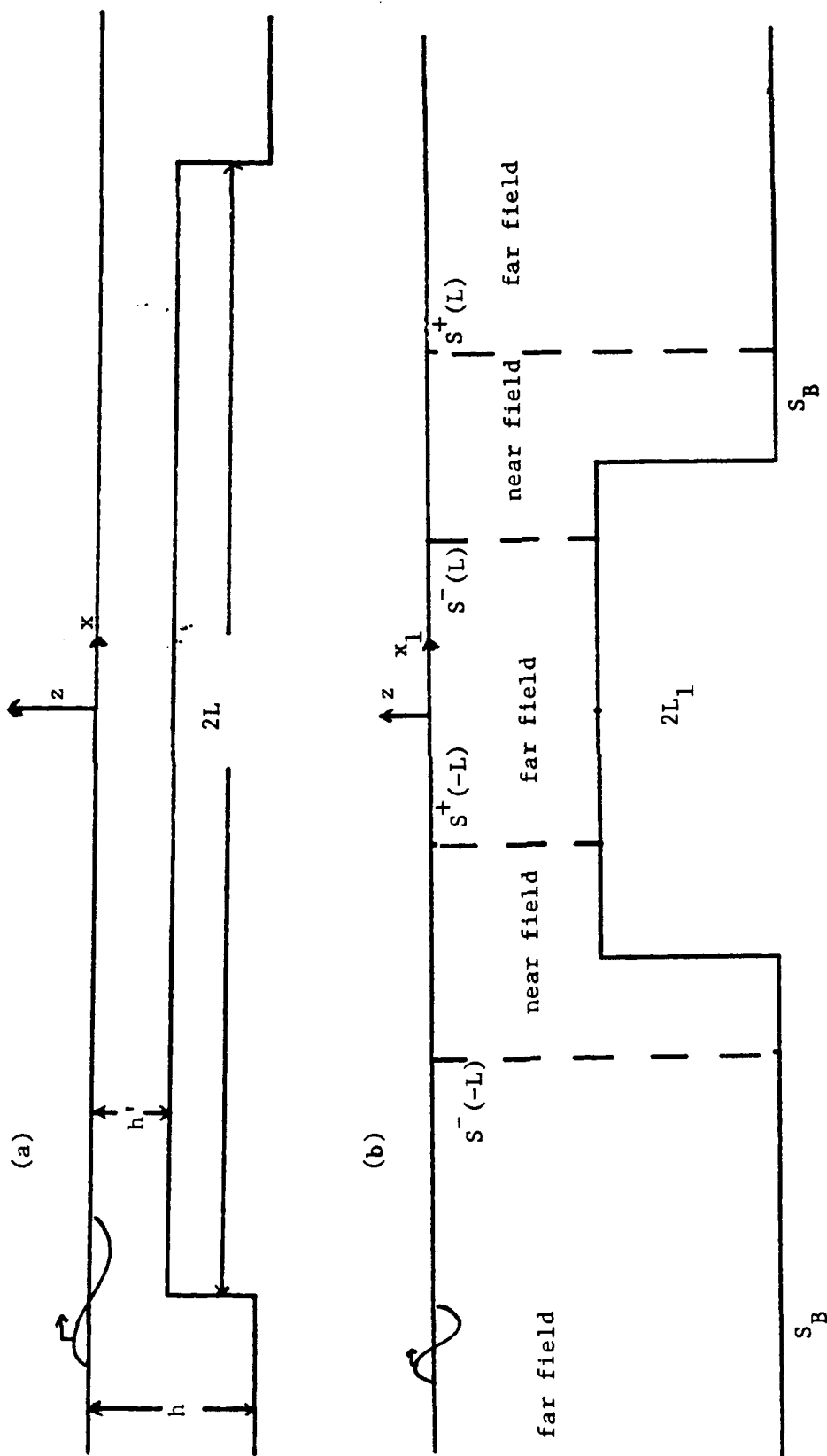
Figure 4.1   a)   The Ridge Geometry

4.1   b)   The Matching Boundaries for a Ridge

93

Figure 4.2 Top View of the Waves on a Ridge.
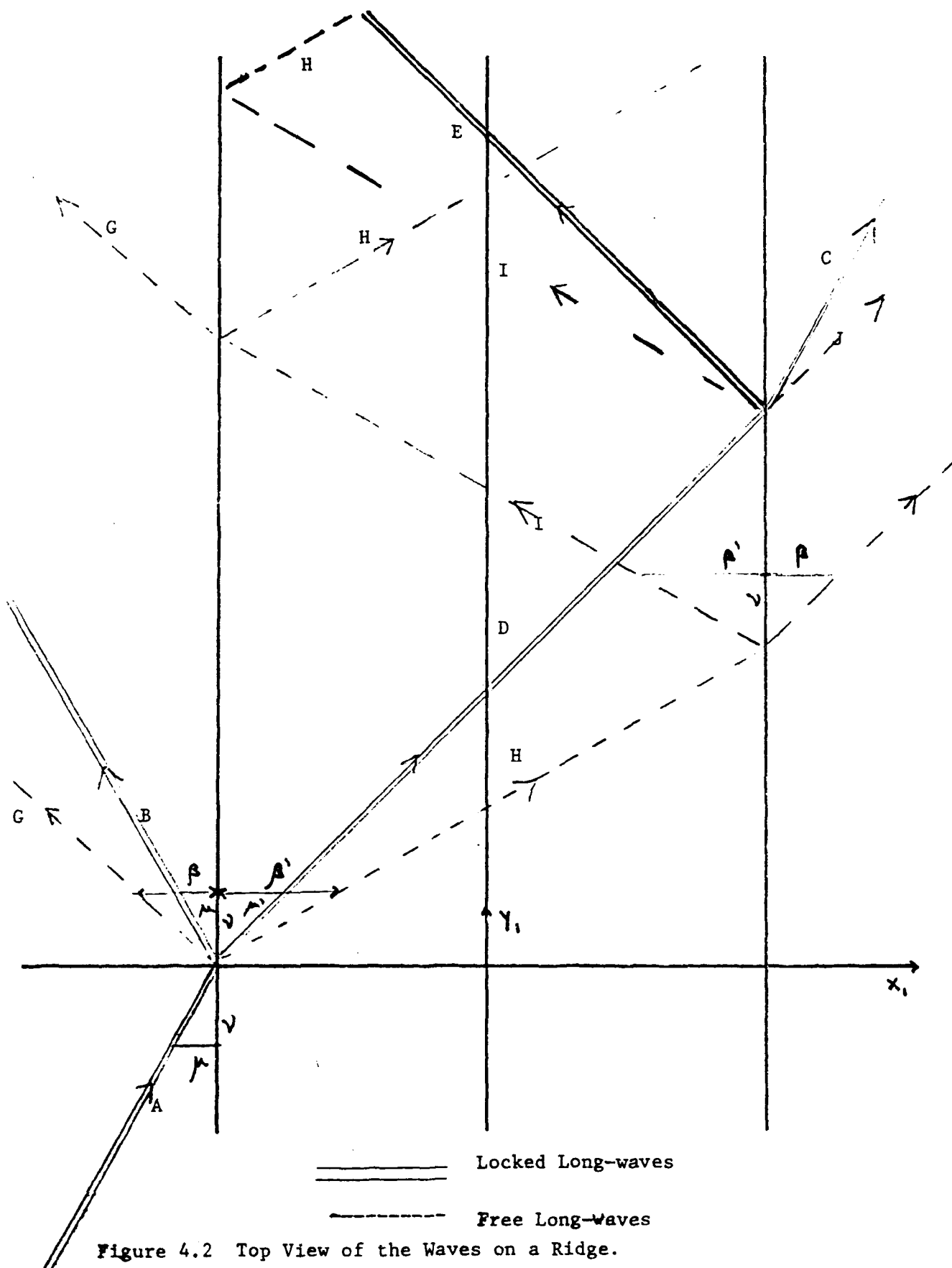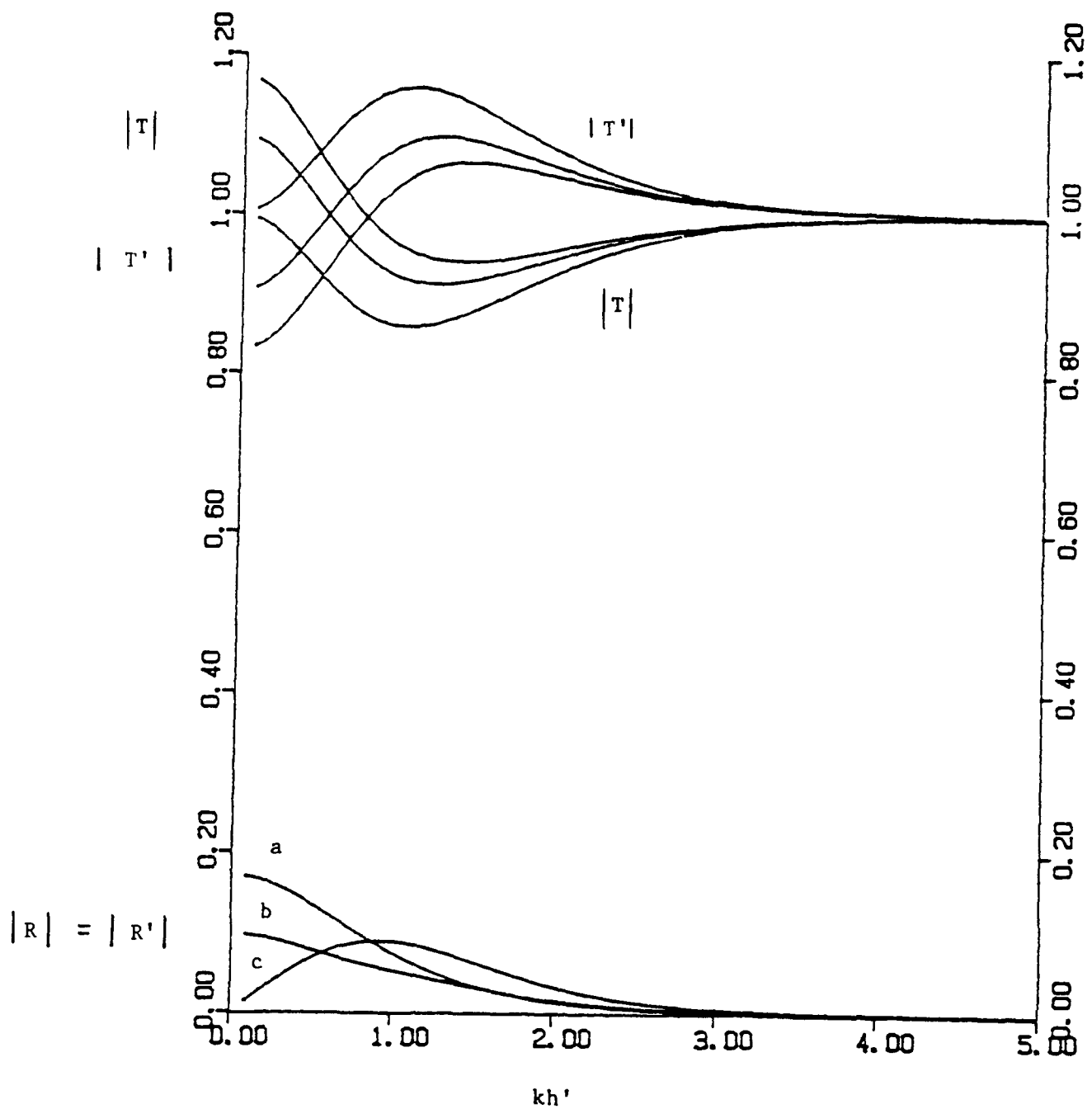
Figure 4.3 The Reflection Coefficients ($|R| = |R'|$') and Transmission Coefficients (T and T') for a Single Step versus kh'; h'/h $\approx$ 0.5. The Angles of Incidence are: a) 0^0(normal), b) 40^0 and c) 55^0.

$$T'D \ e^{i\alpha'L} = C \ e^{i\alpha L}$$

$$R'D \ e^{i\alpha'L} = E \ e^{-i\alpha'L}$$

(4.2.5)

at $(x = L)$

In general, A, B, C, D, and E should be treated as functions of long time scale. However, for a sinusoidal envelope it is easier to decompose the incident wave as follows:

$$A \ e^{i(\alpha x + \gamma y - \omega t)} = A^+ \ e^{i(\alpha^+ x + \gamma^+ y - \omega^+ t)}$$
$$+ A^- \ e^{i(\alpha^- x + \gamma^- y - \omega^- t)}$$

(4.2.6)

where $A^+ = A^-$ is a real constant,

$$A = \text{Re} \ \{(A^+ + A^{-*}) \ e^{-i\Omega(t_1 - \mu x_1 - \nu y_1)}\}$$

(4.2.7)

$$\mu = \frac{\alpha}{kC_g} \ ; \quad \nu = \frac{\gamma}{kC_g}$$

(4.2.8)

and

$$\alpha^+ = \alpha + \varepsilon\Omega \ ; \ \alpha^- = \alpha - \varepsilon\Omega; \ \omega^+ = \omega + \varepsilon\omega \ ; \ \omega^- = \omega - \varepsilon\Omega \ ; \ \varepsilon\Omega/\omega = O(\varepsilon)$$

(4.2.9)

The rest of the amplitude functions are written:

$$B = \text{Re} \ \{(B^+ + B^{-*}) \ e^{-i\Omega(t_1 + \mu x_1 - \nu y_1)}\}$$

$$C = \text{Re} \ \{(C^+ + C^{-*}) \ e^{-i\Omega(t_1 - \mu x_1 - \nu y_1)}\}$$

$$D = \text{Re} \ \{(D^+ + D^{-*}) \ e^{-i\Omega(t_1 - \mu' x_1 - \nu y_1)}\}$$

$$E = \text{Re} \ \{(E^+ + E^{-*}) \ e^{-i\Omega(t_1 + \mu' x_1 - \nu y_1)}\}$$

(4.2.10)

where

$$\mu'^2 + \nu^2 = C_g'^{-2} \qquad\qquad (4.2.11)$$

or, equivalently in the form of (4.2.6).

Substituting $A^\pm$, $B^\pm$, $C^\pm$, $D^\pm$, and $E^\pm$ in place of A, B, C, D, and E in (4.2.4) and (4.2.5) results in a matrix equation:

$$
\begin{bmatrix}
e^{i\alpha^\pm L} & 0 & 0 & -T'e^{i\alpha^{\pm'}L} \\
0 & 0 & e^{-i\alpha^\pm L} & -R'e^{i\alpha^{\pm'}L} \\
0 & -e^{i\alpha^\pm L} & T'e^{i\alpha^{\pm'}L} & 0 \\
0 & 0 & R'e^{i\alpha^{\pm'}L} & -e^{-i\alpha^{\pm'}L}
\end{bmatrix}
\cdot
\begin{bmatrix}
B^\pm \\ C^\pm \\ D^\pm \\ E^\pm
\end{bmatrix}
=
\begin{bmatrix}
RA^\pm e^{-i\alpha^+ L} \\
TA^\pm e^{-i\alpha^+ L} \\
0 \\
0
\end{bmatrix}
$$

which can be inverted to give:

$$
\begin{bmatrix}
B^\pm \\ C^\pm \\ D^\pm \\ E^\pm
\end{bmatrix}
= \frac{A^\pm}{1-R'^2 \exp(4i\alpha^{\pm'}L)}
\begin{bmatrix}
R' \exp(-i\alpha^\pm L) + R'TT' \exp[i(4\alpha^{\pm'}-\alpha^\pm)L] \\
T'T \exp[2i(\alpha^{\pm'}-\alpha^\pm)L] \\
T \exp[i(\alpha^{\pm'}-\alpha^\pm)L] \\
R'T \exp[i(3\alpha^{\pm'}-\alpha^\pm)L]
\end{bmatrix}
\qquad (4.2.12)
$$

cf. Newman (1965).

Values of $B^\pm/A^\pm$ are plotted in Figure 4.4. Since the small differences between α^+ and α^- have an $O(1)$ effect on the phase for waves travelling across the whole shelf, the amplitudes for the two components, $()^\pm$, differ. The solution given by (4.2.12) could be found without using the far spacing approximation. An exact solution for B and C was given by Mei and Black (1969) using a variational method. Their results for $h'/h = 0.5$ and $L/h = 3$ given in their Figure 2 are in excellent agreement with the present results where we assume a long shelf – in the range of frequencies corresponding

97
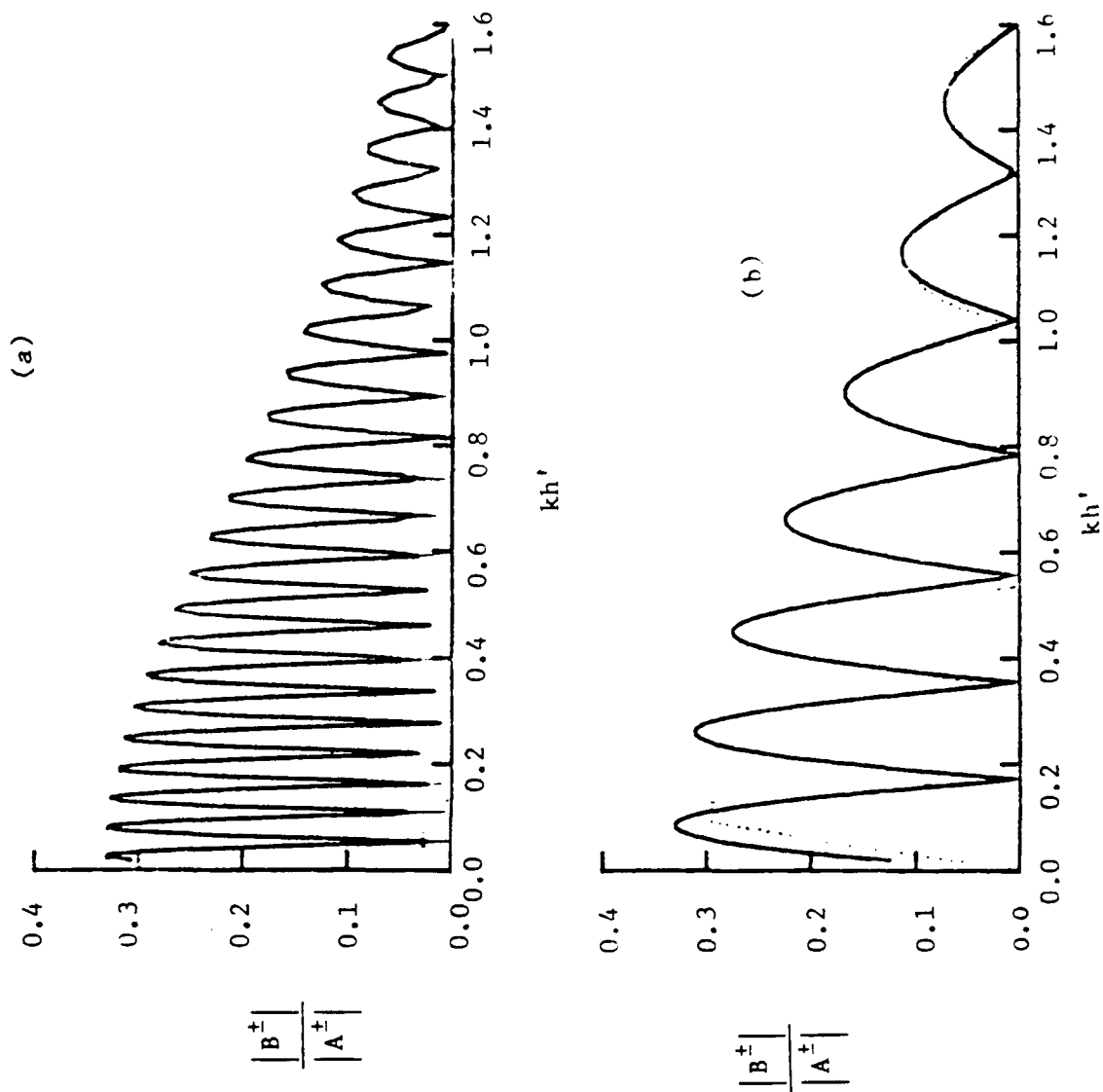
Figure 4.4 The Reflection Coefficient $|B^{\pm}/A^{\pm}|$ for a Ridge versus kh'. h'/h = 0.5; a) L/h = 10, b) L/h = 3. Results of Mei & Black (1969) are Shown in a Dotted Line for Case b.

to (4.1.3)) as shown in Figure 4.4. For a transient problem A, B, C, D, and E are more general functions of x_1, y_1, t_1. Results of using (4.25) (which relies on the multiple scale approach) for transient envelopes will be presented later. For a sinusoidal envelope we can substitute (4.2.8) and (4.2.10) into (4.2.5). We end up with the same solutions for B^+, B^-, C^+, C^-,...

An alternative to (4.2.12) is to decompose the short wave potential at, say, ω^+, into a component that is symmetric with respect to $(x = 0)$ and an antisymmetric component. This results in four sets of equations, for two unknowns each. The results are, of course, the same.

This completes the determination of the propagating short waves. We may turn to the long-wave potential.

4.3 The Long-wave Potential

The governing wave equation for the slow potential in the far field is (2.4.18). We are still considering the monochromatic envelope input (4.2.6) and wish to study the oscillatory motion that results from it. There are two types of long waves. One is locked to the short wave groups, and is similar to the waves given by (3.1.9). The only difference is in the direction in which these waves propagate. Off the shelf, where the short waves are unidirectional, the locked long waves are given by the solution to (2.4.20).

$$\phi^{(\chi)}_{10t_1} = \text{Re } \chi e^{-2i\Omega(t_1 \pm \mu x_1 - \nu y_1)} \equiv \left|\chi\right|^2 \frac{f_0^2(0) \ c_g^2}{gh - c_g^2} (k^2 - \sigma^2 + \frac{2\omega k}{c_g}) \quad (4.3.1)$$

where

99

$$\chi = A, B, C \qquad (4.3.2)$$

A,B,C,D, and E refer to the four wave trains given by (4.2.7) and (4.2.10); (−) is taken for A and C; (+) is taken for B.

On the shelf, the dispersion makes the wave envelopes propagate at a different direction from the short waves. From (2.4.18) we get:

$$\phi_{10t_1}^{(\chi)} = |\chi|^2 \; \frac{f_0'^2(0) \; C_g'^2}{gh' - C_g'^2} \; (k'^2 - \sigma^2 + 2\omega \, (\alpha' \; \mu' + \gamma\nu)) \qquad (4.3.3)$$

where

$$\chi = D, E \qquad (4.3.4)$$

(−) is taken for D and (+) for E.

There will also be free waves, propagating away from the edges. The free waves are solutions of the D'Alembert equation:

$$\phi_{10t_1t_1}^{F} - gh \; \nabla_1^2 \phi_{10}^{F} = 0 \qquad (4.3.5)$$

where h is replaced by h' on the shelf.

Because the potential is periodic in y_1 for the periodic envelope (4.2.6), the free waves, too, must be periodic with the same wavenumber as $|A|^2$, namely $2\Omega\nu$.

The x_1 (cross-ridge) wavenumbers of the free waves $2i\Omega\beta$, $2\Omega\beta'$, must satisfy:

$$-\beta^2 + \nu^2 = (gh)^{-1} \qquad (4.3.6)$$

$$\beta'^2 + \nu^2 = (gh')^{-1} \qquad (4.3.7)$$

β, β' will be real or imaginary, depending on the signs of β^2, β'^2. We shall study the interesting case where the free long waves are trapped as propagating modes on the ridge, and are evanescent off the ridge. In this case resonance may occur. The free waves will have the form:

$$\phi_{10}^F = \phi_{10}^G = \text{Re } \underline{G} \, e^{-2i\Omega(t_1 - \nu y_1) + 2\Omega\beta x_1} \qquad (x_1 < -L_1)$$

$$\phi_{10}^F = \phi_{10}^H + \phi_{10}^I \qquad\qquad\qquad (|x_1| < L_1)$$

with

$$\phi_{10}^H = \text{Re } \underline{H} \, e^{-2i\Omega(t_1 - \beta' x_1 - \nu y_1)} \qquad\qquad (4.3.8)$$

$$\phi_{10}^I = \text{Re } \underline{I} \, e^{-2i\Omega(t_1 + \beta' x_1 - \nu y_1)}$$

and

$$\phi_{10}^F = \phi_{10}^J = \text{Re } \underline{J} \, e^{-2i\Omega(t_1 - \nu y_1) - 2\Omega\beta x_1} \qquad (x_1 > L_1)$$

with

$$-\beta^2 = \frac{1}{gh} - \nu^2 < 0 < \beta'^2 = \frac{1}{gh'} - \nu^2 \qquad\qquad (4.3.9)$$

$\underline{G}$, $\underline{H}$, $\underline{I}$, and $\underline{J}$ will be determined by matching to the near field potential.

The total far field is:

$$\phi_{10} = \phi_{10}^A + \phi_{10}^B + \phi_{10}^G \qquad\qquad (x_1 < -L_1)$$

$$\phi_{10} = \phi_{10}^D + \phi_{10}^E + \phi_{10}^H + \phi_{10}^I \qquad (|x_1| < L_1) \qquad (4.3.10)$$

$$\phi_{10} = \phi_0^C + \phi_{10}^J \qquad\qquad\qquad (x_1 > L_1)$$

from (4.3.1) and (4.3.8)

In the near field, the geometry is the same as in the wide gap case Section 3.3.1. Due to the arguements of Section 3.3.1 (Equation 3.3.16), the slow potential ψ_{10} is independent of short scale (x, y, z). It does, however, depend on y_1 due to variation along the shelf:

$$\psi_{10}^{\pm} = \psi_{10}^{\pm} (y_1, t_1) \tag{4.3.11}$$

where ψ_{10}^{+} is the potential at the right edge and ψ_{10}^{-} is the potential at the left edge of the shelf.

Just as in Section 3.3.1, ψ_{10} does not depend on x_1 and the second order slow drift velocity in the x direction is accounted for by ψ_{20x}. Integrating the normal derivative of ψ_{20} around the 'boundaries' of the near field S_{∞}^{+}, S_{∞}^{-}, S_B and S_F (see Figure 4.1) at say $(x_1 = -L_1 \equiv - \epsilon L)$, we find as in Section 3.3.1 a result similar to (3.3.34). It is:

$$\int_{S_{\infty}^{+}(-L)} \psi_{20x} \, dz - \int_{S_{\infty}^{-}(-L)} \psi_{20x} \, dz = -[h'U(-L+\infty) - h \, U(-L-\infty)] \tag{4.3.12a}$$

where $S_{\infty}^{\pm}(-L)$ and $(x \rightarrow - L \pm \infty)$ both stand for the matching boundaries to the right and to the left of the edge at $(x_1 = -L_1)$. The derivation of (4.3.12) is even simpler than that of (3.3.34) in the floating body case, since there are no moving boundaries. At $(x_1 = L_1)$, we have, similarly,

$$\int_{S_{\infty}^{+}(L)} \psi_{20x} \, dz - \int_{S_{\infty}^{-}(L)} \psi_{20x} \, dz = -[hU(L+\infty) -h'(U(L-\infty)] \tag{4.3.12b}$$

To match with the near field near the depth discontinuity at $(x = -L)$, we may write the inner expansion of ϕ_{10} (see 3.1.11) as follows:

$$\phi_{10} \sim [\phi_{10}^A + \phi_{10}^B + \phi_{10}^G]_{x_1 = -L_1} + x_1 \{[-\mu \, \phi_{10}^A + \mu \, \phi_{10}^B]_{t_1} + \phi_{10x_1}^G \}$$
$$(x_1 \rightarrow - L_1^-)$$

$$\phi_{10} \sim [\phi_{10}^D + \phi_{10}^E + \phi_{10}^H + \phi_{10}^I]_{x_1 = -L_1} + x_1 [-\mu' \, \phi_{10}^D + \mu' \, \phi_{10}^E - \beta' \, \phi_{10}^H + \beta' \, \phi_{10}^I]_{t_1}$$
$$(x_1 \rightarrow - L_1^+)$$

$$\phi_{10} \sim [\phi_{10}^D + \phi_{10}^E + \phi_{10}^H + \phi_{10}^I]_{x_1 = L_1} + x_1 [-\mu' \, \phi_{10}^D + \mu' \, \phi_{10}^E - \beta' \, \phi_{10}^H - \beta' \, \phi_{10}^I]_{t_1}$$
$$(x_1 \rightarrow L_1^-)$$

$$\phi_{10} \sim [\phi_{10}^C + \phi_{10}^J]_{x_1 = L_1} + x_1 [-\mu \, \phi_{10t_1}^C + \phi_{10x_1}^J] \qquad (x_1 \rightarrow L_1^+) \qquad (4.3.13)$$

Use has been made of the simple relations between t_1 and x_1 derivatives of these terms.

Matching (4.3.13) to the outer expansion of the slow potential from (4.3.11) and (4.3.12) we get:

$$\phi_{10}^A + \phi_{10}^B + \phi_{10}^G = \psi_{10}^- = \phi_{10}^D + \phi_{10}^E + \phi_{10}^H + \phi_{10}^I \qquad (x_1 = -L_1)$$

$$\phi_{10}^D + \phi_{10}^E + \phi_{10}^H + \phi_{10}^I = \psi_{10}^+ = \phi_{10}^C + \phi_{10}^J \qquad (x_1 = L_1)$$

$$h \, [-\mu \, \phi_{10t_1}^A + \mu \, \phi_{10t_1}^B + \phi_{10x_1}^G] - h'[-\mu' \, \phi_{10}^D + \mu' \, \phi_{10}^E - \beta' \, \phi_{10}^H + \beta' \, \phi_{10}^I]_{t_1}$$

$$= h' \, U(-L + \infty) - h \, U(-L - \infty) \qquad (x_1 = -L_1)$$

$$h' \, [-\mu' \, \phi_{10}^D + \mu' \, \phi_{10}^E - \beta' \, \phi_{10}^H + \beta' \, \phi_{10}^I]_{t_1} - h[-\mu \, \phi_{10t_1}^C - \phi_{10x_1}^J] =$$

$$= h \, U(L + \infty) - h' \, U(L - \infty) \qquad (x_1 = L_1) \qquad (4.3.14)$$

On the other hand, the Stokes drift terms hU and $h'U$ are determined from (3.3.27) as in (3.3.33). They are:

$$hU = h \operatorname{Re} \underline{U}^{(1)} e^{-2i\Omega t_1} \equiv \frac{2\omega\alpha}{g} f_0^2(0) \left(\left|\tilde{A}\right|^2 - \left|\tilde{B}\right|^2 \right) \qquad (x_1 = -L_1^-)$$

$$h'U = h' \operatorname{Re} \underline{U}^{(2)} e^{-2i\Omega t_1} \equiv \frac{2\omega\alpha'}{g} f_0'^2(0) \left(\left|\tilde{D}\right|^2 - \left|\tilde{E}\right|^2 \right) \qquad (x_1 = -L_1^+)$$

$$\quad (4.3.15)$$

$$h'U = h' \operatorname{Re} \underline{U}^{(3)} e^{-2i\Omega t_1} \equiv \frac{2\omega\alpha'}{g} f_0'^2(0) \left(\left|\tilde{D}\right|^2 - \left|\tilde{E}\right|^2 \right) \qquad (x_1 = L_1^-)$$

$$hU = h \operatorname{Re} \underline{U}^{(4)} e^{-2i\Omega t_1} \equiv \frac{2\omega\alpha}{g} f_0^2(0) \left|\tilde{C}\right|^2 \qquad (x_1 = L_1^+)$$

where $\left|\tilde{}\right|^2$ stands for the oscillatory part of $\left|\right|^2$ and has an exponential factor as in (4.3.1).

We note that in contrast to the cases of Section 3.3, where the Stokes' Drift terms eventually cancelled, they have a non zero net contribution in the present problem. The reason is that in the floating body problem, conservation of energy was equivalent to conservation of mass in the drift terms, since the depth and wavenumber were the same on both sides of the body. At the present case the depth difference results in a net mass flux.

When (4.3.1), (4.3.3) and (4.3.8) are substituted into (4.3.14) we arrive at four linear equations for $\underline{G}$, $\underline{H}$, $\underline{I}$, and $\underline{J}$. These can be solved to yield a full solution for the long waves, without having to explicitly solve for the full second order potential.

We get:

$$[b] \begin{bmatrix} \underline{G} \\ \underline{H} \\ \underline{I} \\ \underline{J} \end{bmatrix} = \begin{bmatrix} a_1 \\ a_2 \\ a_3 \\ a_4 \end{bmatrix}$$

(4.3.16)

where the matrix b is given by:

$$\begin{bmatrix} e^{-2\Omega\beta L_1} & -e^{-2i\Omega\beta' L_1} & -e^{2i\Omega\beta' L_1} & 0 \\ 0 & e^{2i\Omega\beta' L_1} & e^{-2i\Omega\beta' L_1} & -e^{-2\Omega\beta L_1} \\ 2\Omega h\beta e^{-2\Omega\beta L_1} & -2i\Omega h'\beta' e^{-2i\Omega\beta' L_1} & 2i\Omega h'\beta' e^{2i\Omega\beta' L_1} & 0 \\ 0 & -2i\Omega h'\beta' e^{2i\Omega\beta' L_1} & 2i\Omega h'\beta' e^{-2i\Omega\beta' L_1} & -2\Omega h\beta e^{-2\Omega\beta L_1} \end{bmatrix}$$

(4.3.17)

and a_1, a_2, a_3, and a_4 are the locked wave components in (4.3.14):

$$a_1 = -\underline{A}\, e^{-2i\Omega\mu L_1} - \underline{B}\, e^{2i\Omega\mu L_1} + \underline{D}\, e^{-2i\Omega\mu L_1} + \underline{E}\, e^{2i\Omega\mu L_1}$$

$$a_2 = \underline{C}\, e^{2i\Omega\mu L_1} - \underline{E}\, e^{-2i\Omega\mu L_1} - \underline{D}\, e^{2i\Omega\mu L_1}$$

$$a_3 = -h[(-\mu\underline{A}\, e^{-2i\Omega\mu L_1} + \mu\underline{B}\, e^{2i\Omega\mu L_1})(-2i\Omega) + \underline{U}^{(1)}]$$

$$+ h'[(-\mu'\underline{D}\, e^{-2i\Omega\mu' L_1} + \mu'\underline{E}\, e^{2i\Omega\mu' L_1})(-2i\Omega) + \underline{U}^{(2)}]$$

$$a_4 = -h[(-\mu'\underline{E}\, e^{-2i\Omega\mu' L_1} + \mu'\underline{D}\, e^{2i\Omega\mu' L_1})(-2i\Omega) + \underline{U}^{(3)}]$$

$$+ h'[-\mu'\underline{C}\, e^{2i\Omega\mu L_1}(-2i\Omega) + \underline{U}^{(4)}]$$

The matrix (4.3.17) becomes singular when:

$$\text{Im}[(\beta h + i\beta' h')^2 \, e^{4i\Omega\beta' L_1}] = 0 \qquad (4.3.18)$$

(see Mei (1983, p. 141)) which means that there is infinite resonance of the trapped free waves at the frequencies

$$2\Omega_n \beta' L_1 = tg^{-1} \frac{\beta h}{\beta' h'} + \frac{1}{2} n\pi \qquad (4.3.19)$$

We note that the second and third columns of (4.3.17) are complex conjugates of each other. This means that

$$\underline{I}(2\Omega) = -\underline{H}^*(2\Omega) \qquad (4.3.20)$$

Hence the free wave on the shelf is of the form

$$\text{Re}[\underline{H} \, e^{2i\Omega(t_1 - \beta' x_1 - vy_1)} - \underline{H}^* e^{2i\Omega(t_1 + \beta' x_1 - vy_1)}]$$

$$= \text{Re}[|\underline{H}| \, e^{2i\Omega(t_1 - vy_1)}] \sin(2\Omega\beta' x_1 - arg\underline{H})$$

which is a standing wave in the x_1 direction, propagating in the y_1 direction.

$\underline{H}$ is found from (4.3.16) by Cramer's method:

$$\underline{H} = \frac{\begin{bmatrix} e^{-2\Omega\beta L_1} & a_1 & -e^{2i\Omega\beta' L_1} & 0 \\ 0 & a_2 & e^{-2i\Omega\beta' L_1} & -e^{-2\Omega\beta L_1} \\ 2\Omega h\beta e^{-2\Omega\beta L_1} & a_3 & 2i\Omega h'\beta' e^{2i\Omega\beta' L_1} & 0 \\ 0 & a_4 & 2i\Omega h'\beta' e^{-2i\Omega\beta' L_1} & -2\Omega h\beta e^{-2\Omega\beta L_1} \end{bmatrix}}{4\Omega^2 \sin 2\beta' L_1 (2\Omega - 2\Omega_0)} \qquad (4.3.21)$$

where the left hand side of (4.3.18) was written as a sine.

Figure 4.5 shows the variation of the normalized $h\left|\underline{H}\right|/A^2$ with Ω/ω. The resonant frequencies correspond to the roots of (4.3.19). The spacing between them is simply $\pi/(4\beta'L_1)$.

The location of the first resonance Ω_0 is given by

$$2\Omega_0 = \frac{1}{\beta'L_1}\ tg^{-1}\ \frac{\beta h}{\beta'h'} \qquad (4.3.22)$$

The leading behaviour of Ω_0 is due to the factor $1/(\beta'L_1)$. In Figure 4.6, Ω_0 is plotted versus the angle of incidence of the waves.

In the special case of normal incidence ($\gamma = \nu = 0$), Equation (4.3.8) is replaced by:

$$\phi_{10}^F = \phi_{10}^G = \text{Re}\underline{G}\ e^{-2i\Omega(t_1 + x_1/\sqrt{gh})} \qquad (x_1 < -L_1)$$

$$\phi_{10}^F = \phi_{10}^H + \phi_{10}^I \qquad (\left|x_1\right| < L_1)$$

with

$$\phi_{10}^H = \text{Re}\underline{H}\ e^{-2i\Omega(t_1 - x_1/\sqrt{gh'})} \qquad (4.3.23)$$

$$\phi_{10}^I = \text{Re}\underline{I}\ e^{-2i\Omega(t_1 - x_1/\sqrt{gh'})}$$

and

$$\phi_{10}^F = \phi_{10}^J = \text{Re}\underline{J}\ e^{-2i\Omega(t_1 - x_1/\sqrt{gh})} \qquad (x_1 > -L_1)$$

The free wave off the shelf is now propagating. Equations (4.3.16) and (4.3.17) are still valid (with β imaginary). The normalized $h\left|\underline{H}\right|/A^2$ is plotted in Figure 4.5. No infinite resonance occurs, and the variation with Ω or L is minute.
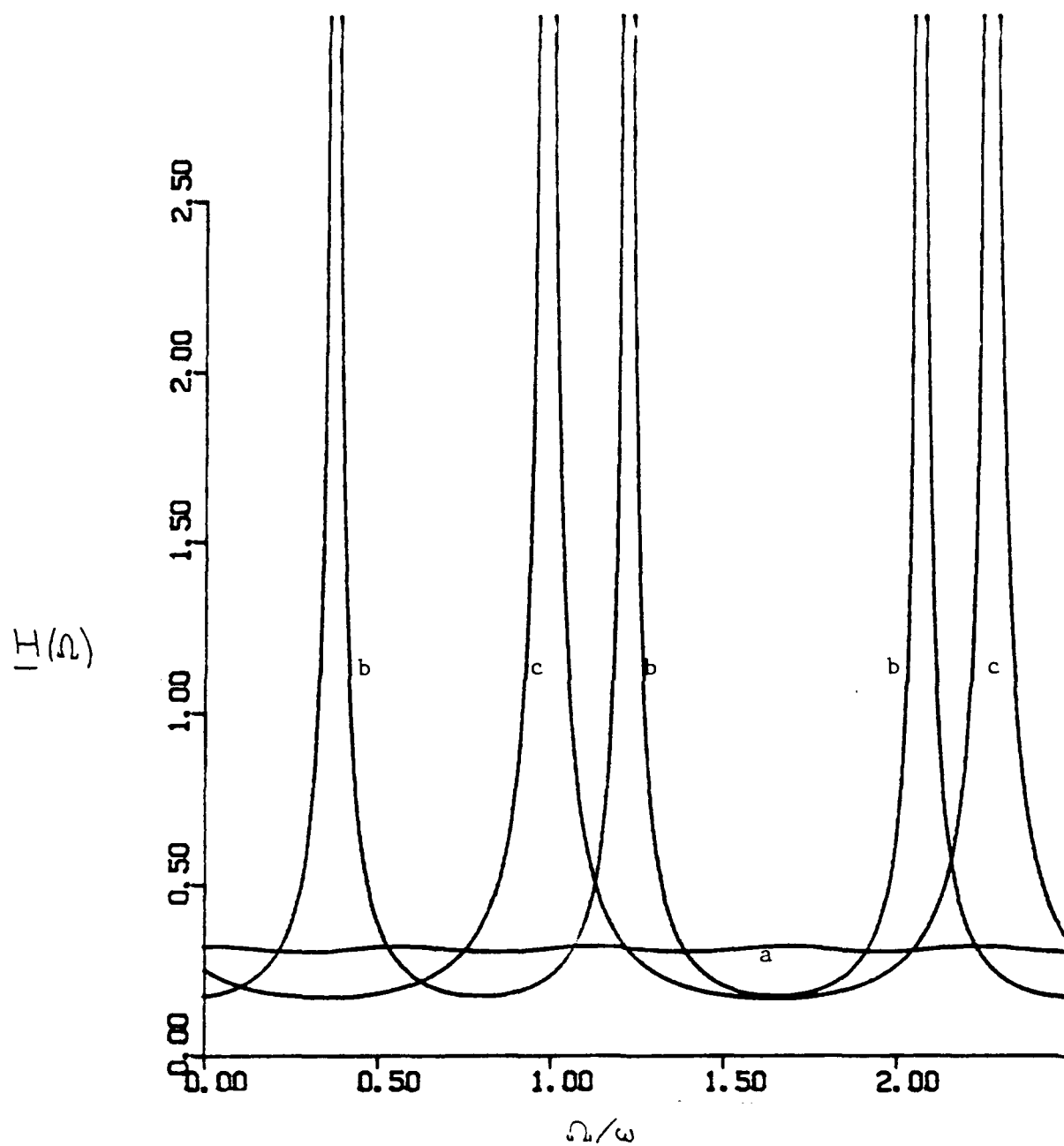
Figure 4.5   The Frequency Response $\underline{H}(\Omega)$ Normalized by a^2/h, versus Ω/ω (L/h = 10., L'/h = 0.5, σh = 1) for Three Angles of Incidence: a) Normal Incidence (0^0) b) 40^0 and c) 50^0.
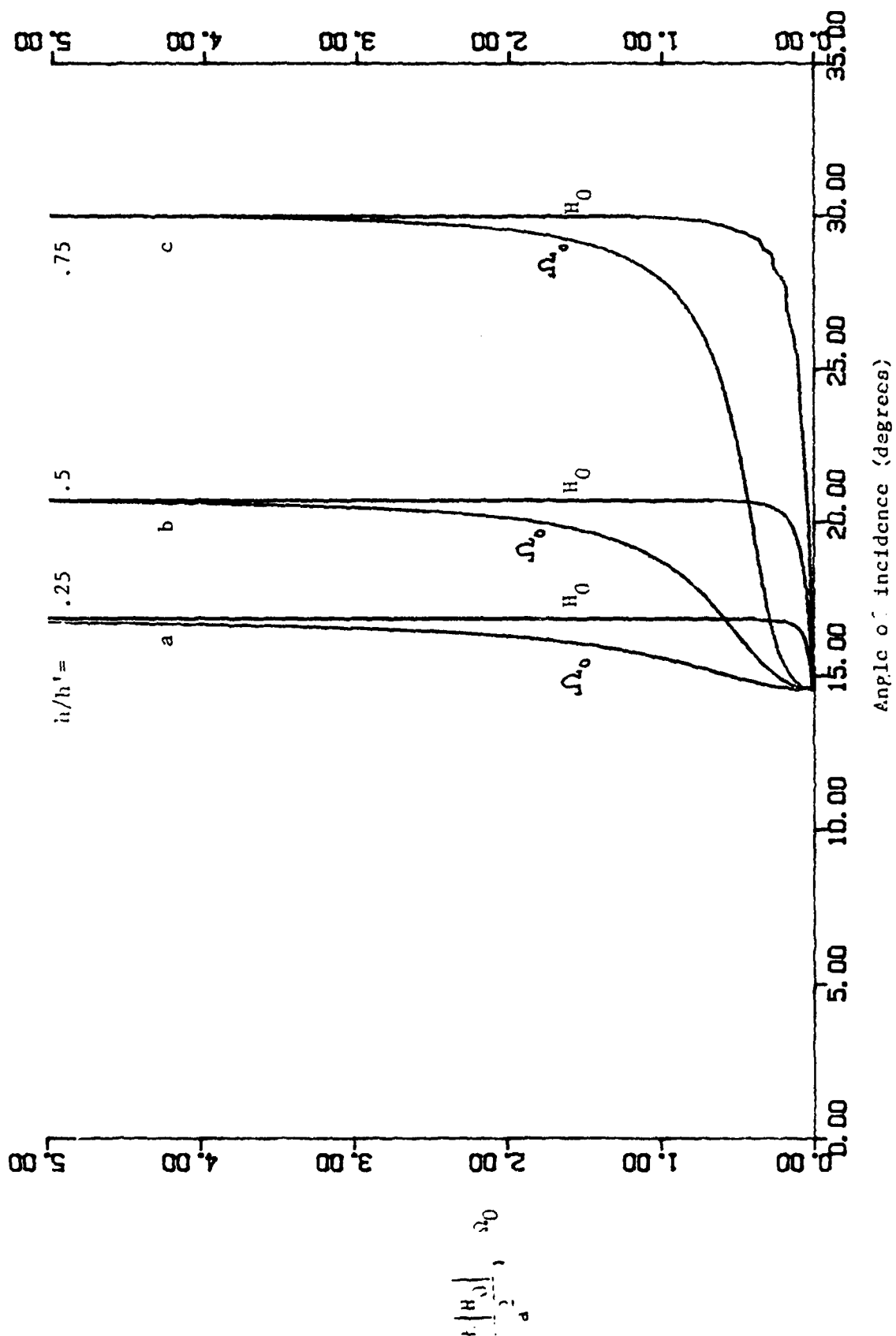
Figure 4.6 The Modulation Frequency Ω_0 at Which the First Pole Occurs and the Value of H_0, the Residue at Ω_0 for Three Depth Ratios: a) $h'/h = 0.25$, b) $h'/h = 0.5$ and c) $h'/h = 0.75$; ($L/h = 10.$, $\sigma h = 4.$).

109

4.4 Transient Response

We have found that the trapped long waves due to obliquely incident short waves can have an infinite resonance at certain modulation frequencies. This, of course, is physically impossible. Note, however, that the present theory relates to times on the scale of t_1, whereas the frequency response is calculated for a periodic incident wave envelope. Longer time scales, and hence, higher order effects need to be considered. Foda & Mei (1981) have derived a nonlinear Schrödinger Equation for the development of the resonated long waves on a mildly sloping ridge. They found that a higher order radiation damping limits the magnitude of resonance. We shall examine instead the transient response of the ridge to a narrow banded incident wave of finite duration on the time scale of t_1. In particular, for oblique incidence we shall focus on the case where the spectrum peak coincides with a resonant frequency.

We start by looking at the case of normal incidence, which does not lead to wave trapping, but is the easiest to perform experiments for.

When $-\beta^2$ is positive, the governing equation for ϕ_{10} can be easily solved using finite differences in time. The response is passive, and the free waves and the forced waves 'echo' on both edges of the shelf.

The method of solution is as follows: first we solve for the short waves. Given $A(L_1, t_1)$ we note that:

$$D(L_1, t_1) = D(-L_1, t_1 - L_1/C_g'); \quad E(-L_1, t_1) = E(L_1, t_1 - L_1/C_g')$$

making use of these relations to account for the propagation across the ridge, we solve (4.2.4) and (4.2.5) at each time step, to find the short-wave

amplitudes: A, B, D and E at $(x_1 = L_1)$ and C, D and E at $(x_1 = L_1)$, see Figures 4.7a. The locked long-waves are computed from these amplitudes through (4.3.1) and (4.3.3) and the Stokes' drift terms are found from (4.3.15).

We can now eliminate the x_1 derivative from (4.3.14) via:

$$\phi^G_{10_{x_1}} = -|\beta|\ \phi^G_{10_{t_1}} ; \qquad \phi^J_{10_{x_1}} = |\beta|\ \phi^J_{10_{t_1}}$$

to get coupled equations for $\phi^{(\alpha)}_{10}$ $(\alpha = G, H, I, J)$ that involve only t_1 derivatives. Making use of

$$\phi^H_{10}(L_1, t_1) = \phi^H_{10}(-L_1, t_1 - L_1/\sqrt{gh'}); \quad \phi^J_{10}(L_1, t_1) = \phi^J_{10}(-L_1, t_1 - L_1/\sqrt{gh'})$$

We integrate (4.3.14) numerically with respect to time from $(t_1=0)$ on and determine the free long waves at $-L_1$ and at L_1.

In Figure 4.7b the wave characteristics of the long waves are sketched in an (x_1, t_1) diagram.

The resulting transient response to a sinosoidal packet at the left edge $(x_1 = -L_1)$ and at the right edge $(x_1 = L_1)$ is plotted in Figure 4.8. Interference of the free waves and the locked waves can be seen after one reflection. At later times the response is negligible.

For oblique incidence with wave trapping, ϕ^F_{10} becomes evanescent off the shelf and we shall use a Fourier Transform of the incident wave in conjunction with the frequency response to determine the transient response. Let the incident wave envelope be a Gaussian:

111

(a) The Short-wave Groups and their Amplitudes.

$E = R'D = R'TA$

$-C_g'$ C_g

$C = T'D$
$= T'TA$

t_1

$D = TA$

$B = RA$

$-C_g$ C_g'

A

C_g

L L x_1
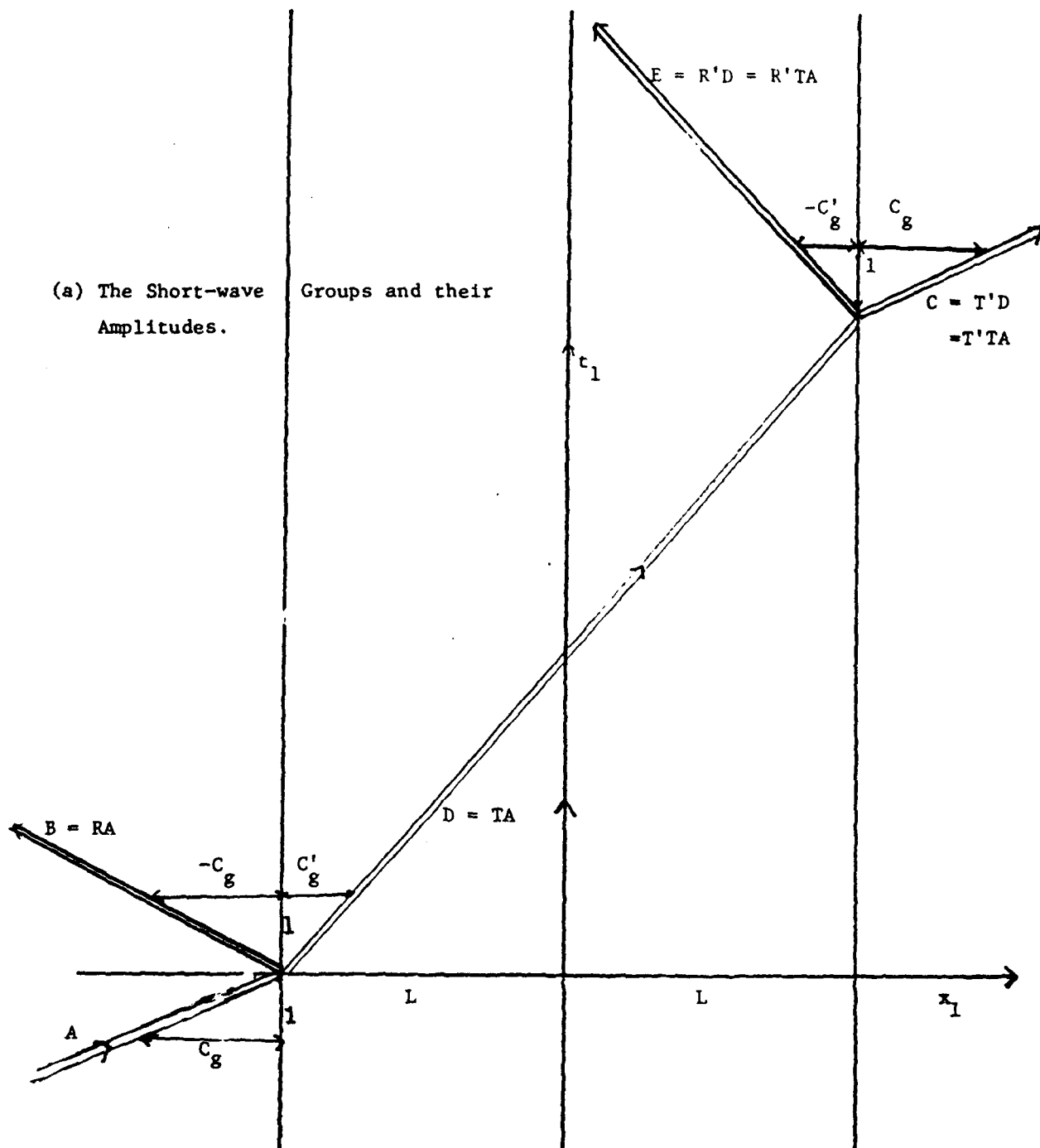
Figure 4.7 An (x_1, t_1) Diagram of the Long-waves for Normal Incidence
on a Shelf.

112

Figure 4.7

Legend:
——————— Locked Long-waves
– – – – – Free Long-waves

113
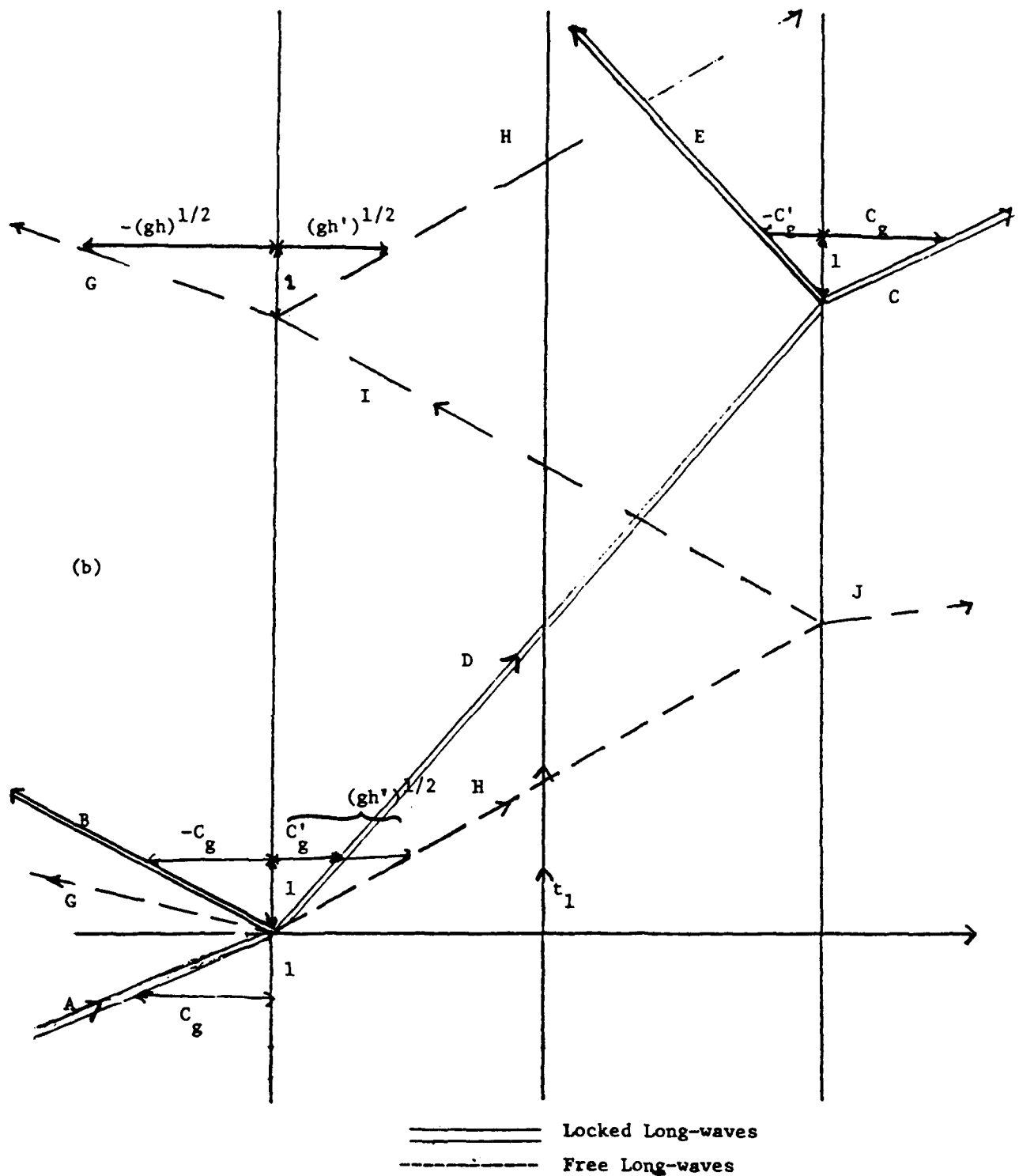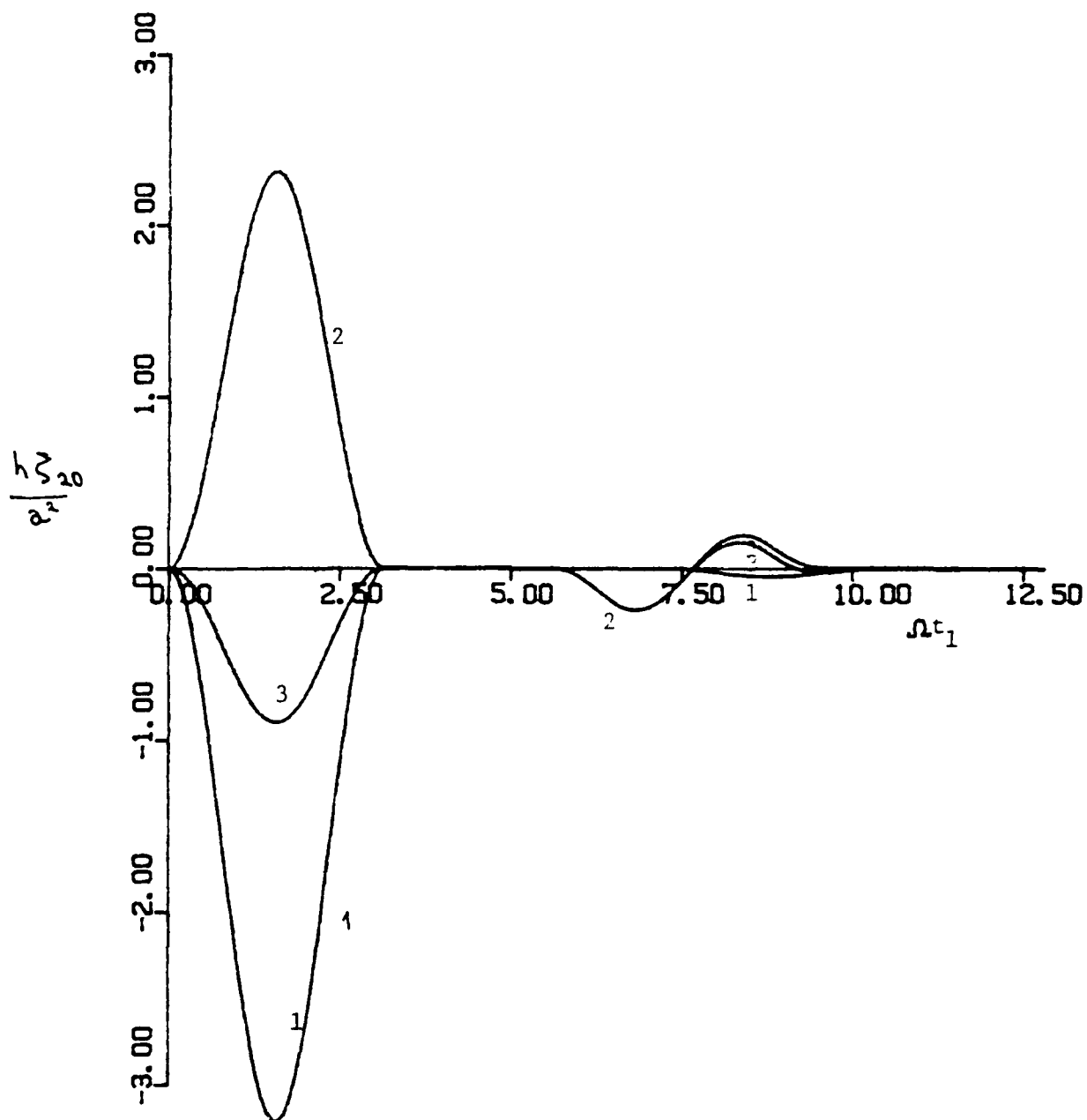
Figure 4.8 The Long-wave Transient Response of a Ridge to Normally Incident Waves
$h\zeta_{20}/a^2$, a) at the Left Edge and b) at the Right Edge of the Shelf,
versus Ωt, (h'/h = 0.5, L/h = 10, σh = 1, Ω/ω = 1) 1) the locked
Waves, 2) the Free Waves, and 3) the Total Slow-wave.

114

(b)
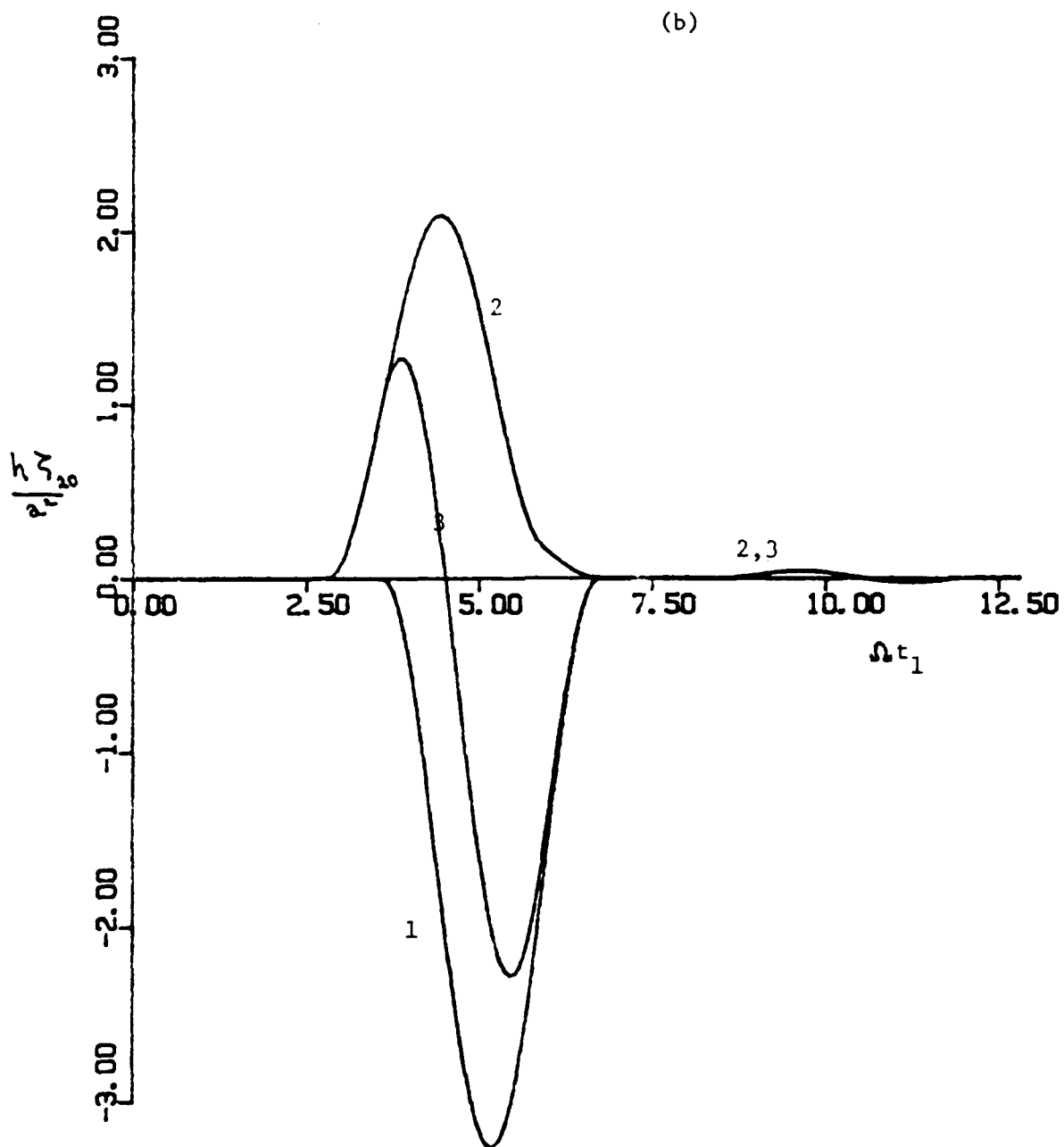
Figure 4.8

$$A = \text{Re } e^{-i\Omega_0 \rho - \frac{1}{2} w^2 \rho^2} \tag{4.4.1}$$

where ρ is the phase function:

$$\rho \equiv t_1 - \mu_1 x_1 - \nu y_1 \tag{4.4.2}$$

and

$$w \ll \Omega_0 \tag{4.4.3}$$

is the characteristic length of the packets.

The Fourier Transform of $|A|^2$ with respect to 2Ω is

$$F.T.(|A|^2) \equiv \frac{1}{2\pi} \int_{-\infty}^{\infty} d\rho \ |A|^2 \ e^{2i\Omega\rho}$$

$$= F.T. \ (\frac{1}{2} e^{-w^2\rho^2} + \frac{1}{4} e^{2i\Omega_0\rho - w^2\rho^2} + \frac{1}{4} e^{-2i\Omega_0\rho - w^2\rho^2}) \tag{4.4.4}$$

$$= \frac{1}{8w\sqrt{\pi}} \ [2e^{-\Omega^2/w^2} + e^{-(\Omega-\Omega_0)^2/w^2} + e^{-(\Omega+\Omega_0)^2/w^2}]$$

Let us examine the transient response for H, the right going free wave on the shelf at a point along the axis ($x_1 = 0$, $y_1 = 0$).

$$H(0, 0, t_1) = 2\text{Re} \int_{-\infty}^{\infty} d2\Omega \ \underline{H}(2\Omega) \ e^{-2i\Omega t_1} \ F.T.|A|^2) \tag{4.4.5}$$

since $\underline{H}$ (2Ω) is the complex amplitude of the frequency response to a component of $|A|^2$ in the form

$$\frac{1}{2} \text{Re } e^{-2i\Omega\rho} \tag{4.4.6}$$

116

To accentuate the resonance effect, we choose $2\Omega_0$ that lies on a pole of $\underline{H}(2\Omega)$. The leading term of (4.4.5) will be the contribution from that pole. The Gaussian dependence will make all other contributions negligible because of (4.4.3), and only the second term of (4.4.4) should be kept. The result is

$$H(0, 0, t_1) \simeq \frac{1}{4w\sqrt{\pi}} \, \text{Re} \int_{-\infty}^{\infty} d\,(2\Omega)\frac{H_0}{2(\Omega-\Omega_0)} e^{-2i\Omega t_1 - (\Omega-\Omega_0)^2/w^2} \qquad (4.4.7)$$

where H_0 is the residue of $\underline{H}$ at the pole of H as a function of 2Ω at $2\Omega = 2\Omega_0$. The values of H_0 will be discussed later.

The integration path is slightly above the real axis in order to make H tend to zero as t_1 goes to $-\infty$. This integral can be analyzed by the method of steepest descent. In the complex plane 2Ω, the phase function

$$g(2\Omega) = -2i\Omega t_1 - \frac{(\Omega-\Omega_0)^2}{w^2} \qquad (4.4.8)$$

has a saddle point s at:

$$2\Omega = 2\Omega_0 - 2iw^2 t_1 \qquad (4.4.9)$$

(see Figure 4.9). We transform the integration path to a path through s:

$$H(0, 0, t_1) \simeq \frac{1}{4w\sqrt{\pi}} \, \text{Re} \int_{-\infty-2iw^2 t_1}^{\infty-2iw^2 t_1} d2\Omega \, \frac{H_0}{2(\Omega-\Omega_0)} e^{-2i\Omega t_1 - (\Omega-\Omega_0)^2/w^2}$$

$$\qquad (4.4.10)$$

$$+ \, U(t_1) \, \text{Re}\left[-2\pi i \, \frac{H_0}{4w\sqrt{\pi}} e^{-2i\Omega_0 t_1}\right]$$

where U is the unit step function and the last term is due to the residue and is added by Cauchy's theorem when the pole at $2\Omega_0$ is traversed for positive
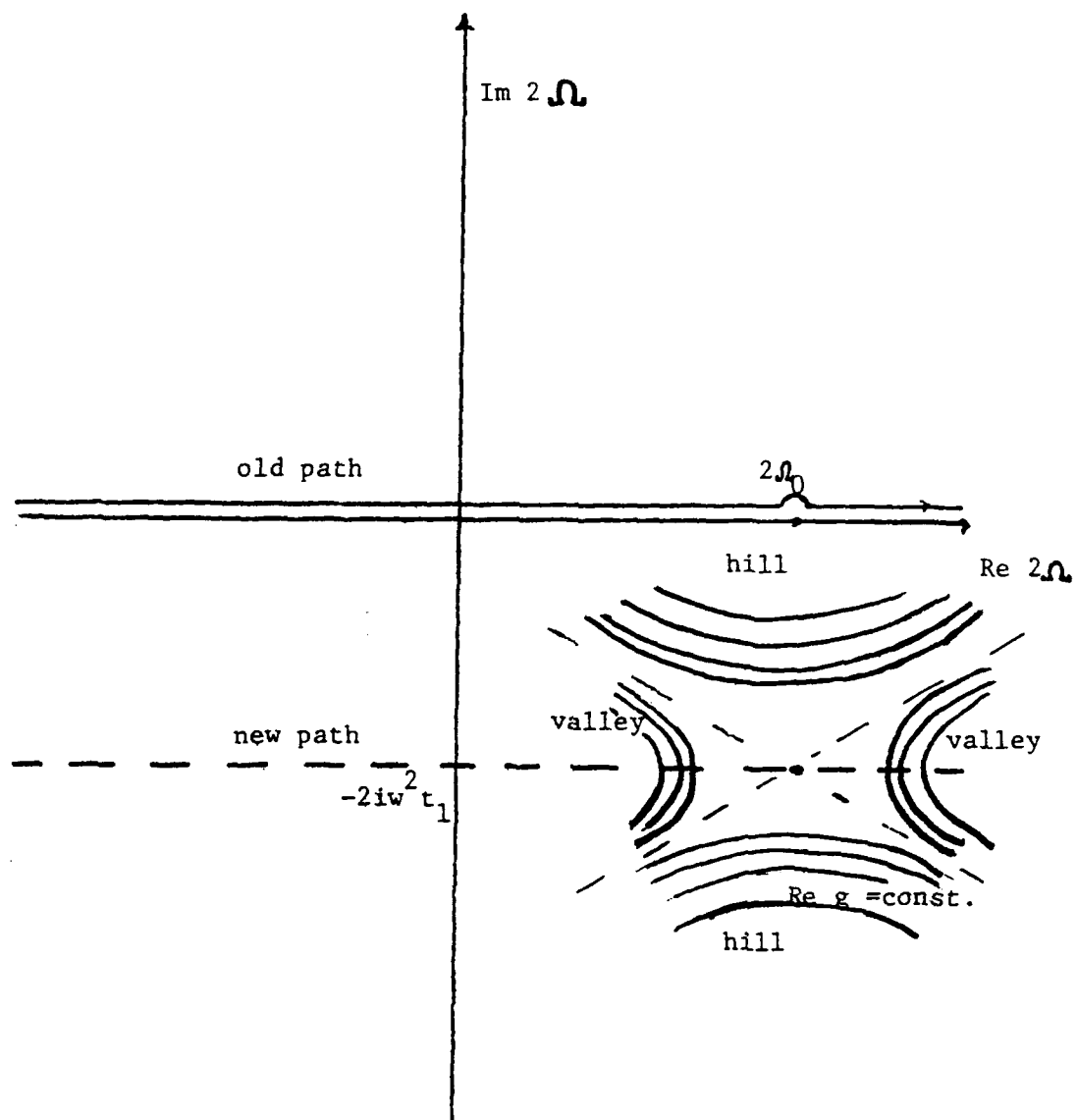
Figure 4.9 The Complex 2Ω Plane; s is the Saddle Point of Re g.

t_1. The contributions from the vertical segments connecting the present path with the real axis at both infinities vanish because of the Gaussian factor.

The integral in (4.4.10) can be evaluated by the following change of variable:

$$\sigma = 2\Omega - 2\Omega_0 + 2iw^2 t_1 \qquad (4.4.11)$$

It becomes

$$\frac{H_0}{4w\sqrt{\pi}} e^{-w^2 t_1^2 - 2i\Omega_0 t_1} \int_{-\infty}^{\infty} d\sigma \frac{e^{-\sigma^2/4w^2}}{\sigma - 2iw^2 t_1} \qquad (4.4.12)$$

This last integral has been evaluated (Carrier 1970) and is given by

$$\text{sgn}(t_1) \, i\pi \, e^{w^2 t_1^2} [1 - \text{erf } w|t_1|] \qquad (4.4.13)$$

(4.4.10), (4.4.12) and (4.4.13) can be combined to give:

$$H(0, 0, t_1) \simeq \text{Re } \frac{iH_0\sqrt{\pi}}{4w} \{\text{sgn}(t_1) [1 - \text{erf } w|t_1|] - 2 U(t_1)\} e^{-2i\Omega_0 t_1} \qquad (4.4.14)$$

Equation (4.3.21) describes the spatial structure of the total free wave on the shelf.

The strength of the transient response (4.4.14) depends on the energy in the input packet via $1/w$ which represents its length, and on H_0.

To find H_0, we replace the denominator of (4.3.21) by $2\beta'L_1$, hence H_0 is proportional to $1/(\beta'L_1)$ and is an almost linear functions of Ω_0 cf. (4.3.22). In Figure 4.6 H_0 is plotted versus the angle of incidence of the short waves.

Figure 4.10 shows the response of the trapped waves to the transient input (4.4.1). As seen in (4.4.14) there is a transient part that builds up before the arrival of the peak of the envelope and decays after its arrival, and a steady 'wake' due to the contribution from the pole, that follows the short-wave groups passage along the ridge and keeps oscillating at the resonance frequency on the ridge, long after all other waves are gone. The steady reverberation in the wake is, of course valid only for time scales that are within the scope of the theory, namely on the t_1 scale. Over much longer time scales, higher order effects will diminish the wake. This behaviour is typical of various wave guides.

We now turn to the diffraction of slowly varying waves in a two layer fluid.
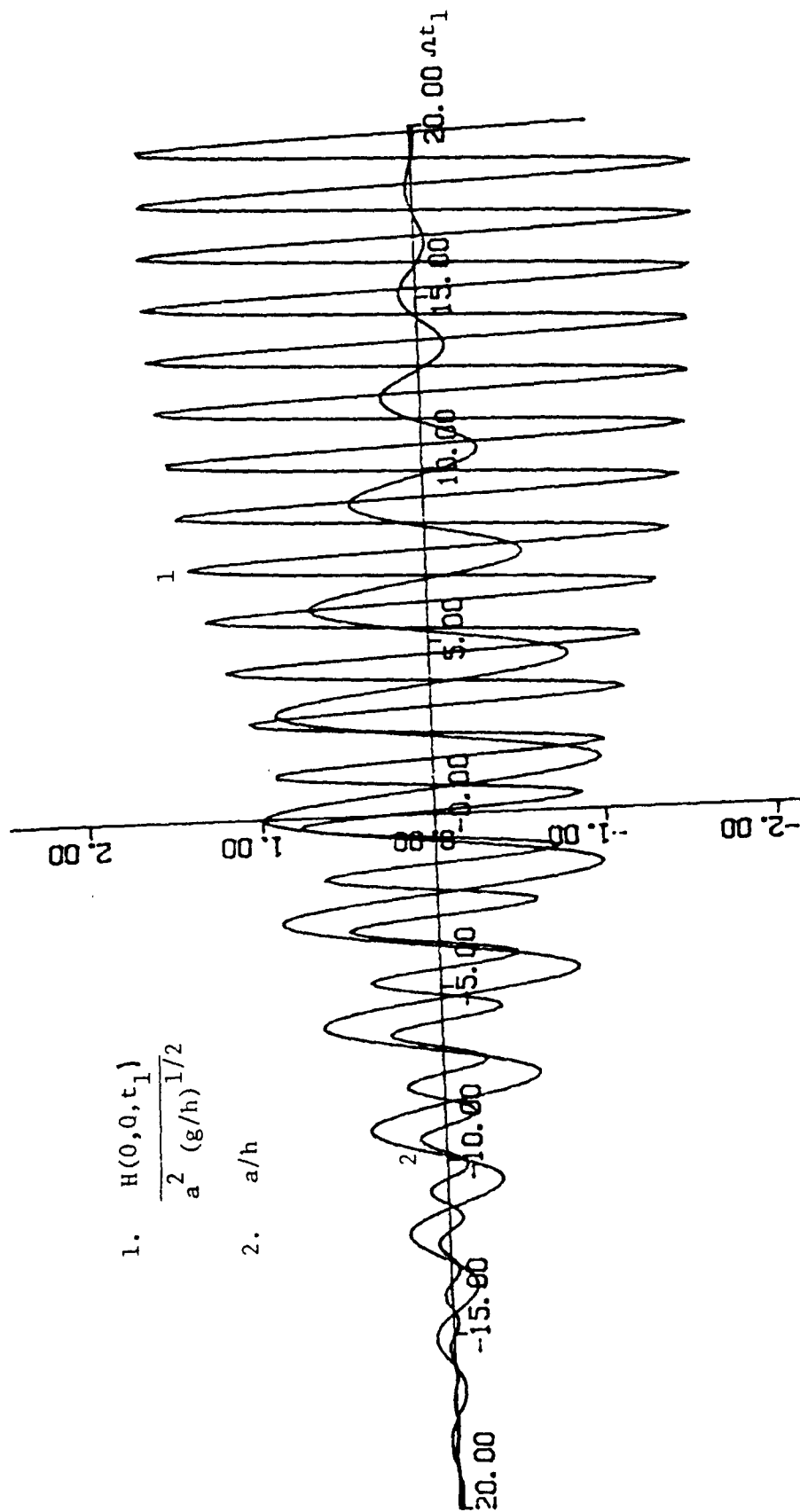
Figure 4.10 Transient Response for an Obliquely Incident Gaussian Wave Packet. The Incident Short-wave Amplitude and the Value of H $(0, 0, t_1)$ are Plotted versus t_1. Angle of Incidence is $20.7°$, $h'/h = 0.5$, $L/h = 10$, $\sigma h = 1$, Ω/ω is 2.07 and $H_0 = 0.16 - .0791$; in a) $w = 0.1$ and in b) $w = 0.2$

Figure 4.10

(b)

1. $\dfrac{H(0,0,t_1)}{a^2}\,(g/h)^{1/2}$

2. a/h
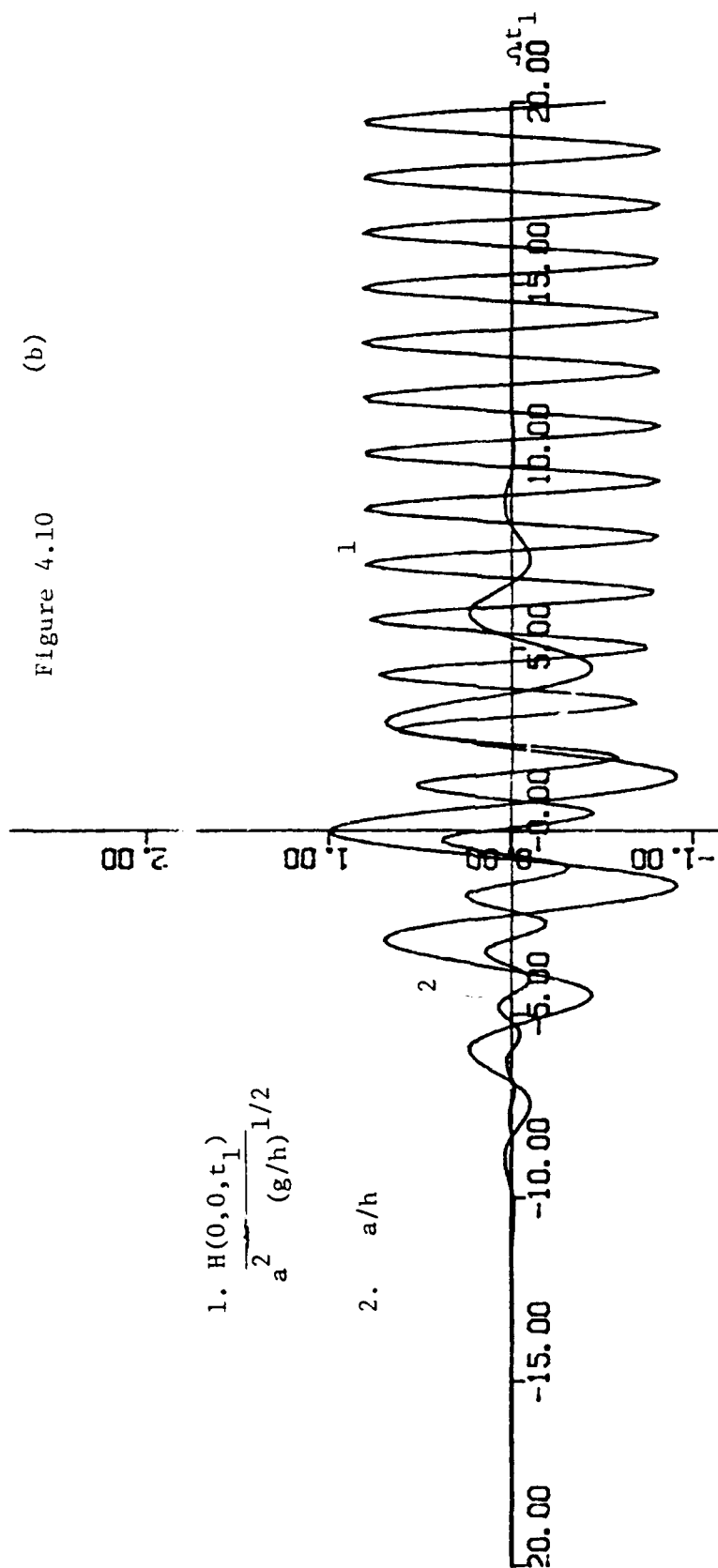
5. EXCITATION OF INTERNAL WAVES IN THE LEE OF A BREAKWATER BY SLOWLY VARYING SURFACE WAVES

5.1 Introduction and Definitions

It is well known that surface waves can interact nonlinearly to produce internal waves. Past research in this field has been concentrated on the resonant interaction of two surface wave components with an internal wave, in an open sea. This type of work was started by Ball (1964) and is still being continued (c.f. Dysthe and Das (1981) and references therein). In this chapter we shall study the interaction away from resonance combined with diffraction by a long breakwater. The short-wave groups and the "locked" internal waves propagating with them will be shown to exist in the lit zone but not in the shadow zone. Free internal waves will be required to maintain continuity of the long wave field across the shadow boundary. We shall see that the free long waves are slower than the locked long waves and hence the free long waves will radiate away from the shadow boundary into the shadow zone (and the lit zone). This mechanism can be important for resonant excitation in bays and behind straits. The method of solution will again involve the use of multiple scales and asymptotic matching of near fields and far fields.

The sea is modeled as a two layer fluid with the lower layer of density ρ and depth h, and the upper layer of density ρ' and depth h'. The origin of the coordinate system is chosen at the interface between the two layers with

123

the z axis pointing upwards. The breakwater is lying on the positive y axis and the waves are normally incident from $(x \to -\infty)$ (see Figure 5.1).

Let us first determine the forced internal wave in an _open_ sea. As in Lamb (1932, p. 372) the short waves have a potential

$$\phi_{11} = A_0 f_0 \, e^{ikx} \equiv A_0 \cosh k(z+h) \, e^{ikx} \qquad (-h < z < 0) \quad (5.1.1)$$

in the lower layer, and

$$\phi'_{11} = A_0 f'_0 \, e^{ikx} \equiv A_0 \, (C \cosh kz + B \sinh kz) e^{ikx} \qquad (0 < z < h') \quad (5.1.2)$$

in the upper layer.

Matching the vertical velocities at $(z=0)$ we get:

$$-k \sinh kh = -kB = i\omega b \qquad (5.1.3)$$

where $A_0 b$ is the interface displacement amplitude for the short wave. Matching the pressures at the interface gives:

$$\rho(i\omega \cosh kh - gb) = \rho'(i\omega C - gb) \qquad (5.1.4)$$

At the free surface $(z = h')$ the usual boundary condition leads to

$$\omega^2(C \cosh kh' + B \sinh kh') = gk(C \sinh kh' + B \cosh kh') \qquad (5.1.5)$$

b, B and C may be determined from (5.1.3) and (5.1.4):

$$b = ik/\omega \sinh kh$$

$$B = \sinh kh \qquad (5.1.6)$$

$$C = \rho/\rho' \cosh kh - gk/\omega^2 \, (\rho-\rho')/\rho' \sinh kh$$

Substituting these in (5.1.5) yields the dispersion relation

$$\omega^4 \, (\rho \coth kh \coth kh' + \rho') - \omega^2 \, \rho(\coth kh' + \coth kh) \, gk$$

$$+ (\rho - \rho') \, g^2 k^2 = 0 \qquad (5.1.7)$$

reflection zone

far field

breakwater

shadow zone

reflection boundary

shadow boundary

near
field

near field

far field

TOP VIEW

ρ'

h'

z

x

ρ

h
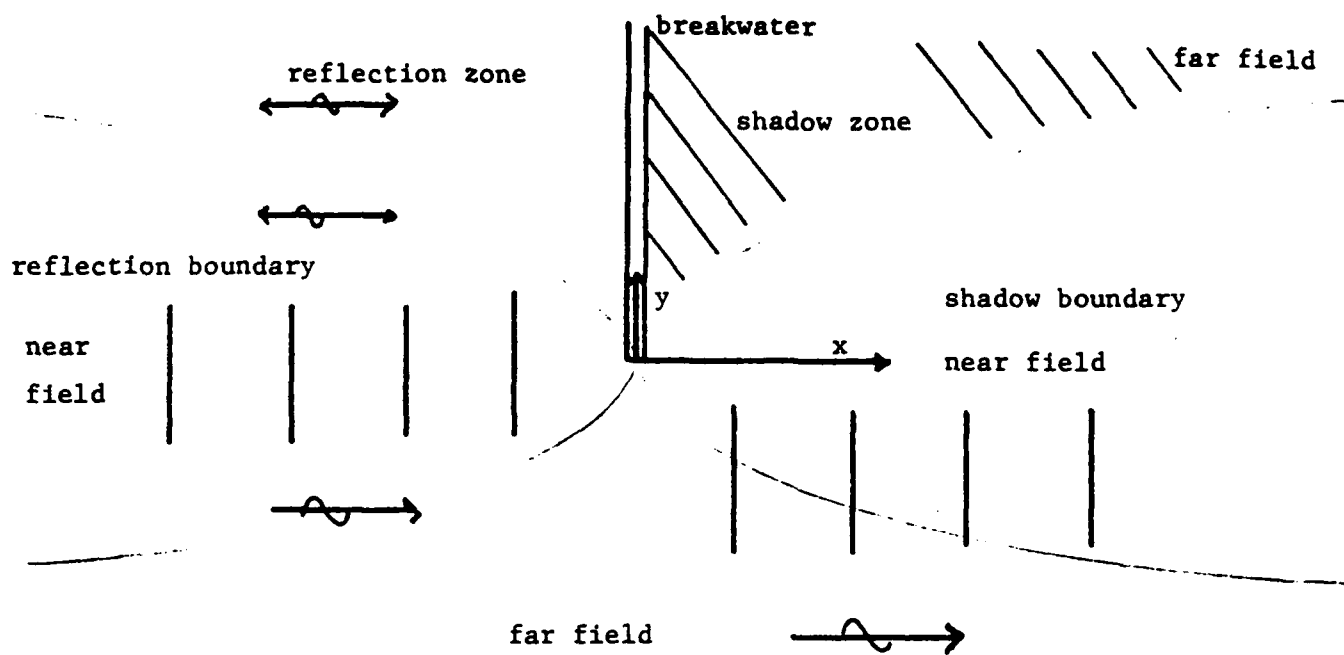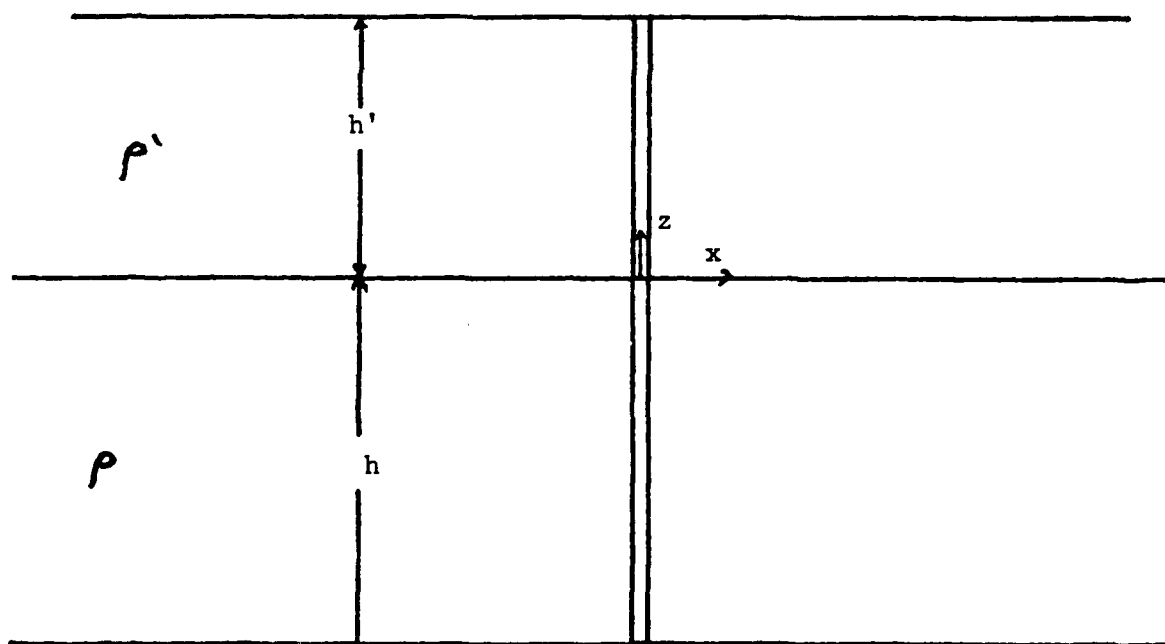
SIDE VIEW

Figure 5.1 Definition Sketch.

For a fixed k this is a quadratic equation for ω^2. The surface wave mode corresponds to the larger frequency of the two positive roots of (5.1.6).

The internal wave mode corresponds to the smaller ω. When one mode is selected, Equation (5.1.7) can be substituted in (5.1.2) to define f_0'. For reference numerical solutions for $\omega/k/\sqrt{g(h + h')}$ versus $k(h + h')$ are shown in Figure 5.2 for both surface and internal modes, with $(\rho-\rho')/\rho = 0.01$; $h'/(h + h') = 0.05$, .01 and 0.2.

5.2 The Locked Long-wave

We shall assume that ϕ_{11} and ϕ_{11}' correspond to the surface wave mode. To determine the long waves we follow the procedure of Section 2.4. For the lower layer, the equivalent of (2.4.16) and (2.4.17) is:

$$\bar{\zeta}_{20t_1} + h\ \phi_{10x_1x_1} + (\zeta_{11}^*\ \phi_{11_x} + *)_{x_1} = 0 \qquad (z = 0) \quad (5.2.1)$$

where ζ is the displacement of the interface. For the upper layer, both the free surface (ζ') and the interface must be considered:

$$\bar{\zeta}_{20t_1}' - \bar{\zeta}_{20t_1} + h'\ \phi_{10x_1x_1}' + (\zeta_{11}'^*\ \phi_{11_x}'\ (z=h') + *)_{x_1}$$

$$\qquad\qquad (5.2.2)$$

$$- (\zeta_{11}^*\ \phi_{11_x}'\ (z=0) + *)_{x_1} = 0$$

The equivalent of Bernoulli's Equation (2.4.14) are, at the free surface:

$$-g\ \bar{\zeta}_{20}' = \phi_{10t_1}' + \left|\nabla\ \phi_{11}'\right|^2 + (i\omega\zeta_{11}'\ \phi_{11_z}'^* + *) \qquad (z=h') \quad (5.2.3)$$

and at the interface:

$$\rho'[g\ \bar{\zeta}_{20} + \phi_{10t_1}' + \left|\nabla\phi_{11}'\right|^2 + (i\omega\zeta_{11}\ \phi_{11z}'^* + *)]$$

126
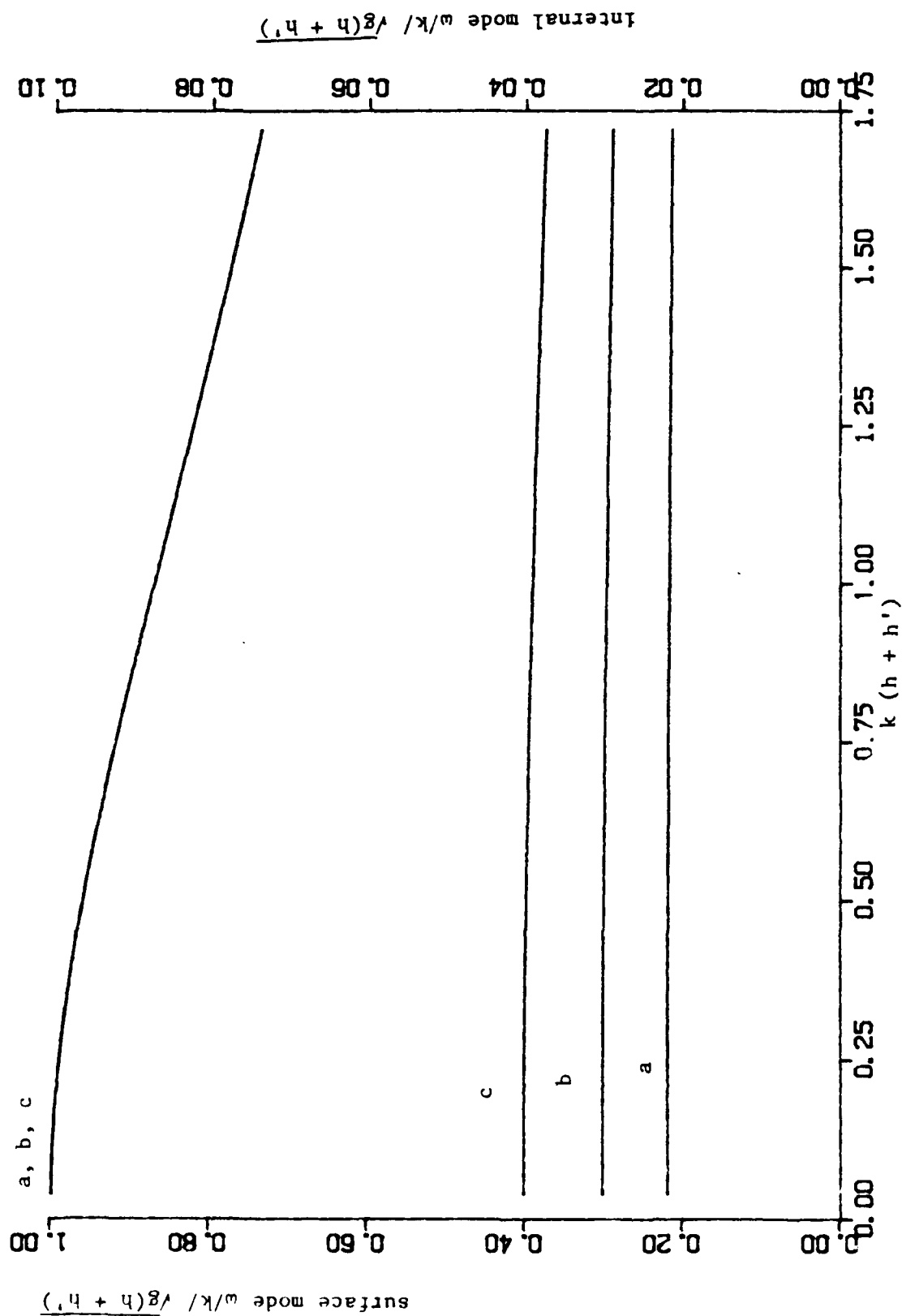
Figure 5.2   The Normalized Phase Velocity, $\omega/k/\sqrt{g(h+h')}$, for Surface and Internal Waves versus $k(h+h')$: $\rho'/\rho = 0.99$; $h'/(h+h')$ is a) 0.05, b) 0.1 and c) 0.2.

$$= \rho[g \, \bar{\zeta}_{20} + \phi_{10t_1} + |\nabla \phi_{11}|^2 + (i\omega\zeta_{11} \, \phi_{11}^* + *)] \quad (z=0) \qquad (5.2.4)$$

Equations (5.2.1) - (5.2.4) can be solved for ϕ_{10}, ϕ_{10}', $\bar{\zeta}_{20}$ and $\bar{\zeta}_{20}'$. Let us assume that ζ_{11}' has a monochromatic envelope:

$$\zeta_{11}' = [Re \; a \; exp \; -i\Omega \; (t_1 - \frac{x_1}{C_g})] \; e^{ikx} \qquad (5.2.5)$$

where C_g is the group velocity of the short surface wave mode.

The slow potential is forced by the square of the short wave. It will have a component that is time harmonic and proportional to $exp(-2i\Omega t_1)$ and a steady component. From here on we shall study only the first one. We proceed to determine the amplitudes of the harmonic components of ϕ_{10}', $\bar{\phi}_{10}$, $\bar{\zeta}_{20}$ and $\bar{\zeta}_{20}$. For the locked long waves that propagate at the velocities $\pm C_g$, the homogeneous part of Equations (5.2.1) - (5.2.4) has the following coefficient matrix:

$$b = \begin{bmatrix} \dfrac{-4\Omega^2}{C_g^2} h & 0 & -2i\Omega & 0 \\ 0 & \dfrac{-4\Omega^2}{C_g^2} h' & 2i\Omega & -2i\Omega \\ 2\rho i\Omega & -2\rho' i\Omega & \rho' g - \rho g & 0 \\ 0 & 2i\Omega & 0 & -g \end{bmatrix} \qquad (5.2.6)$$

The determinant of (5.2.6) is

$$\frac{\Omega^4}{C_g^4} \{\rho \; C_g^4 - \rho \; g(h + h') \; C_g^2 + (\rho - \rho') \; gh \; gh'\} \qquad (5.2.7)$$

This is a second order polynomial in C_g^2 which has zeros at the roots of the dispersion relation (5.1.5) (as a functon of ω/k) in the long waves limit kh →

128

0 and $kh' \to 0$. This means that the short-wave groups will resonate the long internal waves when they propagate at the same velocity, as is well known. Equation (5.2.7) can be written as

$$\frac{\Omega^4}{c_g^4} \rho \ (c_g^2 - c_1^2)(c_g^2 - c_1'^2) \tag{5.2.8}$$

where C_1' and C_1 are the phase velocities of the long surface and internal modes respectivley. This factor is similar to the factor $(gh - c_g^2)$ in Section 2.

Equation (5.2.8) is equivalent to (5.1.6) in the limit of shallow water waves. C_1 and C_1' are given by:

$$c_1^2 = g/2 \ \{h+h' - [(h-h')^2 + 4 \ (\rho'/\rho)h \ h']^{1/2}\} \tag{5.2.9}$$

$$c_1'^2 = g/2 \ \{h+h' + [(h-h')^2 + 4 \ (\rho'/\rho)h \ h']^{1/2}\} \tag{5.2.10}$$

The long-waves solutions of (5.2.1) − (5.2.4) will include locked and free long-waves. The locked long waves are found by solving the matrix equation:

$$[b] \begin{bmatrix} \phi_{10}^L \\ \phi_{10}^{L'} \\ \zeta_{20}^{-L} \\ \zeta_{20}^{-L'} \end{bmatrix} = \begin{bmatrix} a_1 \\ a_2 \\ a_3 \\ a_4 \end{bmatrix} \tag{5.2.11}$$

where $\{a_1, \ a_2, \ a_3, \ a_4\}$ are the forcing terms in (5.2.1) − (5.2.4):

$$a_1 = - (\zeta_{11}^* \phi_{11x} + *)_{x_1} \qquad\qquad (z = 0)$$

$$a_2 = (\zeta_{11}^* \phi_{11x}'(z=0) + *)_{x_1} - (\zeta_{11}' \phi_{11x}'(z=h') + *)_{x_1}$$

$$a_3 \quad \rho[|\nabla\phi_{11}|^2 + (i\omega\zeta_{11}\phi_{11z}^* + *)] - \rho'[|\phi_{11}'|^2 + (i\omega\zeta_{11}\phi_{11z}'^* + *)] \quad (z = 0)$$

$$a_4 = |\nabla\phi_{11}'|^2 + (i\omega\zeta_{11}'\phi_{11z}'^* + *) \qquad\qquad (z = h')$$

The values of a_1, a_2, a_3 and a_4 are given by:

$$
\begin{bmatrix} a_1 \\ a_2 \\ a_3 \\ a_4 \end{bmatrix}
= k^2 |\tilde{A}_0|^2
\begin{bmatrix}
\dfrac{-2i\Omega}{\omega g C_g} \sinh 2kh \\[2ex]
\dfrac{-2i\Omega}{\omega g C_g} [(B^2 + C^2) \sinh 2kh' + 4BC \sinh^2 kh'] \\[2ex]
\rho - \rho' (C^2 - B^2) \\[2ex]
C^2 - B^2
\end{bmatrix}
\qquad (5.2.13)
$$

where $|\tilde{A}_0|^2$ is the harmonic part of $|A_0|^2$. It is given (from (5.2.5)) by:

$$|\tilde{A}_0|^2 = \frac{1}{2} \left| \frac{ga}{2i\omega f_0'(h')} \right|^2 \mathrm{Re}\, e^{-2i\Omega(t_1 - \frac{x_1}{C_g})} \qquad (5.2.14)$$

as in (3.3.13).

We denote the complex amplitudes of ϕ_{10}^L and $\phi_{10}^{L'}$ by E and E', respectively:

$$\phi_{10}^{L} = \text{Re } E \exp -2i\Omega(t_1 - x_1/C_g) \quad ; \qquad \phi_{10}^{L'} = \text{Re } E' \exp -2i\Omega(t_1 - x_1/C_g) \quad (5.2.15)$$

and those of $\bar{\zeta}_{20}$ and $\bar{\zeta}_{20}'$ by Z and Z' respectively:

$$\bar{\zeta}_{20} = \text{Re } Z \exp -2i\Omega(t_1 - x_1/C_g) \quad ; \qquad \bar{\zeta}_{20}' = \text{Re } Z' \exp -2i\Omega(t_1 - x_1/C_g) \quad (5.2.16)$$

After eliminating the factor $\exp -2i\Omega(t_1 - x_1/C_g)$, the coefficients E, E',
and Z' are found from the matrix equation (5.2.11) numerically.

Figure 5.3 shows the locked long waves amplitudes Z and Z' versus
$k(h + h')$. The parameters are $h/(h +h') = 0.4$, 0.5, 0.6 and $(\rho - \rho')/\rho = 0.1$.
The resonance at the roots of (5.2.8) is apparent.

The free long-wave will be determined in Section 5.4.

5.3 • The Short-wave Diffraction

For simplicity we shall only consider normal incidence of a surface wave
train from $x \sim -\infty$. For a uniform wavetrain the diffraction can be written
in terms of the well known diffraction factor. We write ϕ_{11} as the sum of a
right going wave and a left going (reflected) wave (see Figure 5.1):

$$\phi_{11} = A_0 f_0(\phi^+ e^{ikx} + \phi^- e^{-ikx}) \quad ; \qquad \phi_{11}' = A_0 f_0'(\phi^+ e^{ikx} + \phi^- e^{-ikx})$$

where in f_0 and f_0', ω^2 must be associated with the large (surface mode)
solution of (5.1.7).

The diffraction factors ϕ^+ and ϕ^- are:
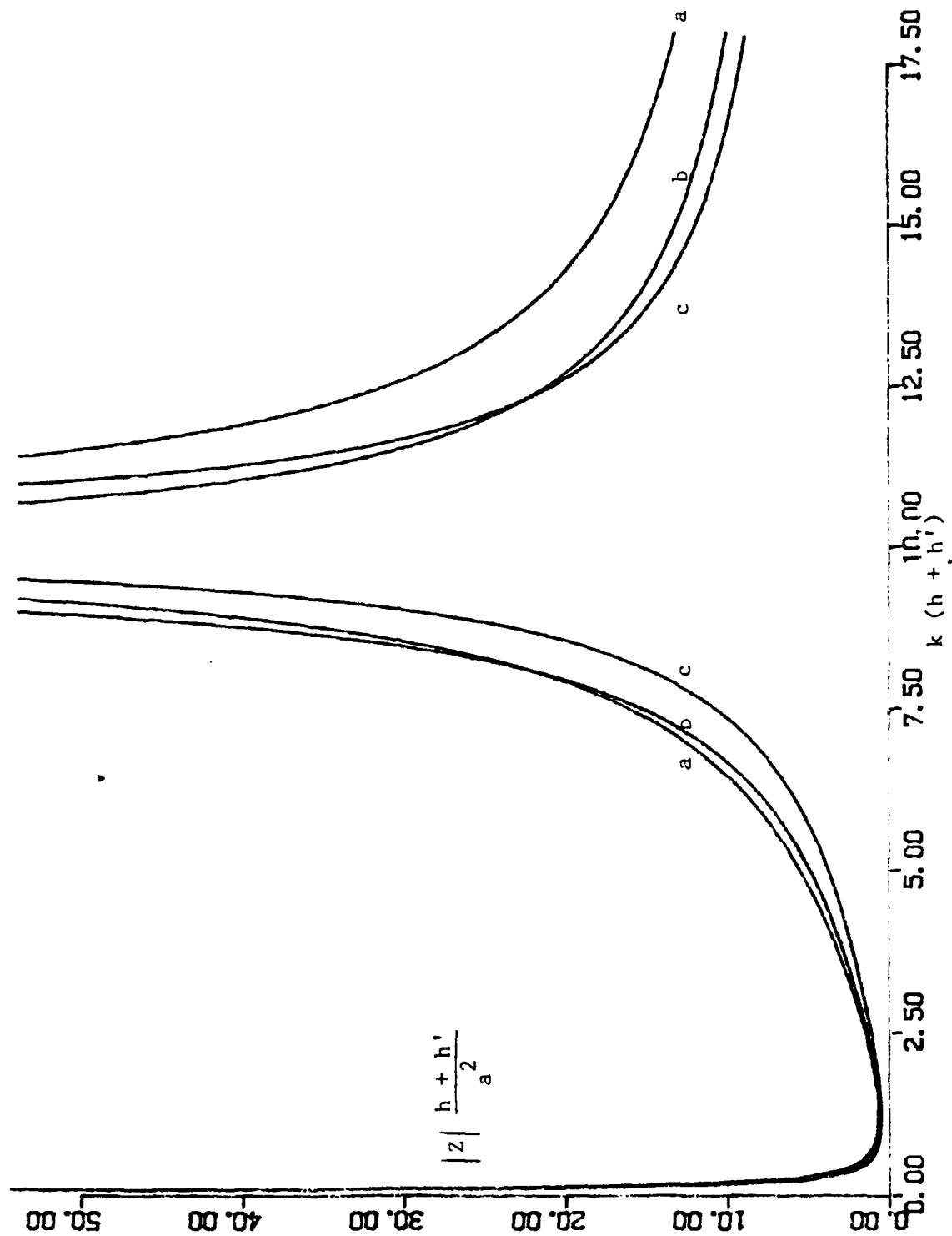
Figure 5.3 a)   The Locked Internal Long-wave Amplitudes $|z|$;
$((\rho'-\rho)/\rho = 0.1)$, $h'/(h+h')$ is a) 0.4, b) 0.5 and c) 0.6.

132
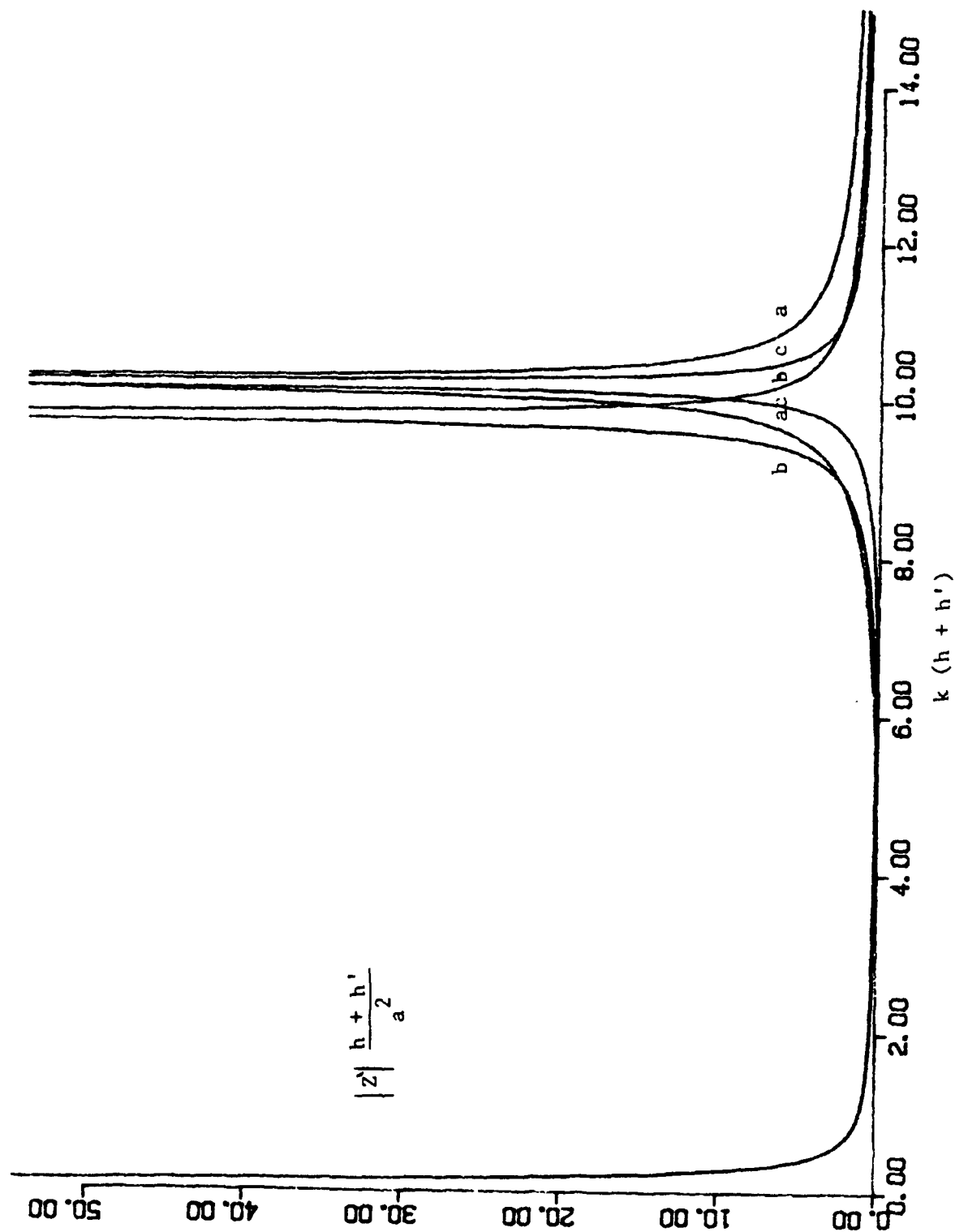
Figure 5.3 b)   The Locked Surface Long-wave Amplitudes $|z'|$;
$((\rho'-\rho)/\rho = 0.1)$, $h'/(h+h')$ is a) 0.4, b) 0.5 and c) 0.6.

$$\phi^+ = \begin{cases} D(-y, \ \sqrt{x}) & (x > 0) \\ 1 & (x < 0) \end{cases} \tag{5.3.1}$$

$$\phi^- = \begin{cases} 0 & (x > 0) \\ D(y, \ \sqrt{-x} & (x < 0) \end{cases}$$

where

$$D(y, \ \left|x\right|^{1/2}) \to 0 \qquad (x > 0 \ , \quad y \to -\infty)$$

$$D(y, \ \left|x\right|^{1/2}) \to 1 \qquad (x > 0 \ , \quad y \to \infty) \tag{5.3.2}$$

and D can be found by a parabolic approximation (cf. Mei 1983, pp. 486-490):

$$D(y, \ \sqrt{x}) \simeq \frac{1}{\sqrt{2}} \left\{ \frac{1}{2} + C(\sigma) + i\left[\frac{1}{2} + S(\sigma)\right] \right\} e^{-i\pi/4} \tag{5.3.3}$$

with

$$\sigma \equiv \frac{ky}{\sqrt{\pi kx}} \tag{5.3.4}$$

and C and S are Fresnel cosine and sine integrals.

The derivatives of D with respect to x and y are:

$$\frac{1}{kD} \frac{\partial D}{\partial x} = O(kx)^{-1}$$

$$\frac{1}{kD} \frac{\partial D}{\partial y} = O(kx)^{-1/2} \tag{5.3.5}$$

134

For a slowly varying wave:

$$\phi_{11} = f_0\{\phi^+ A_0(t_1 - \frac{x_1}{C_g}) e^{ikx} + \phi^- A_0(t_1 + \frac{x_1}{C_g}) e^{-ikx}\}$$

$$\phi'_{11} = f'_0\{\phi^+ A_0(t_1 - \frac{x_1}{C_g}) e^{ikx} + \phi^- A_0(t_1 + \frac{x_1}{C_g}) e^{-ikx}\} \tag{5.3.6}$$

If the incident wave is given by (5.2.5) then

$$A_0(t_1) = a \cos \Omega t_1 \ g/(2i\omega f'_0(h'))$$

as in (3.3.13).

The far field is defined by:

$$\sigma > O(\epsilon^{-1}) \tag{5.3.7}$$

since there the leading order derivative is that of the phase factors

$$e^{ikx} \text{ and } e^{-ikx} \tag{5.3.8}$$

and D can be approximated in the far field by its asymptotic value 0 or 1, see (5.3.2).

When we substitute the form of ϕ_{11}, ϕ'_{11} for the diffraction problem into (5.2.1) - (5.2.4), we find right away that the locked long-wave in the far field is given by the solution of (5.2.11) multiplied by the square of the diffraction factor from (5.3.1), which is summarized in the following table:

TABLE 5.1

Quadrant:	I	II	III	IV
Right Going: $\phi+$	0	1	1	1
Left Going: $\phi-$	0	1	0	0

The near field is defined as the region where the diffraction factor variation is significant. It is the inside of the "parabola"

$$\sigma = 0(\epsilon^{-1}) \qquad\qquad (5.3.9)$$

On the scale of x_1, x is $0(\epsilon^{-1})$ and y is $0(\epsilon^{-1/2})$, so that $y_1 \simeq 0$. At the leading order ψ_{10}, ψ'_{10}, the near field slow potentials, are functions of t_1, but not of y_1. Hence we have,

$$\psi_{10} = \psi_{10}(x_1, t_1) \quad \text{and} \quad \psi'_{10} = \psi'_{10}(x_1, \cdot) \qquad (5.3.10)$$

This near field slow potential should be matched to the far field potential:

$$\phi_{10}(y_1 = 0^+, x_1, t_1) = \psi_{10}(x_1, t_1) = \phi_{10}(y_1 = 0^-, x_1, t_1) \qquad (5.3.11)$$

The normal gradient of the slow potential should also be matched as in the previous chapters:

$$\phi_{10y_1}(y_1 = 0^+, x_1, t_1) = \psi_{20_y}(y \to +\infty, x_1, t_1)$$

$$\qquad\qquad\qquad (5.3.12)$$

$$\phi_{10y_1}(y_1 = 0^-, x_1, t_1) = \psi_{20_y}(y \to -\infty, x_1, t_1)$$

In the present problem there are no evanescent modes, and hence ψ_{20} represents a uniform current. To see that, we note that the forcing term for ψ_{20z} at $(z = 0)$ as given in (2.2.6) and (3.3.26) can be evaluated as follows (using a well known vector identity):

$$g \psi_{20z} = \nabla_h \cdot [i\omega\psi_{11} \nabla_h \psi_{11}^* + *] = \nabla_h \cdot [i\omega\psi_{11} \nabla_h \psi_{11}^* - i\omega \psi_{11}^* \nabla_h \psi_{11}]$$

$$= i\omega\psi_{11} \nabla_h^2 \psi_{11}^* - i\omega\psi_{11}^* \nabla_h^2 \psi_{11} =$$

$$\qquad\qquad\qquad (5.3.13)$$

$$= i\omega\psi_{11} [- k^2 \psi_{11}] - i\omega\psi_{11} [- k^2 \psi_{11}] = 0$$

since ψ_{11} solves a single Helmholz equation and has no evanescent modes.
This means that ψ_{20} is divergence-free and we may write

$$\phi_{10y_1}(y_1 = 0^+, x_1, t_1) = \psi_{20_y}(y \to \pm\infty, x_1, t_1) = \phi_{10y_1}(y_1 = 0^-, x_1, t_1) \quad (5.3.14)$$

where ψ_{20y} has the same value at both matching boundaries

$$y_1 = 0^+ , \quad y \to +\infty \quad \text{and} \quad y_1 = 0^- , \quad y \to -\infty \qquad (5.3.15)$$

for any given x_1, t_1. This is again a simple special case of (3.3.34) where
the net mass flux through the near field must be zero. At the outer limits of
the near field, the y component of Stokes' drift is zero since the waves are
propagating in the x direction. Hence, ψ_{20y} accounts for the total drift
current in the y direction. ϕ'_{10}, ψ'_{10} and ψ'_{20} satisfy equations identical
to (5.3.11) and (5.3.14). The near field is, in effect, transparent to the
long-wave and the matching is carried out between the far field potentials, on
both sides of the shadow and reflection boundaries. The near field merely
smooths the transition. The locked waves are already known and we now
determine the free waves.

5.4 The Free Long-wave

Let us write the slow far field potentials, ϕ_{10} and ϕ'_{10}, as sums of
locked long-waves: ϕ^L_{10}, $\phi^{L'}_{10}$; and free long-waves: ϕ^F_{10}, $\phi^{F'}_{10}$:

$$\phi_{10} = \phi^L_{10} + \phi^F_{10} \; ; \qquad \phi'_{10} = \phi^{L'}_{10} + \phi^{F'}_{10} \qquad (5.4.1)$$

The governing equations for ϕ^F_{10}, $\phi^{F'}_{10}$ are then obtained from the homogen-
eous counterparts of (5.2.1) through (5.2.4) with $\partial/\partial x_1$ replaced by ∇_h,
i.e.,

$$\bar{\zeta}^F_{20t_1} + h\nabla^2_1\phi^F_{10} = 0$$

$$\bar{\zeta}^{F'}_{20t_1} - \bar{\zeta}^F_{20t_1} + h'\nabla^2_1\phi^{F'}_{10} = 0$$

$$-g\bar{\zeta}^{F'}_{20} = \phi^{F'}_{10t_1}$$

$$\rho'(g\bar{\zeta}^F_{20} + \phi^{F'}_{10t_1}) = \rho(g\bar{\zeta}^F_{20} + \phi^F_{10t_1})$$

(5.4.2)

Eliminating $\bar{\zeta}_{20}$ and $\bar{\zeta}'_{20}$ yields

$$(\frac{\partial^2}{\partial t^2} - c^2_1\,\nabla^2_1)(\frac{\partial^2}{\partial t^2} - c_i'^2\,\nabla^2_1)\begin{bmatrix}\phi^{F'}_{10}\\ \phi^F_{10}\end{bmatrix} = 0 \qquad (5.4.3)$$

From (5.3.11) and (5.3.12) we get the boundary conditions:

$$\phi^F_{10}\begin{vmatrix}y_1 = 0^+\\ y_1 = 0^-\end{vmatrix} = -\phi^L_{10}\begin{vmatrix}y_1 = 0^+\\ y_1 = 0^-\end{vmatrix} \qquad (5.4.4a)$$

$$\phi^{F'}_{10}\begin{vmatrix}y_1 = 0^+\\ y_1 = 0^-\end{vmatrix} = -\phi^{L'}_{10}\begin{vmatrix}y_1 = 0^+\\ y_1 = 0^-\end{vmatrix} \qquad (5.4.4b)$$

$$\phi^F_{10y_1}\begin{vmatrix}y_1 = 0^+\\ y_1 = 0^-\end{vmatrix} = -\phi^L_{10y_1}\begin{vmatrix}y_1 = 0^+\\ y_1 = 0^-\end{vmatrix} = 0 \qquad (5.4.5a)$$

$$\phi^{F'}_{10y_1}\begin{vmatrix}y_1 = 0^+\\ y_1 = 0^-\end{vmatrix} = -\phi^{L'}_{10y_1}\begin{vmatrix}y_1 = 0^+\\ y_1 = 0^-\end{vmatrix} = 0 \qquad (5.4.5b)$$

$(\phi_{10}^{L}$ and $\phi_{10}^{L'}$ are not functions of y_1). From Equations (5.4.4), (5.4.5) and the form of ϕ_{10}^{L}, $\phi_{10}^{L'}$ we immediately see that ϕ_{10}^{F}, $\phi_{10}^{F'}$ are antisymmetric in x_1 and in y_1. It is therefore sufficient to solve for the free potentials in, say, the first quadrant. The boundary conditions are:

along the breakwater:

$$\phi_{10x_1}^{F} = \phi_{10x_1}^{F'} = 0 \qquad\qquad \text{on} \qquad \begin{array}{l}(x_1 = 0)\\(y_1 \geq 0)\end{array} \qquad (5.4.6a)$$

and along the line $y_1 = 0$:

$$\begin{bmatrix} \phi_{10}^{F'} \\ \phi_{10}^{F} \end{bmatrix} = \frac{1}{2} \, \text{Re} \, \begin{bmatrix} E' \\ E \end{bmatrix} e^{-2i\Omega(t_1 - \frac{x_1}{C_g})} \qquad \begin{array}{l}(y_1 = 0)\\(x_1 \geq 0)\end{array} \qquad (5.4.6b)$$

Because of the form of the boundary condition (5.4.6b), we expect the solutions of ϕ_{10}^{F}, $\phi_{10}^{F'}$ to have a wavenumber $2\Omega/C_g$ in the x_1 direction. Equation (5.4.3) describes waves of two types. One mode is the barotropic surface mode with horizontal wavenumber $2\Omega/C_i'$ and the other, the baroclinic internal mode with horizontal wave number $2\Omega/C_i$. For a wide range of parameters, $2\Omega/C_g$ lies between these two, i.e.,

$$\frac{2\Omega}{C_i'} \; < \; \frac{2\Omega}{C_g} \; < \; \frac{2\Omega}{C_i}$$

This means that the internal mode of the free waves will be propagating and have real wavenumbers in both the x_1 and y_1 directions, while the free surface mode will be evanescent in the y_1 direction (since the x_1 wavenumber is

greater than the total horizontal wave number).

Away from the shadow boundary for the free waves, which will be defined shortly, we have

$$\phi_{10}^F \sim \mathrm{Re}[\phi_{bt}\, e^{-2i\Omega(t_1 - \frac{|x_1|}{c_g} - iv_{bt}|y_1|)} + \phi_{bc}\, e^{-2i\Omega(t_1 - \frac{|x_1|}{c_g} - v_{bc}|y_1|)}]$$

$$\phi_{10}^{F'} \sim \mathrm{Re}[\phi_{bt}'\, e^{-2i\Omega(t_1 - \frac{|x_1|}{c_g} - iv_{bt}|y_1|)} + \phi_{bc}'\, e^{-2i\Omega(t_1 - \frac{|x_1|}{c_g} - v_{bc}|y_1|)}]$$

(5.4.7)

where the subscripts bt and bc stand for the surface (barotropic) and the internal (baroclinic) modes, respectively, and

$$-v_{bt}^2 + c_g^{-2} = c_i'^{-2}$$

$$v_{bc}^2 + c_g^{-2} = c_i^{-2}$$

The direction of the internal mode forms an angle

$$\theta = \cos^{-1}\frac{c_i}{c_g} \tag{5.4.8}$$

with the positive x_1 axis. There will be a parabolic transition zone between the area into which the free internal waves are emitted and the area near the y_1 axis where there are no free waves. This transition can be described in terms of a diffraction factor, similar to D of (5.3.3)

$$D_1(y_1', \overline{\sqrt{x_1'}}) = \frac{1}{\sqrt{2}} \{\tfrac{1}{2} + C(\sigma') + i\,[\tfrac{1}{2} + S(\sigma')]\}e^{-i\pi/4} \tag{5.4.9}$$

$$\text{with } \sigma' = \frac{-Ky_1'}{\sqrt{\pi K x_1'}} \quad ; \quad K = \frac{2\Omega}{c_i} \tag{5.4.10}$$

and (x_1', y_1') is a Cartesian coordinate-system with x'_1 inclined at ϕ with respect to the x_1 axis:

$$\begin{bmatrix} x_1' \\ y_1' \end{bmatrix} = \begin{bmatrix} \cos\theta & \sin\theta \\ -\sin\theta & \cos\theta \end{bmatrix} \begin{bmatrix} x_1 \\ y_1 \end{bmatrix} \qquad (5.4.11)$$

The diffraction factor D_1 multiplied by the periodic waves of Equation (5.4.7) describes the 'diffracted' free long-wave field in the first quadrant $(x_1, y_1 > 0)$. The significance of the existence of free waves is greatest in this region. The free waves elsewhere are simply given by the free wave field being antisymmetric with respect to both x_1 and y_1.

In Figure 5.4 the transition zones for the emitted free waves are sketched. We see that free internal waves are emitted into the "shadow zone" behind the breakwater, where no short-waves or locked long-waves are present.

To determine the amplitude of the free internal waves, we first write down the ratio of the amplitudes of the potentials for the two modes, the barotropic (bt) and the baroclinic (bc). For the surface (bt) mode of the free long-waves, we replace all ∇_1^2 operators in the equations (5.4.2) by $1/C_1'^2 \partial^2/\partial t_1^2$. We then eliminate $\bar{\zeta}_{20}'$ and $\bar{\zeta}_{20}$ integrate with respect to t_1 and determine the ratio ϕ_{bt}/ϕ_{bt}':

$$\alpha \equiv \frac{\phi_{bt}}{\phi_{bt}'} = \frac{gh' - C_1'^2}{gh} > 0 \qquad (5.4.12)$$

Replacing $C_1'^2$ by C_1^2, we get for the internal wave (bc) mode:
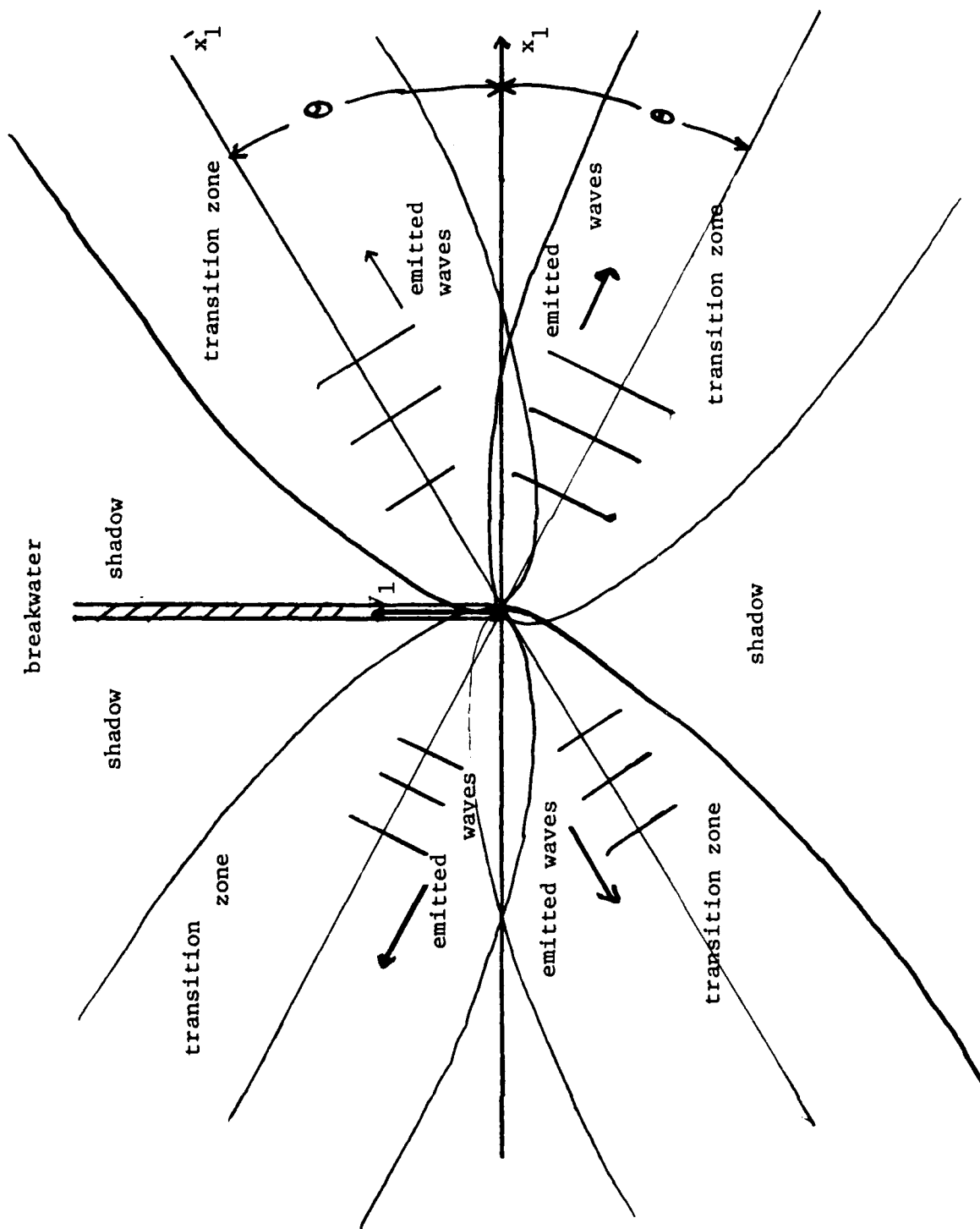
Figure 5.4 The Diffraction Transition Zones for the Free Long-waves.

142

$$\beta \equiv \frac{\phi_{bc}}{\phi'_{bc}} = \frac{gh' - c_1^2}{gh} < 0 \qquad (5.4.13)$$

Note that the signs of ϕ_{10}^F and $\phi_{10}^{F'}$ for the internal wave mode are opposite.

From (5.4.6b) and (5.4.7) we have:

$$\phi_{bc} + \phi_{bt} = \frac{1}{2} E \; ; \quad \phi'_{bc} + \phi'_{bt} = \frac{1}{2} E' \qquad (5.4.14)$$

Equations (5.4.12) – (5.4.14) can be immediately solved to give ϕ_{bc}, ϕ_{bt}, ϕ'_{bc} and ϕ'_{bt}. In particular:

$$\phi_{bc} = \frac{1}{2} [E - \alpha E'] / (1 - \frac{\alpha}{\beta}) \qquad (5.4.15)$$

The baroclinic (propagating) component of the interface displacement is found directly from (5.2.1):

$$\zeta_{bc} = \frac{2i\Omega h}{c_1^2} \phi_{bc} \qquad (5.4.16)$$

In Figure 5.3a, Z, the normalized amplitude of the locked long internal waves, ζ_{20}^{-L}, is plotted versus $k(h + h')$. The resonance at $(kh \to 0)$ is due to C_g coinciding with C_1', whereas the higher frequency resonance is due to C_g coinciding with C_1. In Figure 5.5, the normalized ζ_{bc} of Equation (5.4.16) is plotted versus $k(h + h')$. When the depths of the two layers are equal the high wave number resonance is absent in the baroclinic mode. This is because the forcing is barotropic, E and E' are both large, but the barolinic mode (see 5.4.15) remains finite. When the layer depths are different the resonance of the locked wave is reflected in the free waves. Near the resonance, however, θ
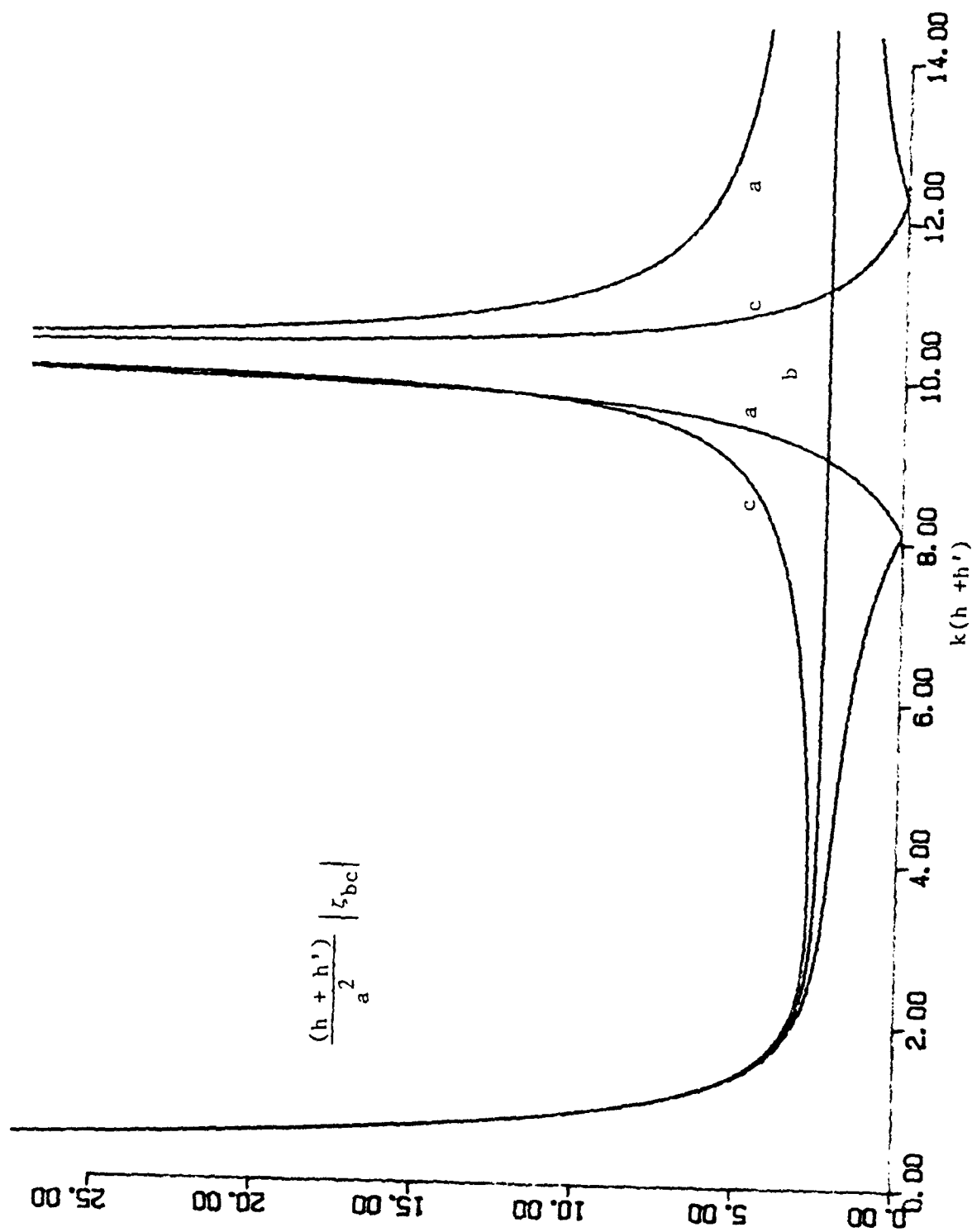
Figure 5.5 a)   The Free Internal Long-wave Amplitude $|\zeta_{bc}|$:
$(\rho'-\rho)/\rho = 0.1$, $h'/(h+h')$ is a) 0.4, b) 0.5 and c) 0.6.

144
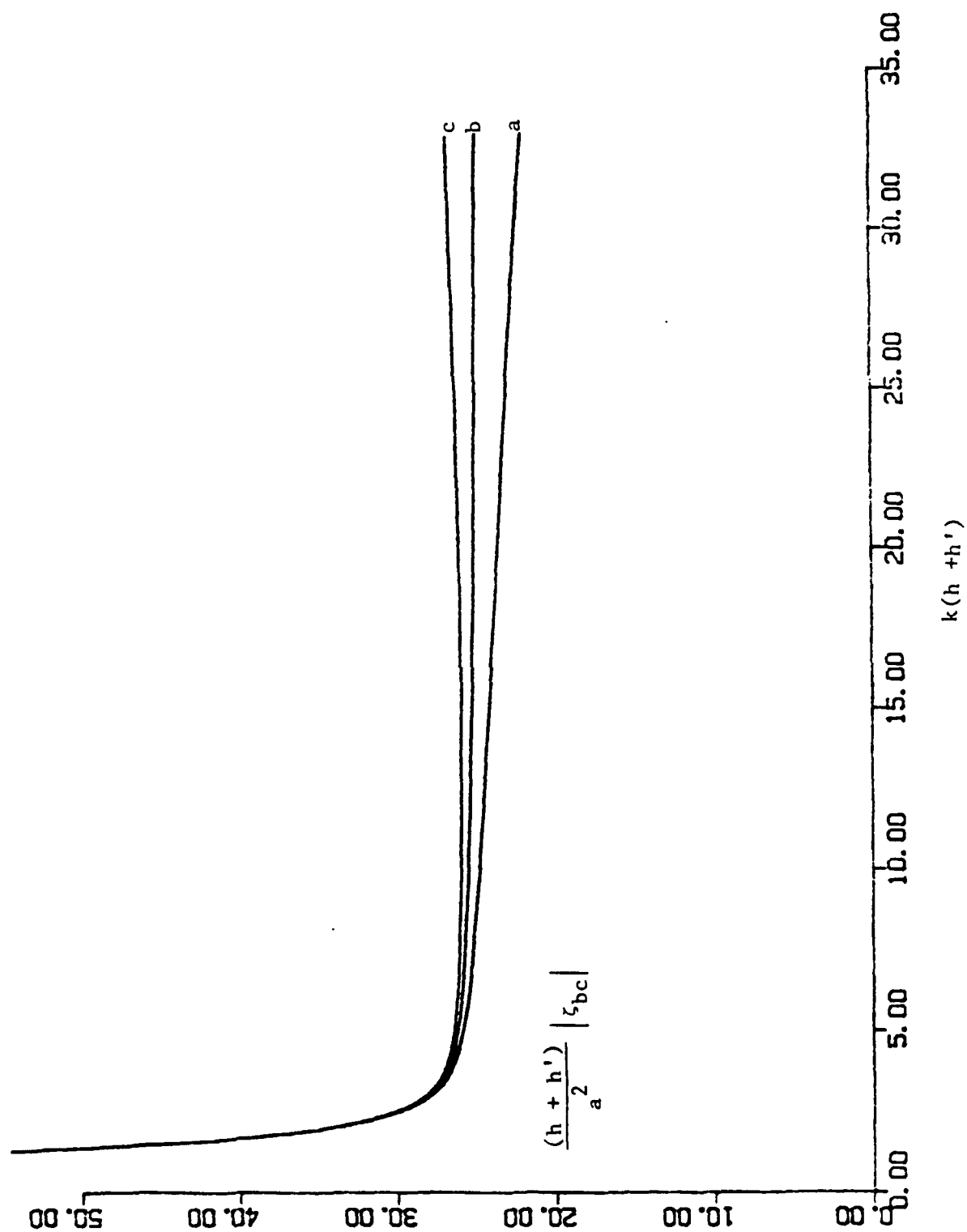
Figure 5.5   b)   The Free Internal Long-wave Amplitude $|\zeta_{bc}|$:
$(\rho'-\rho)/\rho = 0.01$, $h'/(h+h')$ is a) 0.4, b) 0.5 and c) 0.6.

of Equation (5.4.8) is nearly zero. This means that the free waves penetration angle into the shadow zone is very small, and the free waves are almost parallel to the already existing locked long-waves. For waves with larger wave-numbers than the resonant wave-number, the internal waves are evanescent. The values at which ζ_{bc} becomes zero represent a change in phase of the free internal waves. We expect the interface displacement to grow with decreasing reduced gravity as seen when comparing Figure 5.5 (a) and (b).

This concludes our treatment of slowly varying waves in a stratified fluid. The significance of our findings is in the propagation of energy into the sheltered region in the lee of the breakwater. It is of interest to study the possibility of resonance in a basin sheltered by a peninsula or a strait. Additional aspects include the effect of continuous stratification and bottom topography. The related problem of harbour resonance in a homogenous fluid will be commented on in the following, conclusion chapter.

6. CONCLUSION

6.1 Summary

In this work we have strived to gain insight into the interplay between wave scattering and diffraction by floating bodies and topographical features – and the wave nonlinearity. The waves were assumed to be slowly varying. The water depth and the short wave-length are comparable. We carried out a multiple scale perturbation expansion in both time and the horizontal space coordinates. The governing equation in open water was formulated, purposefully allowing for waves propagating in a few directions at the same location. Locked long-waves were found that are forced by, and travel with the short-wave groups.

We found that when the short-waves were modified by a floating body, depth variations or a breakwater, so were the locked long-waves. The changes in the mean mass flux and free surface elevation associated with these modifications are balanced by the generation of free shallow water waves that are radiated away from the region of short-wave modification. Specific problems were then solved by studying the near field of the wave modification regions and asymptotically matching to the far field.

The lion share of the thesis treats the drift motion of a floating body. Specifically, the leading order slow drift forces on a swaying horizontal rectangular cylinder were studied in detail. Various mooring stiffnesses and depth-draught ratios were examined. The method demonstrated can be readily applied to more general body shapes and modes of motion. We have studied the practically important case in which the slow drift amplitude is large and

147

comparable to the short-wave length. The present work justifies the results of the more intuitive engineering solutions that have been in use. It also defines the limitations on its validity.

We have found that there is a first order slow potential that corresponds to a second order pressure and second order slow surface elevation. This pressure is at the leading order slow pressure and has not been considered before. The force due to that pressure was determined. It was found to be small for quite a general class of geometries. The slow first order potential is coupled to the slow second order potential. In particular, the effect of the second order potential on the leading order slow motion and waves was derived without explicitly solving for any second order potential. We have not computed the third order drift force due to the second order slow potential, nor the damping due to the interaction of the slow sway with the short waves. However, the simplicity of the formulation facilitates extension of the treatment to determine higher order corrections. In all the cases studied both periodic and transient envelopes were investigated. The sway response and the long-wave field were determined. For several configurations resonance was identified.

We have also studied the trapping of long waves on a shelf/ridge by obliquely incident slowly varying waves. Here, too, emphasis was placed on the new aspects: those of partial reflection of the modulated short-waves - and the resulting local second order slow potential which is coupled to the long waves. Due to the depth difference between the two sides of the shelf edge there is a net slow mass flux gradient associated with the short-waves that contributes to the long-wave generation. Free shallow water waves are emit-

ted away from the shelf edges. These free waves can be trapped on the shelf and resonance may occur.

At the leading order the resonance appears infinite in the frequency response formulation. We have chosen to study the excitation of an edge wave by a transient envelope. After the input short-waves and locked long-waves have passed, the trapped oscillation (which is a standing wave in the cross-shelf direction and propagating along the shelf) remains behind as a wake, which can be described as a 'ringing effect'. This effect can be of quiet a large amplitude. At longer times, higher order effects that have not been included will diminish the wake. Results for the response to normally incident waves were also included. No trapping occurs and the response is passive. Possible extensions of the theory include application to standing internal waves, which have been observed on seamounts, and combining the effects of shear currents (that can also trap waves) and rotation.

Finally we have considered the diffraction of slowly varying waves in a two layer fluid. In addition to the surface waves, interfacial waves are also present. When the short waves are diffracted by a long breakwater, the locked long surface and internal waves are modified. We had asymptotically matched the far field in the lee of the breakwater, through the shadow boundary to the 'lit zone'. We found that free baroclinic long-waves are emitted from the shadow boundary into both regions. Long waves are emitted from the reflection boundary as well.

The free internal waves propagate obliquely into the shadow zone at an angle that depends on the ratio of the internal wave velocity to the larger surface-waves group-velocity. These internal waves can resonate in a basin. Even small internal waves can be important to mixing processes and to bio-

logical phenomenon. Space shuttle pictures of the straits of Gibraltar show internal waves propagating obliquely into the lee of the straits.

All of the problems studied were designed to bring out the physics of short waves - long waves interaction. the formal assumptions of the asymptotic theory were: i) small waves steepness and ii) narrow wave spectrum. For steeper waves and wider spectra, higher order corrections need to be considered. The simplicity of the present formulation facilitates such extension. The asymptotoic results should be compared with more accurate results to assess their range of validity. An additional difficulty is associated with a directional spread of the waves. When the range of wave directions is continuous, the difference wave-numbers form a continuum and are not strictly multiple scales. It is likely that this obstacle can be overcome by observing that the physical quantity of the gradient of the slow potential is second order. More work along these lines may allow easier treatment of three dimensional problems. The various features described can be combined with additional ingredients to study realistic, complex situations. Finally, let us sketch our approach to the interesting problem of harbour reasonance.

6.2 Epilogue: Harbour Resonance

Harbours are known to undergo seiches at their natural frequencies which are of the order of several minutes. Several mechanisms have been suggested to be associated with the excitation of such oscillations. These include surf-beats and edge waves. Bowers (1977) has studied the problem of waves incident in a narrow channel terminated by a narrower basin. He did not consider the local field near the basin entrance. The present theory shows that since in uniform depth energy conservation translates to mass conservation in the drift terms, the final result is not affected. We choose to study a more realistic configuration, where the ocean is three dimensional. Consider, for definiteness the configuration given in Figure 6.1. The short-wave groups are incident on the breakwater and diffracted by it. As in Chapter 5 there is no slow locked waves inside the harbour, while there is a slow standing wave outside. Matching the two regions through the shadow boundary (that is studied by conformal mapping) the free slow oscillations can be determined. Since the eigenfrequencies of the harbour can fall in the ranre of the modulation frequency of the short waves, harbour resonance will be excited. In contrast to the internal waves studied previously, the free waves outside the harbour will be evanescent, since they are faster than the locked long-waves. A full solution to that problem will be completed in the future.

151
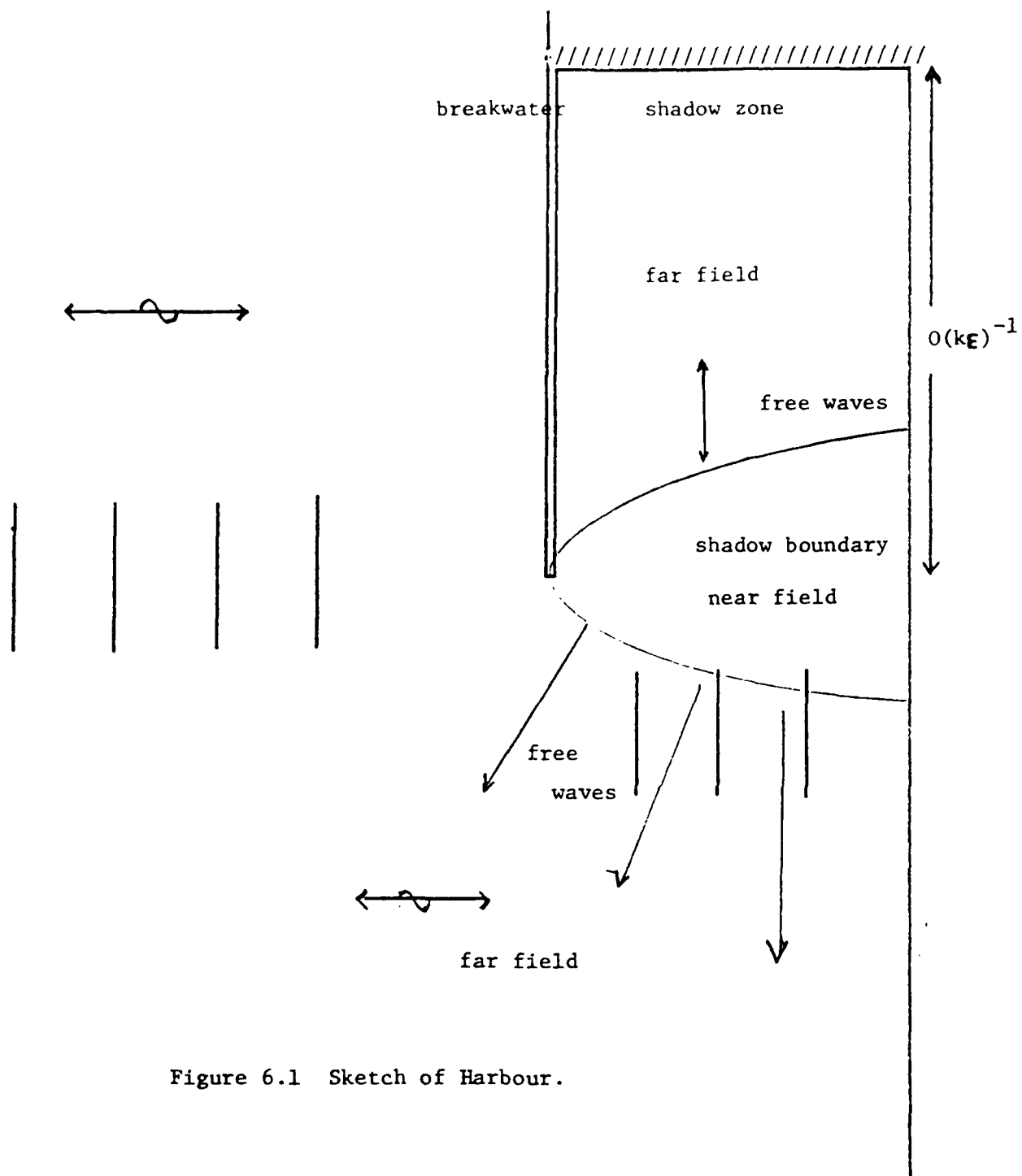
Figure 6.1 Sketch of Harbour.

REFERENCES

Agnon, Y. and Mei, C. C., 1985a, Slow drift motion of a two dimensional block in beam seas, J. Fluid Mech., 151, 279-294.

Agnon, Y. and Mei, C. C., 1985b, Slow drift motions of a floating body in narrow-banded seas, Proc. BOSS '85 Symp. on Behaviour of Offshore Structures, Delft.

Ball, F. K., 1964, Energy transfer between external and internal gravity waves, J. Fluid Mech., 19, 465-478.

Beck, R. and Tuck, E. O., 1982, Computation of Shallow water ship motions, Proc. Symp. on Naval Hydrodynamics, Paris, pp. 1543-1587.

Benney, D. J., 1962, Nonlinear gravity wave interactions, J. Fluid Mech., 14, 574-584.

Black, J. L., 1970, Scattering and radiation of water waves, Sc.D. Thesis, Department of Civil Engineering, MIT.

Bowers, E. C., 1976, Long period oscillations of moored ships subject to short wave seas, Trans. Roy. Inst. of Naval Arch., 118, 181-191.

Bowers, E. C., 1977, Harbour resonance due to set down beneath wave groups, J. Fluid Mech., 79, 71-92.

Carrier, G. F., 1970, The dynamics of Tsunamis, Mathematical Problems in Geophysical Fluid Dynamics, American Mathematical Society, Providence, RI, 157-181.

Dysthe, K. B. and Das, K. P., 1981, Coupling between a surface-wave spectrum and an internal wave: modulational interaction, J. Fluid Mech., 104, 483-503.

Faltinsen, O. M. and Løken, A. E., 1979, Slow drift oscillations of a Ship in irregular waves, Appl. Ocean Res., 1, 21-31.

Flagg, C. N. and Newman J. N., 1971, Sway added-mass coefficients for rectangular profiles in shallow water, J. Ship Res., 15, 257-267.

Foda, M. A. and Mei, C. C., 1981, Nonlinear excitation of long trapped waves by a group of short swells, J. Fluid Mech., 111, 319-345.

Hsu, F. H. and Blenkarn, K. A., 1970, Analysis of peak mooring forces caused by slow vessel drift oscillations in random seas, Proc. Offshore Technol. Conf., Houston, Paper 1159.

Huijsmans, R.H.M. and Hermans, A.J., 1985, A fast algorithm for computation of 3-D ship motions at moderate forward speed, Sixth Internat'l Conf. on Numerical Ship Hydrodynamics.

Lamb, H., 1898, On the reflection and transmission of electric waves by a metal grating, Proc. Lond. Math. Soc., 29, 523-544.

Lamb, H., 1945, Hydrodynamics, Dover, New York.

Longuet-Higgins, M. S., 1977, The mean forces exerted by waves on floating or submerged bodies, with applications to sand bars and wave-power machines, Proc. Roy. Soc. Lond. A, 352, 463-480.

Longuet-Higgins, M. S. and Stewart, R. W., 1962, Radiation stress and mass transport in gravity waves, with applications to surf-beats, J. Fluid Mech., 13, 481-504.

Longuet-Higgins, M. S. and Stewart, R. W., 1964, Radiation stress in water waves; a physical discussion, with applications, Deep Sea Res., 11, 529-562.

Martinsen, T., 1983, Calculation of slowly varying drift forces, Appl. Ocean Res., 5, 141-144.

Maruo, H., 1960, The drift of a body floating on waves, J. Ship Res., 4: 3, 1-10.

Mei, C. C., 1983, The Applied Dynamics of Ocean Surface Waves, Wiley-Interscience, New York.

Mei, C. C. and Benmoussa, C., 1984, Long waves induced by short-wave groups over an uneven bottom, J. Fluid Mech., 139, 219-235.

Mei, C. C. and Black, J. L., 1969, Scattering of surface waves by rectangular obstacles in waters of finite depth, J. Fluid Mech., 38, 499-511.

Molin, B. and Bureau, G., 1980, A Simulation model for the dynamic behavior of tankers moored to single point moorings, International Symp. on Ocean Engineering Ship Handling, Swedish Maritime Research Center, Gothenburg.

Newman, J. N., 1965, Propagation of water waves past long two dimensional obstacles, J. Fluid Mech., 23, 23-29.

Newman, J. N., 1967, The drift force and moment on ships in waves, J. Ship Res., 11, 51-60.

Newman, J. N., 1969, Lateral motion of a slender body between two parallel walls, J. Fluid Mech., 39, 97-115.

Newman, J. N., 1974, Second order, slowly varying forces on vessels in irregular waves, Proc. Int. Symp. on Dynamics Marine Vehicles and Offshore Structures in Waves, University College, London.

Newman, J. N., 1977, Marine Hydrodynamics, The MIT Press.

Ogilvie, T. F., 1983, Second-order hydrodynamic effects on ocean platforms, Proc. Int'l Workshop on Ship and Platform Motions, Univ. of California at Berkeley.

Pinkster, J. A., 1980, Low frequency second order wave exciting forces on floating structures, Netherlands Ship Model Basin, Publ. No. 650.

Remery, G. F. M. and Hermans, A. J., 1971, The slow drift oscillations of a moored object in random seas, Proc. Offshore Technol. Conf., Houston.

Roberts, J. B., 1981, Nonlinear analysis of slow drift oscillations of moored vessels in random seas, J. Ship Res., 25, 130-140.

Symonds, G. and Bowen, A. J., 1984, Interactions of nearshore bars with incoming wave groups, J. Geoph. Res., 89, C2, 1953-1959.

Triantafyllou, M. S., 1982, A consistent hydrodynamic theory for moored and positioned vessels, J. Ship Res., 26, 97-105.

Tuck, E. O. and Taylor, P. J., Shallow water problems in ship hydrodynamics, Proc. 8th Symp. on Naval Hydrodynamics, Pasadena, pp. 627-659.

Ursell, F., 1950, On the theoretical form of ocean swell on a rotating earth. Mon. Not. Roy. Astro. Soc., (Geophys. Suppl.), 6, No. 1, 1-8.

Verhagen, J. H. G. and Van Sluijs, M. F., 1970, The low-frequency drifting force on a floating body in waves, Int. Shipbuild. Prog., 17, 136-145.

APPENDIX A

On The Scattering and Radiation of Regular Waves by a Semi-immersed Rectangular Cylinder

In this appendix we supply some details on the determination of the reflection coefficient, the hydrodynamic force for the scattering of regular waves, the radiated waves, and the added mass and damping coefficients for harmonic sway motion of a semi-immersed horizontal rectangular cylinder.

Multiplying (3.2.14) by $\{F_0, \ldots, F_N\}$ and integrating with respect to z from $-h$ to $-D$ we obtain, from (3.2.16) and from the orthonormality of $\{F_N\}$ the following $N+1$ linear algebraic equations.

$$-2b_0 \, P_{00} = g^A_{00} \, B_0 F_0 + \sum_{n=1}^{\infty} B_n \, k_n \, \cos \, k_n \, B \, g^A_{0n}$$

$$\begin{matrix} \cdot & & \cdot & & \cdot \\ \cdot & & \cdot & & \cdot \\ \cdot & & \cdot & & \cdot \end{matrix}$$

$$-2b_0 \, P_{0N} = g^A_{0N} \, B_0 F_0 + \sum_{n=1}^{\infty} B_n \, k_n \, \cos \, k_n \, B \, g^A_{Nn}$$

(A.1)

where

$$P_{mn} \equiv \int_{-h}^{-D} dz \, f_m \, F_n \tag{A.2}$$

$$g^{[^S_A]}_{mn} \equiv \int_{-h}^{-D} \int_{-h}^{+D} F_m(2) \, F_n(z') \, G^{[^S_A]} \, (z, \, z') \, dz \, dz' \tag{A.3}$$

From 3.2.16 we get

$$g^{[^S_A]}_{nm} = g^{[^S_A]}_{mn} = \frac{1}{k} \, P_{1m} \, P_{1m} + \sum_{\ell=1}^{\infty} \frac{P_{\ell n} P_{\ell m}}{k_\ell}$$

$$- \sum_{\ell=1}^{\infty} \begin{bmatrix} \coth \, k_\ell B \\ \tanh \, k_\ell B \end{bmatrix} \frac{\delta_{\ell n} \delta_{\ell m}}{K_\ell}$$

(A.4)

From (3.2.15) multiplied by $\{F_1, \ldots F_N\}$

$$-2a_0 P_{01} = \sum_{n=1}^{N} -A_n K_n \sinh K_n B \, g_{1n}^S$$

$$\vdots \qquad\qquad \vdots$$

$$\vdots \qquad\qquad \vdots \qquad\qquad\qquad (A.5)$$

$$\vdots \qquad\qquad \vdots$$

$$-2a_0 P_{0N} = \sum_{n=1}^{N} -A_n K_n \sinh K_n B \, g_{Nn}^S$$

We need to find R_S and R_A which are given by (3.2.13a),

$$a_0 \, R_S = \frac{1}{k} \left[\sum_{n=1}^{N} - A_n K_n \sinh K_n B \, P_{0n} \right] + 1 \qquad\qquad (A.6)$$

$$b_0 \, R_A = \frac{1}{k} \left[B_0 P_{00} + \sum_{n=1}^{N} - B_n K_n \cosh K_n B \, P_{0n} \right] + 1 \qquad (A.7)$$

(A.1) can be rearranged to be a system of equations in terms of $\{R_A,$ $B_0, \ldots B_N\}$ and (A.5) can be written as a system of equations for $\{R_S,$ $A_1, \ldots A_N\}$, then using Cramer's method R_S and R_A are computed.

The hydrodynamic force can be evaluated directly. The symmetric component yields no net horizontal force, so that for an incident wave of unit amplitude:

$$F = \frac{1}{2} F_A = i\omega\rho' \int_{S_0^-} \phi_{11} \, da = i w\rho \left[(1+R_A) M_0 \, a_0 + \sum_{n=1}^{N} M_n \, a_n \right] \qquad (A.8)$$

where

$$M_n \equiv \int_{-D}^{0} f_n \, dz \qquad n = 0, 1, \ldots$$

and from (3.3.13), (3.2.7)

$$a_0 = \frac{g}{2i\omega f_0(0)} e^{ikB} \qquad\qquad (A.9)$$

Alternatively, F can be found from Haskind relationship as will be discussed later. In Figure A.1 the values of

$$\left| R_d \right| = \frac{1}{2} \left| (R_S + R_A) \right| \tag{A.10}$$

are plotted. They agree with those of Mei and Black (1969 (Figure 6)) and Black (1970 (Figure 9.9)) within graphic accuracy. The order of the determinant was 10 for R_A and 9 for R_S. 40 terms are used in the series of (A.4). The resulting errors are less than one percent.

For the radiation problem, the potential is antisymmetric, (3.3.9) is replaced by

$$\psi_{11}^A = f_0 b_0\, e^{-ik(x+B)} + \sum_{n=1}^{\infty} b_n\, f_n\, e^{k_n(x+B)} \qquad (x < -B) \tag{A.11}$$

the boundary condition on the sides of the swaying cylinder is (3.2.20). Instead of (3.2.14), the following integral equation holds:

$$-\left(\frac{iM_0 f_0}{k} + \sum_{n=1}^{\infty} \frac{M_n f_n}{k_n} \right) = \int_{-h}^{-D} dz'\, G^A(z,z')\, U_A(z') \tag{A.12}$$

Mutliplying (A.12) by $\{F_0, \ldots F_N\}$ and integrating with respect to z from $-h$ to $-D$, we get for a unit sway velocity:

$$
\begin{aligned}
-q_0 &= q_{00}\, B_0 + \sum_{n=2}^{N} g_{0n}\, B_n\, K_n \cosh K_n B \\
\ &\quad \vdots \\
-q_N &= q_{0N}\, B_0 + \sum_{n=2}^{N} g_{Nn}\, B_n\, K_n \cosh K_n B
\end{aligned}
\tag{A.13}
$$

where

$$q_n = \frac{i}{k} M_0\, P_{0n} + \sum_{m=1}^{\infty} M_n\, P_{mn}/k_n$$

$\bar{B} \equiv \{B_0, \ldots B_N\}$ is found by solving the set of equations (A.13).

Now

$$-ikb_0 = M_0 \, B_0 P_{00} + \sum_{n=1}^{N} g_{Nn} \, B_n \, K_n \, \cosh K_n \, B \qquad (A.14)$$

which is used to determine b_0. From (3.3.13) we get the amplitude of the radiated wave in terms of the sway velocity:

$$X_{11} \, R_r = -\frac{i\omega f_0(0)}{g} \, b_0 \, V_{11} \, e^{-ikB} \qquad (A.15)$$

but

$$V_{11} = -i\omega X_{11} \qquad (A.16)$$

hence

$$R_r = \sigma \, f_0(0) b_0 \, e^{-ikB} \qquad (A.17)$$

Haskind relation is:

$$F = \frac{2\rho g \, e^{2ikB}}{f_0^2(0) \, \sigma} \, R_r \qquad (A.18)$$

In Figure A.1 the values of $\left| R_r \right|$ are plotted. They also agree with the values of Black (1970, Figure 3.20) within graphic accuracy as do the values of F computed from (A.8) or from (A.18).

The hydrodynamic force on the swaying cylinder can be written in terms of the real valued added mass m and damping coefficient λ defined by

$$-(-\omega^2 \, m - i\omega\lambda) \, X_{11} = 2i\omega\rho \int_{S_0^-} \phi_{11} \, dz \qquad (A.19)$$

From (A.11) and (A.16) we get:

$$\qquad\qquad\qquad\qquad\qquad\qquad\qquad\qquad\qquad\qquad\qquad (A.20)$$
$$-(-\omega^2 \, m - i\omega\lambda) \, X_{11} \simeq 2i\omega\rho \left(\frac{i}{k} \, M_0^2 + \sum_{n=1}^{\infty} \frac{M_n^2}{kn} + q_0 B_0 + \sum_{n=1}^{N} q_n \, B_n \, K_n \, \cosh K_n B \right.$$

Since $\bar{B}$ is known, $(-\omega^2 m - i\omega\lambda)$ is determined from (A.20). The damping coefficient can be related to R_r via energy balance as follows:[1]

---

[1] cf. Newman (1977)

159
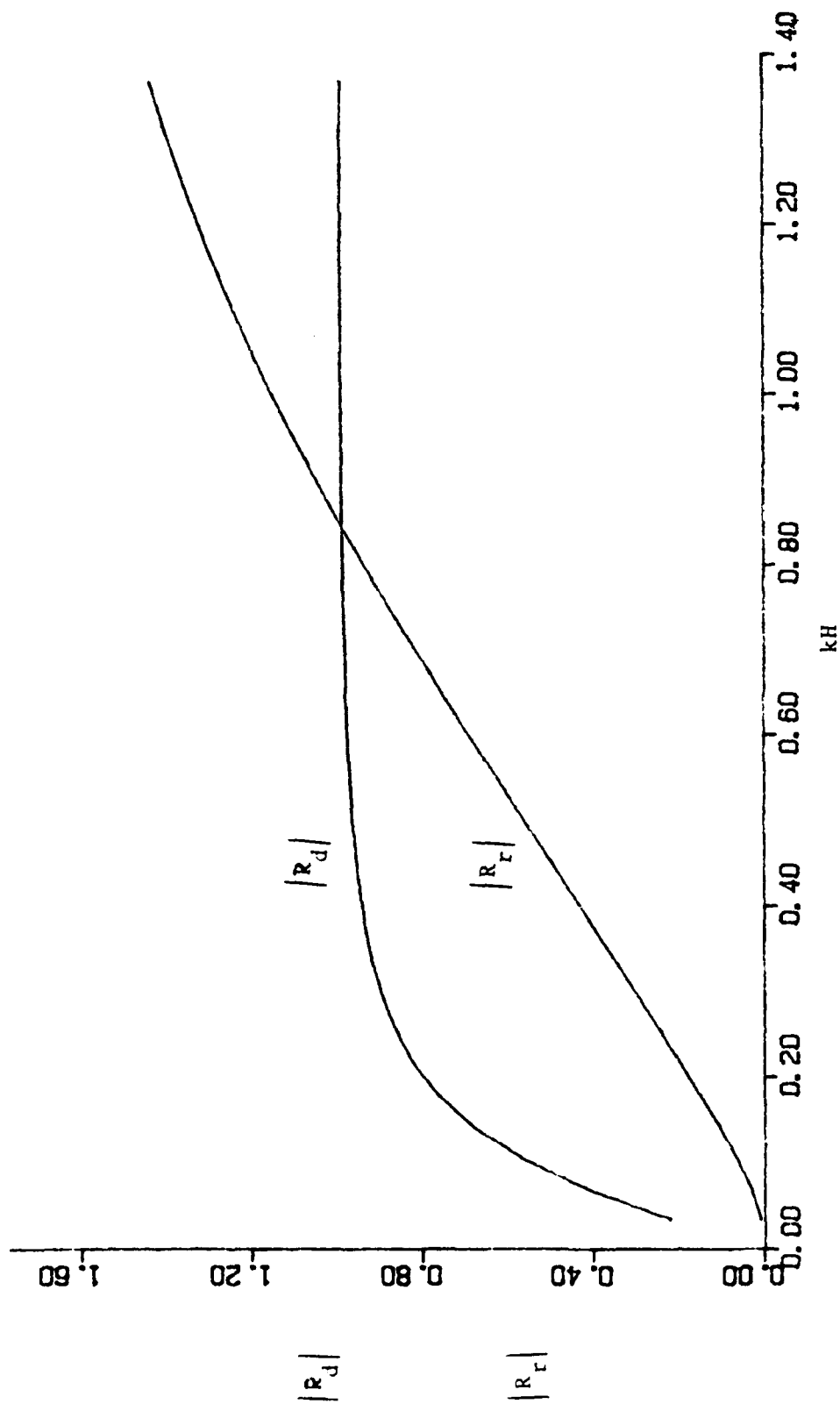
Figure A.1 Reflection Coefficient $|R_d|$ and Sway Radiation Coefficien $|R_r|$ For a Semi-immersed Rectangular Block; B/h = 1.5, H/h = 0.5.

$$\lambda = 2\omega\rho k \left| \frac{b_0}{V_{11}} \right|^2 \tag{A.21}$$

where b_0 is given by (A.14).

The value of λ computed from b_0 (or R_r in Figure A.1) according to (A.20) and (A.21) agree each with the other.

APPENDIX B

Derivation of R, the Reflection Coefficient for the Short Waves,

for a Swaying Block with a Narrow Gap, or no Gap Underneath

As discussed in Section 3.3.2, the short-wave potential ψ_{11} is not affected by the existence of a narrow ($h/L = O(\epsilon)$) gap underneath the rectangular horizontal cylinder. The solution for a sliding block was given in Agnon and Mei (1985a) and is repeated here.

(2.3.4) is written in the form:

$$\psi_{11} = \begin{cases} (a_0^+ - b_0^+) \, f_0 e^{ikx} + \sum_{n=1}^{\infty} b_n^+ f_n e^{-k_n x} & (x > 0) \\[12pt] (a_0^- e^{ik_x} + b_0^- e^{-ikx}) \, f_0 + \sum_{n=1}^{\infty} - b_n^- f_n e^{k_n x} & (x < 0) \end{cases} \tag{B.1}$$

from (3.2.4) get

$$a_0^- = a_0^+ \equiv A_0$$

$$b_0^- = b_0^+ \equiv B_0 \tag{B.2}$$

$$b_n^- = b_n^+ \equiv B_n$$

When (B.1) is substituted into (3.2.6) and the scalar product of the resulting equation is taken with f_n for each n, we find

$$A_0 = B_0 = - \frac{2i\rho}{k_0 M} \left(-B_0 \, F_0 + \sum_{m=1}^{\infty} B_m \, F_m\right) F_0 \tag{B.3a}$$

and

$$B_n = \frac{-2\rho}{k_n M} \, F_n \left(-B_0 \, F_0 + \sum_{m=1}^{\infty} B_m \, F_m\right) \tag{B.3b}$$

where

$$F_n \equiv \int_{-n}^{0} f_n \, dz \tag{B.4}$$

Define

$$C \equiv \sum_{n=1}^{\infty} B_n F_n \tag{B.5}$$

$$D \equiv \frac{-2\rho}{M} \sum_{n=1}^{\infty} \frac{F_n^2}{kn} \tag{B.6}$$

Then substituting (B.3b) into (B.5) gives:

$$C = (-B_0 F_0 + C) D \tag{B.7}$$

From which

$$C = \frac{B_0 F_0 D}{D - 1} \tag{B.8}$$

which substituted into (B.3a) yields:

$$A_0 - B_0 = \frac{-i F_0}{k_0 M} 2\rho \frac{B_0 F_0}{D - 1} \tag{B.9}$$

which can be solved for $R = B_0/A_0$

$$B_0 = A_0 \left\{ 1 + \frac{i F_0^2}{k_0} \Big/ \Big[\sum_{n=1}^{\infty} \frac{F_n^2}{k_n} + \frac{M}{2\rho} \Big] \right\}^{-1} \tag{B.10}$$

Similarly we get:

$$B_n = A_0 \frac{F_n F_0}{k_n} \Big[\frac{i F_0^2}{k_0} + \sum_{n=1}^{\infty} \frac{F_n^2}{k_n} + \frac{M}{2\rho} \Big]^{-1} \tag{B.11}$$

The values of $|R|^2$ are plotted in Figure B.1.

163
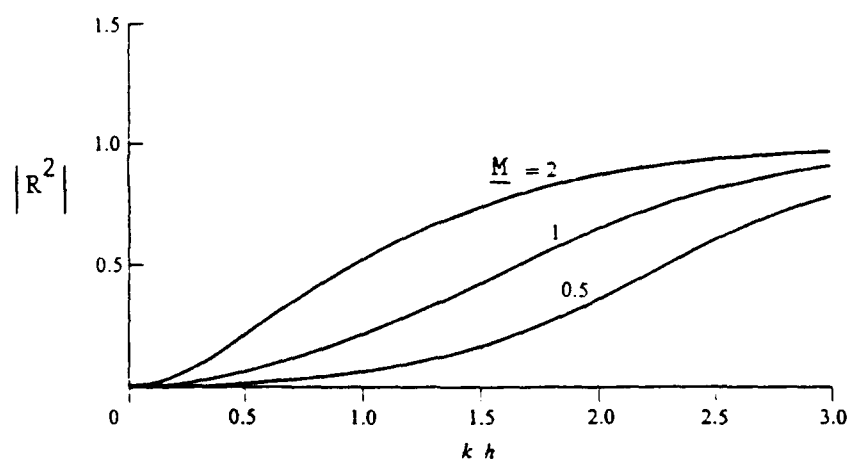
Figure B.1 Square of Reflection Coefficient For Sliding Block.

APPENDIX C

Derivation of the Ordinary Differential Equation for the Slow Sway in Terms

of the Radiation Stress

The derivation of the Ordinary Differential Equation for the slow sway was outlined in Section 3.3.1. When (3.3.63) is differentiated with respect to t_1 and substituted into (3.3.64), we get:

$$K\, X_{10} = \rho h\, 2c_1\, \left[\left(-\frac{\phi_{10}^T}{C_g} - \frac{\phi_{10}^+}{\sqrt{gh}} \right)_{t_1 t_1} - X_{10 t_1 t_1} + U_{t_1} \right] \qquad \text{(C.1)}$$

$$+ \rho g\, \left| A^2 \right|\, \left| R^2 \right|\, \frac{C_g}{C}$$

we now substitute for $\phi_{10}{}_{t_1}$, using (3.3.65), to get:

$$K\, X_{10} = 2\rho h\, c_1\, \left\{ \left[-\frac{\phi_{10 t_1 t_1}^T}{C_g} - X_{10 t_1 t_1} + U_{t_1} \right] \right. \qquad \text{(C.2)}$$

$$\left. - \frac{1}{\sqrt{gh}} \left[\frac{K X_{10 t_1}}{2\rho h} + \phi_{10 t_1}^R - \frac{g}{2h} \left| A \right|_{t_1}^2 \left| R \right|^2 \frac{C_g}{c} \right] \right\} + \rho g\, \left| A \right|^2 \left| R^2 \right| \frac{C_g}{C}$$

Rearranging, we get, using (3.1.6), (3.1.8), (3.1.9) and (3.3.33).

$$X_{10 t_1 t_1} + \frac{K}{2\rho h \sqrt{gh}}\, X_{10 t_1} + \frac{K}{2\rho h c_1}\, X_{10} = \frac{g}{2h c_1} \left| A \right|^2 \left| R \right|^2 \frac{C_g}{C}$$

$$+ \frac{\partial}{\partial t_1}\, \left\{ (1 - \left| R \right|^2)[\phi_{10 t_1}^I - \frac{2\omega k}{gh}\, C_g\, f_0^2(0) \left| A_0^2 \right|] \right. \qquad \text{(C.3)}$$

$$+ \left| R \right|^2 \frac{C_g}{\sqrt{gh}}\, [\phi_{10 t_1}^I - \frac{g}{2h} \left| A \right|^2 \frac{C_g}{C}] \right\}\, (\frac{-1}{C_g})$$

from (3.3.13) it is seen that

$$\frac{2\omega k}{gh} C_g f_0^2(0) |A_0|^2 = \frac{g}{2h} |A|^2 \frac{C_g}{C} \qquad (C.4)$$

From (3.1.8, 3.1.9) we get

$$\phi_{10t_1}^{I} = |A_0|^2 C_g \frac{f_0^2(0)}{gh - Cg^2} [(k^2 - \sigma^2) C_g + 2\omega k] \qquad (C.5)$$

but

$$k^2 - \sigma^2 = k^2 (1 - \tanh^2 kh) = k^2/ch^2 kh \qquad (C.6)$$

and

$$2 C_g = \frac{g}{\omega} \frac{sh\ kh\ ch\ kh + kh}{ch^2\ kh} \qquad (C.7)$$

$$C = \frac{\omega}{k} = \frac{g}{\omega} th\ kh \qquad (C.8)$$

hence

$$k^2 - \sigma^2 = \frac{k\omega}{gh} (2C_g - C) \qquad (C.9)$$

and

$$\phi_{10t_1}^{I} - \frac{2\omega k}{gh} C_g f_0^2(0) |A_0|^2$$

$$= \frac{\omega k\ f_0^2(0)}{gh - C_g^2} [2 \frac{C_g - C}{gh} + \frac{2}{C_g} - \frac{2(gh - C_g^2)}{ghC_g}] |A_0|^2 c_g^2 \qquad (C.10)$$

$$= \frac{\omega k\ f_0^2(0)}{gh - C_g^2} [4 \frac{C_g - C}{gh}] |A_0|^2 c_g^2$$

Defining

$$S \equiv \frac{2C_g}{C} - \frac{1}{2} \qquad (C.11)$$

166

we may write (C.3) (using (3.3.13)) as:

$$X_{10t_1t_1} + \frac{K}{2\rho h\sqrt{gh}}\ X_{10t_1} + \frac{K}{2\rho hc_1}\ X_{10}$$

$$= [-(\frac{C_g}{\sqrt{gh}}\ |R|^2 + 1 - |R|^2)\ \frac{C_g}{gh-C_g^2}\ \frac{g}{2h}\ S\ \frac{\partial}{\partial t_1} + \frac{C_g}{C}\ |R|^2\ \frac{g}{2hc_1}]\ |A|^2$$

(3.3.66)

APPENDIX D

Evaluation of the Steady Drift Force on a Floating Rectangular Cylinder

in Regular Waves

In this appendix, we evaluate the steady drift force on a sliding block in regular waves via direct integration of the mean pressure on the body, and demonstrate that it is equal to that given by the general formula derived by Maruo (1960) and by Newman (1967) via momentum flux consideration, and used in (3.3.19). We shall then generalize the result to a floating cylinder.

In the right hand side of (3.3.8) we let P_{20} be given by (3.3.9) with ψ_{10t_1} set to be zero, for regular waves. We get for the drift force:

$$F = -\rho \left[\int_{S_0^-} P'_{20} \, dz - \int_{S_0^+} P'_{20} \, dz + \delta(i\omega\psi_{11} \, \zeta_{11}^* + *) \right. \tag{D.1}$$

$$\left. + \delta(g \, \zeta_{11} \, \zeta_{11}^*) \right]$$

$$P'_{20} = \left|\nabla\psi_{11}\right|^2 + (i\omega\psi_{11_x}^* \, X_{11} + *) + gz \tag{D.2}$$

The contributions of the terms

$$\left|\psi_{11_x}\right|^2 \quad \text{and} \quad (i\omega\psi_{11_x}^* \, X_{11} + *) \tag{D.3}$$

to the integral are zero because of the kinematic boundary condition (3.2.4). We shall, however, retain the first of these terms for completeness, and because it facilitates the generalization to a floating cylinder. The hydrostatic term can clearly be discarded of since

$$\int_{S_0^-} z \, dz - \int_{S_0^+} z \, dz = 0 \tag{D.4}$$

Integrating $\left|\psi_{11z}\right|^2$ by parts, we find

168

$$\int_{S_0^\pm} \psi_{11} \psi_{11_{xx}}^* \, dz = - \int_{S_0^\pm} \psi_{11} \psi_{11_{zz}}^* + \psi_{11} \psi_{11_z}^* \Big|_{-h}^{-0}$$

$$\text{(D.5)}$$

$$= \int_{S_0^\pm} \psi_{11} \psi_{11_{xx}}^* \, dz + \frac{w^2}{g} |\psi_{11}|^2 {}_{z=0}$$

where use has been made of (2.3.1), (2.3.2) and (2.3.3).

From 3.2.4 we get

$$\int_{S_0^-} (i\omega\psi_{11_x} X_{11} + *) \, dz - \int_{S_0^+} (i\omega\psi_{11_x}^* X_{11} + *) \, dz = 0 \qquad \text{(D.6)}$$

Substituting (D.5) and (D.6) into (D.1) and using

$$\zeta_{11} = \frac{i\omega}{g} \psi_{11} \qquad \text{(D.7)}$$

we get

$$\frac{-F}{\rho} = \int_{S_0^-} (\psi_{11_{xx}} \psi_{11} + |\psi_{11_x}|^2) \, dz - \int_{S_0^+} (\psi_{11_{xx}}^* \psi_{11} + |\psi_{11_x}|^2) \, dz \qquad \text{(D.8)}$$

If we write ψ_{11} in the form:

$$\psi_{11} = \psi_{11}^A + \psi_{11}^S = A_0(e^{ik(x+B)} + R_A e^{-ik(x+B)})f_0 + \sum_{n=1}^{\infty} A_n e^{k_n(x+B)})f_n$$

$$\text{(D.9)}$$

$$+ B_0(e^{ik(x+B)} + R_S e^{ik(x+B)})f_0 + \sum_{n=1}^{\infty} B_n e^{k_n(x+B)} f_n \qquad (x < -B)$$

where for $(x > B)$ ψ_{11} is written in the same form, with ψ_{11}^S symmetric with respect to $(X=0)$ and ψ_{11}^A antisymmetric.

ψ_{11} is decomposed into ψ_{11}^S and ψ_{11}^A so that the result can be generalized to the floating rectangular cylinder case.

Making use of

169

$$\psi_{11}^S (x = B) = \psi_{11}^S (x = -B) \tag{D.10}$$

$$\psi_{11}^A (x = B) = -\psi_{11}^A (x = -B) \tag{D.11}$$

we get from (D.8) that:

$$\frac{-F}{\rho} = 2 \int_{S_0^-} [\psi_{11_{xx}}^{S^*} + \psi_{11_{xx}}^{A^*} \, \psi_{11}^S - (\psi_{11_x}^{S^*} \, \psi_{11_x}^A + *)] dz \tag{D.12}$$

substituting (D.3) into (D.12) and making use of the orthoromality of $\{f_0, f_1 \ldots\}$ we get:

$$\frac{-F}{\rho} = 2 \, [-k^2 \, A_0 B_0^* \, (1+R_A)(1-R_S^*) - \sum_{n=1}^{\infty} k_n^2 \, A_n \, B_n^*$$

$$\tag{D.13}$$

$$- k^2 \, A_0 B_0^* \, (1-R_A)(1-R_S^*) - \sum_{n=1}^{\infty} k_n^2 \, A_n \, B_n^*] + *$$

or

$$\frac{F}{\rho} = 4 \, k^2 \, A_0 B_0^* \, (1 + R_A \, R_S^*) + * \tag{D.14}$$

For a wave incident from $(x = -\infty)$ with amplitude A, we get, from (3.3.13) and (D.9)

$$A_0 = B_0 = \frac{gA}{4i\omega f_0(0)} \tag{D.15}$$

The reflection and transmission coefficients are given by

$$R = \frac{1}{2} (R_S + R_A) , \qquad T = \frac{1}{2} (R_S - R_A) \tag{D.16}$$

Substituting (D.16) into (D.14) we get:

$$\frac{F}{\rho} = 8 \, k^2 \, (1 + |R|^2 - |T|^2) \, \text{Re} \, A_0 B_0^*$$

Substituting (D.15) into (D.17) we get

$$\frac{F}{\rho} = \frac{1}{2} \left(\frac{gk}{\omega f_0(0)}\right)^2 (1 + |R|^2 - |T|^2) \qquad \text{(D.18)}$$

but

$$\frac{2C_g}{C} = \frac{g/\omega \ [\text{sh kh ch kh} + \text{kh}]/\text{ch}^2 \text{ kh}}{g/\omega \qquad \text{th kh}} \qquad \text{(D.19)}$$

making use of (3.3.34) and (D.19), (D.18) can be written as:

$$F = \rho g \ |A|^2 \ |R|^2 \ \frac{C_g}{C} \qquad \text{(D.20)}$$

This result, (3.3.12), can be generalized to a floating rectangular cylinder. If D is smaller than h, we need to subtract from the right hand side of (D.8) the following expression

$$\int_{-h}^{-D} (\psi_{11}^*{}_{xx} \ \psi_{11} + |\psi_{11}{}_x|^2) \ dz \ \Big|_{x = B}^{x = -B} \qquad \text{(D.21)}$$

Integrating the first term by parts, we get, as in (D.5) that

$$\int_{-h}^{-D} \psi_{11}^*{}_{xx} \ \psi_{11} \ dz = \int_{-h}^{-D} |\psi_{11}{}_z|^2 \ dz \qquad \text{(D.22)}$$

Since

$$\psi_{11}{}_z = 0 \qquad (x = \pm B; \quad z = -h, -D) \qquad \text{(D.23)}$$

(cf. (2.3.3), (3.2.5)); Thus (D.10) may be written as:

$$\int_{-h}^{-D} |\nabla\psi_{11}|^2 \ dz \ \Big|_{x = +B}^{x = -B} \qquad \text{(D.24)}$$

which is the net mean horizontal momentum flux into the volume under the floating cylinder. This quantity must be zero since there is no momentum transfer from the swaying cylinder to the fluid below it. We conclude that (3.3.12) is valid for swaying floating rectangular cylinders.

171

APPENDIX E

Derivation of the Added Mass and Damping Coefficient for Large Amplitude

Slow Sway

The presentation in this appendix is based on the work of Professor H. S. Choi from Korea who was visiting Parsons Laboratory during 1985.

The method of a solution involves asymptotically matching a near field solution and a far field solution. The near field is within a few short wavelengths from the body. In the near field a rigid lid upper surface can be assumed for a slow potential. We now apply the same reasoning which led to Equation (3.3.59). Let the ambient flow velocity be ϵv, where we assume that the sway motion has a unit amplitude. The sway velocity is thus

$$\text{Re } -2i\Omega e^{-2i\Omega t_1} \tag{E.1}$$

and its acceleration is

$$\text{Re } -4\Omega^2 e^{-2i\Omega t_1} \tag{E.2}$$

Let the near field potential be

$$\psi = \text{Re } \psi' e^{-2i\Omega t_1} \tag{E.3}$$

ψ' will have the following outer approximation in the body coordinates (i.e., $x'' \equiv x - \text{Re } \exp(-2i\Omega t_1)$):

$$\psi' \rightarrow \epsilon(v' + 2i\Omega) (x'' \pm c) \qquad (kx'' \rightarrow \pm \infty) \tag{E.4}$$

where

$$v = \text{Re } v' e^{-2i\Omega t_1} \tag{E.5}$$

In the fixed frame of reference, we have instead

$$\psi' \rightarrow \epsilon[v'x \pm (v' + 2i\Omega)c] \qquad (kx \rightarrow \pm \infty) \tag{E.6}$$

c, the blockage coefficient was given by Flagg and Newman (1971). In normalized form, we have:

172

$$\underline{c} \equiv \frac{c}{H} = \frac{B}{H} + \frac{2}{\pi} (\ln \frac{h}{4H} + 1) - \frac{B}{h} + O(\frac{H}{h})^2 \qquad (E.7)$$

In the far field, the radiated long waves are

$$\phi = \text{Re } \phi' e^{-2i\Omega t_1} \qquad (E.8)$$

where

$$\phi' = \pm \alpha e^{ik_1|x_1|} \qquad \begin{matrix} (x_1 > 0) \\ (x_1 < 0) \end{matrix} \qquad (E.9)$$

α is an amplitude function and $ghk_1^2 = (2\Omega)^2$. Use has been made of the fact that the slow velocity field due to sway is even in x_1, hence ϕ' is odd in x_1. Note that ϕ is a solution to the long-wave equation; we do not impose a rigid lid condition in the far field.

The inner expansion of ϕ' is:

$$\phi' \to \pm \alpha [1 + ik_1|x_1| + O(kx_1)^2] \qquad \begin{matrix} (x_1 > 0) \\ (x_1 < 0) \end{matrix} \qquad (E.10)$$

Matching the asymptotic expansions (E.6) and (E.10) immediately yields:

$$ik_1 \alpha = v' \qquad (E.11)$$

$$\alpha = \epsilon(v' + 2i\Omega)c \qquad (E.12)$$

from which we find:

$$v' = \frac{-\epsilon 2i\Omega cik_1}{\epsilon ik_1 c - 1} \qquad (E.13)$$

The radiation coefficient, which is defined as the amplitude of the potential $\psi_0^{(2)}$ per unit amplitude of sway displacement, is given by

$$\alpha = \frac{-\epsilon 2i\Omega c}{\epsilon ik_1 c - 1} \qquad (E.14)$$

173

To find the added mass μ, and damping coefficient λ, we compute the horizontal dynamic force on the body:

$$F = \rho[\int_{S^-} \psi_{t_1} \, dz - \int_{S^+} \psi_{t_1} \, dz] = \rho \, \text{Re} \, -2i\Omega e^{-2i\Omega t_1} [\int_{S^-} \psi' \, dz - \int_{S^+} \psi' \, dz] =$$

$$= \rho \, \text{Re}[-2i\Omega e^{-2i\Omega t_1} (h\alpha - 2i\Omega \, 2BD)] \qquad (E.15)$$

(cf. Beck & Tuck (1972)).

The added mass and damping coefficient are defined by:

$$-F = (-4\Omega^2 \mu - 2i\Omega\lambda)e^{-2i\Omega t_1} \qquad (E.16)$$

From (E.15) and (E.16) we find:

$$-4\Omega^2(\mu + M) - 2i\Omega\lambda = 4\Omega^2 \rho h \, \frac{2c}{\varepsilon i k_1 c - 1} \qquad (E.17)$$

since $M = 2\rho BD$.

When the gap H is relatively large, the blockage coefficient tends $2BD/h$ (this is because the increase of the current in the gap is approximately: $h/(h-D) - 1 \rightarrow D/h$ as $D \rightarrow 0$).

The normalized potential jump, $2\alpha/(-2i\Omega)$, is approximated by $-2c$. This implies that the force is mainly in phase with the acceleration:

$$\mu = \rho(-2BD + 2hc) + 2\rho BD \qquad (E.18)$$

which are the values for slow sway in the absence of free surface effects.

174

LIST OF FIGURES AND TABLES

175

DOCUMENT LIBRARY
April 9, 1985
DISTRIBUTION LIST FOR TECHNICAL REPORT EXCHANGE

Institute of Marine Sciences Library
University of Alaska
O'Neill Building
905 Koyukuk Ave., North
Fairbanks, AK

Attn: Stella Sanchez-Wade
Documents Section
Scripps Institution of Oceanography
Library, Mail Code C-075C
La Jolla, CA 92093

Hancock Library of Biology & Oceanography
Alan Hancock Laboratory
University of Southern California
University Park
Los Angeles, CA 90089-0371

Gifts & Exchanges
Library
Bedford Institute of Oceanography
P.O. Box 1006
Dartmouth, NS, B2Y 4A2, CANADA

Office of the International
   Ice Patrol
c/o Coast Guard R & D Center
Avery Point
Groton, CT 06340

Library
Physical Oceanographic Laboratory
Nova University
8000 N. Ocean Drive
Dania, FL 33304

NOAA/EDIS Miami Library Center
4301 Rickenbacker Causeway
Miami, FL 33149

Library
Skidaway Institute of Oceanography
P.O. Box 13687
Savannah, GA 31416

Institute of Geophysics
University of Hawaii
Library Room 252
2525 Correa Road
Honolulu, HI 96822

Library
Chesapeake Bay Institute
4800 Atwell Road
Shady Side, MD 20876

MIT Libraries
Serial Journal Room 14E-210
Cambridge, MA 02139

Director, Ralph M. Parsons Laboratory
Room 48-311
MIT
Cambridge, MA 02139

Marine Resources Information Center
Bldg. E38-320
MIT
Cambridge, MA 02139

Library
Lamont-Doherty Geological Observatory
Colombia University
Palisades, NY 10964

Library
Serials Department
Oregon State University
Corvallis, OR 97331

Pell Marine Science Library
University of Rhode Island
Narragansett Bay Campus
Narragansett, RI 02882

Working Collection
Texas A&M University
Dept. of Oceanography
College Station, TX 77843

Library
Virginia Institute of Marine Science
Gloucester Point, VA 23062

Fisheries-Oceanography Library
151 Oceanography Teaching Bldg.
University of Washington
Seattle, WA 98195

Library
R.S.M.A.S.
University of Miami
4600 Rickenbacker Causeway
Miami, FL 33149

REPORT DOCUMENTATION PAGE	1. REPORT NO. WHOI-86-22	2.	3. Recipient's Accession No.

4. Title and Subtitle	5. Report Date
Nonlinear Diffraction of Ocean Gravity Waves	June 1986
	6.

7. Author(s) Yehuda Agnon	8. Performing Organization Rept. No. WHOI-86-22

9. Performing Organization Name and Address Woods Hole Oceanographic Institution Woods Hole, Massachusetts 02543 and Massachusetts Institute of Technology Cambridge, Massachusetts 02139	10. Project/Task/Work Unit No.
	11. Contract(C) or Grant(G) No. (C) N00014-80-C-531, (G) NR 4332-228

12. Sponsoring Organization Name and Address Office of Naval Research Environmental Sciences Directorate Arlington, VA 22217	13. Type of Report & Period Covered Sc.D. Thesis
	14.

16. Abstract (Limit: 200 words)

In an irregular sea, waves having different wave numbers interact nonlinearly, giving rise to long waves at the difference frequency and wavenumber. The long waves are associated with motions that have large characteristic time and space scales.

The method of multiple scales in time and in space, in conjunction with perturbation expansions, enables us to separate the flow into components for the general case when there are wave-trains propagating in different directions. In particular, it is of great interest to study the effect of modification of the short waves by diffraction, refraction, reflection and radiation. Using the method of matched asymptotics we determine the long-wave, that consists of forced waves travelling with the short-wave groups and of an additional wave that propagates away from the "zone of modification" at the long-wave velocity $(gh)^{\frac{1}{2}}$. The resulting theory has a wide range of applications. We have studied the following problems:

a) Slow Sway of a Moored Floating Body in Water of Finite Depth
b) Wave Trapping on a Shelf
c) Excitation of Interfacial Waves in the Lee of a Breakwater

The present method of analysis, and in particular the multiple scales expansion, proves to be a useful tool in studying modulation and nonlinearity in several aspects at wave propagation, and can be extended to the study of a heretofore unexplored aspect of harbour resonance. The ideas will be sketched in the Epilogue.

17. Document Analysis a. Descriptors
1. surface waves
2. multiple-scales
3. nonlinear waves

b. Identifiers/Open-Ended Terms

c. COSATI Field/Group

18. Availability Statement	19. Security Class (This Report) UNCLASSIFIED	21. No. of Pages 177
Approved for publication; distribution unlimited.	20. Security Class (This Page)	22. Price